2019

Investigation into Photovoltaic Distributed Generation Penetration in the Low Voltage Distribution Network

Shivananda Pukhrem
Technological University Dublin

Investigation into Photovoltaic Distributed Generation Penetration in the Low Voltage Distribution Network

Shivananda Pukhrem

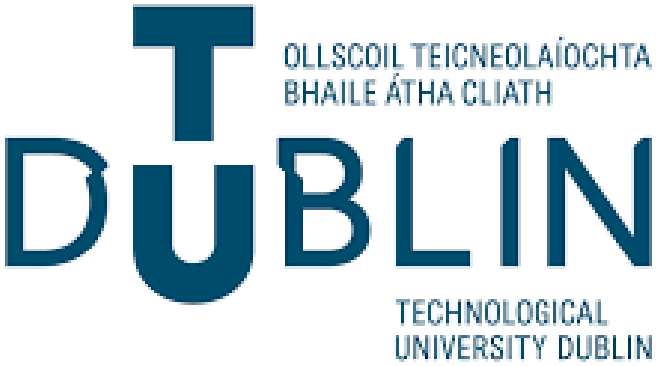

A thesis submitted in fulfillment of the requirements for the degree of

Doctor of Philosophy

School of Electrical and Electronic Engineering

Technological University Dublin

2019

Under the Supervision of

Dr. Malabika Basu and Prof Michael Conlon

To my lovely daughter, Eliza

Abstract

Significant integration of photovoltaic distributed generation (PVDG) in the low voltage distribution network (LVDN) could potentially pose threats and challenges to the core activity of distribution system operators (DSO), which is to transport electrical energy in a reliable and cost-effective way. The main aim of this research is to investigate the active planning and operation of LVDNs with increased PVDG integration through steady state power system analysis. To address the impacts of voltage profile fluctuation due to power flow modification, this research proposes a probabilistic risk assessment of power quality (PQ) variations and events that may arise due to significant PVDG integration. A Monte Carlo based simulation is applied for the probabilistic risk assessment. This probabilistic approach is used as a tool to assess the likely impacts due to PVDG integration against the extreme-case scenarios. With increased PVDG integration, site overvoltage is a likely impact, whereas voltage unbalance reduces when compared with no or low PVDG penetration cases. This is primarily due to the phase cancellation between the phases. The other aspect of the work highlights the fact that the implementation of existing volumetric charges in conjunction with net-metering can have negative impacts on network operator's revenue. However, consideration of capacity charges in designing the existing network tariff structure shows incentivising the network operator to perform their core duties under increased integration of PVDG. The site overvoltage issue was also studied and resolved in a novel way, where the active and reactive power of the PVDG inverters at all the PV installed premises were optimally coordinated to increase the PV penetration from 35.7% to 66.7% of the distribution transformer rating. This work further explores how deficiencies in both reactive power control (RPC) and active power control (APC) as separate approaches can be mitigated by suitably combining RPC and APC algorithms. A novel "Q" or "PF" limiter was proposed to restrict frequent switching between the two droop characteristics while ensuring a stabilizing (smoothened) voltage profile in each of the PV installed nodes. This novel approach not only alleviates the voltage fluctuation but also reduces the overall network losses.

Declaration

I hereby certify that this thesis which I now submit for examination for the award of Doctor of Philosophy, is entirely my own work and has not been taken from the work of others, save and to the extent that such work has been cited and acknowledged within the text of my work.

This thesis was prepared according to the regulations for postgraduate study by research of the Technological University Dublin and has not been submitted in whole or in part for another award in any Institute.

The work reported in this thesis conforms to the principles and requirements of the Technological University Dublin's guidelines for ethics in research.

Technological University Dublin has permission to keep, lend or copy this thesis in whole or in part, on condition that any such use of the material of the thesis be duly acknowledged.

……

Acknowledgements

I am grateful for the opportunity to build my home in this beautiful country, Ireland. I am very blessed to complete my research work successfully and would like to thank sincerely to all who helped me directly and indirectly.

To my colleagues from the School of Electrical and Electronic Engineering, I will never forget the time we spent over these four years. To name few, Michael Farrell, Keith Sunderland, Roberto Sandano, Paul Leamy, Frank Duigan, Ted Burke, Chittesh Veni Chandran, Sandipan Patra and Shahab Sajedi, I cherished your camaraderie.

To my supervisors, Dr. Malabika Basu and Prof. Michael Conlon, your aspiring guidance and valuable criticism over the duration of this research are the indispensable support that led to the successful completion of my work. I am truly grateful and appreciative for all you have done.

To my parents, Birkumar and Bijaya, I thank you for being there always for me by embracing who I am. I cannot ask more than your unconditional love and believing in my potential as long as I could remember. To my dear siblings, Dapu, Mabem and Pingu, I miss so much being around with you all, but I am so thankful that we are keeping our contact and bringing our distance closer.

Lastly, to my dear daughter Eliza, I dedicate this research work to you. Daddy couldn’t be prouder for you. Your presence in my life cannot be compared with any milestone. Daddy loves you more than yesterday!

Abbreviations List

APC	*Active Power Control*
CAPEX	Capital Expenditure
CDF	*Cumulative Distribution Function*
CCDF	*Complimentary Cumulative Distribution Function*
CEER	*Council of European Energy Regulators*
CSB	*Capacitor Switch Banks*
DG	*Distributed Generator*
DSO	*Distribution Network Operator*
DT	*Distribution Transformer*
DUoS	*Distribution Use of System*
EMTP	*Electromagnetic Transient Program*
EPRI	*Electric Power Research Institute*
FACTS	*Flexible AC Transmission System*
GTI	*Grid Tied Inverter*
L	*Load Buses*
LCT	*Low Carbon Technology*
LDC	*Line Drop Compensation*
LSRPP	*Large Scale Renewable Power Plant*
LVDN	*Low Voltage Distribution Network*
MC	*Monte Carlo*
n	*Penetration Level*
N_pv	*Number of PVDG installed customer*
NRA	*National Regulatory Authority*
OpenDSS	*Open Distribution System Simulator*
OPEX	*Operational Expenditure*
OLTC	*On Load Tap Changer*
PF(P)	*Power Factor (PF) as a function of the PVDG active power (P*)
PF(U)	*Power Factor (PF) as a function of the local voltage (U)*
$P^{L}_{N\_pv}$	*Permutation without replacement*
PQ	*Power Quality*
P(U)	*Active Power (P) as a function of the local voltage (U)*
PVDG	*Photovoltaic Distributed Generator*
Q(U)	*Reactive Power (Q) as a function of the local voltage (U)*
RPC	*Reactive Power Control*
SLG	*Single Line to Ground*
SVR	*Step Voltage Regulator*
TUoS	*Distribution Use of System*
TSO	*Transmission System Operator*
UPF	*Unity Power Factor*

Table of Contents

List of Figures

List of Tables

Chapter 1

Introduction

1.1 Background

The low voltage distribution network (LVDN) is primarily designed to transport electric power from the sub-transmission network to the end customer. The part of the transmission system that connects the high voltage substation through step-down transformers to the regional distribution substation is termed the sub-transmission network or medium voltage network. Industrial customers may be connected to the medium voltage level. Capacitor and reactor banks are usually installed in the substations to maintain transmission line voltage. Due to deregulation of the electricity supply industry as seen in [1], no single organization has jurisdiction relating to location and production of individual generating stations. For this reason, distribution system operators (DSOs) are not permitted to own any generating stations or other plant not directly to their main responsibilities which are the security and reliability of the supply of energy. Thus, DSOs in particular have no role in the decision on the siting and sizing of distributed generators (DG) in LVDN [2]. The introduction of renewable base distributed generator (DG) such as solar photovoltaic DG (PVDG) in LVDNs has elevated the complexity of controlling and maintaining the LVDN within acceptable limits. The significant introduction of such PVDGs can impact the performance of the power system.

According to M. Bollen *et al.* [3], the performance of the power system can be quantified based on the primary and secondary aims of the power system. The primary

aims relate to the customer such as reliability of supply, voltage quality and the tariffs. The secondary aims are the internal aims set by the DSOs in achieving these primary aims. The secondary aims could be preventing component overload, correct operation of protection devices, current quality, operational security, and costs. Fulfilling the secondary aims will automatically result in the primary aims being fulfilled. Maintaining the secondary aims in the presence of increased PVDG entails extra expenditure to the DSO. Without the proper mechanism to reward DSO by the national regulatory authority (NRA) in fulfilling their core activities in the presence of increased PVDG may pose a barrier in promoting further PVDG penetration [4]. Through the different types of power system studies, the performance of the power system can be studied in detail.

1.2 Types of power system studies

Generally power system studies are classified according to the temporal behaviour of the power system phenomena under consideration such as the transient model, the dynamic model and the steady state model [5][6][7]. Figure 1.1 categorises the various power system studies.

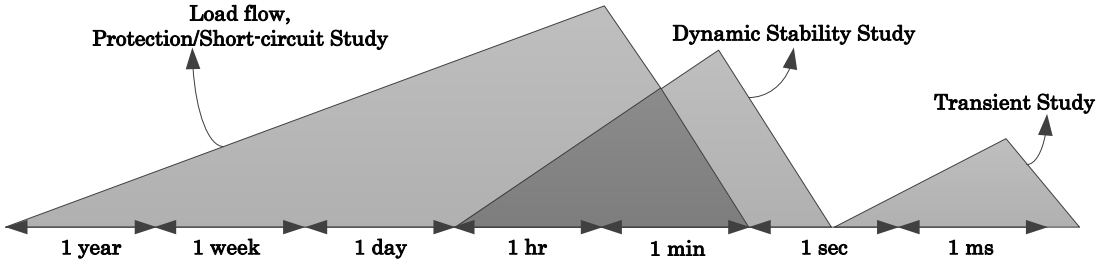

Figure 1.1 : Categorisation of power system studies [7]

i) Transient state: These models refer to the time frame from 1 second down to infinitesimal time. Primarily, this analysis studies electromagnetic transient

phenomena such as transient stability and harmonics. Transient stability includes switching (capacitor banks, re-configuring the electrical network, etc.), short-circuit and lightning phenomena, whereas harmonic study is related to power electronics and magnetic saturation. The transient studies are modelled using differential equations in the time domain. Electromagnetic transient programs (EMTP), namely PSCAD in [8] and PLECS in [9] are generally used to study such detailed transient phenomena and are typically used for detailed analysis of a part of the transmission or distribution system. Further EMTPs are quite useful in detailed modelling of unbalanced three phase systems.

ii) Dynamic state: This model refers the time frame from 1 hour down to 1 second. This model studies electromechanical dynamic stability, such as voltage and power angle stability. It also includes fault recovery studies. This dynamic study is governed by differential/algebraic equations and involves dynamic analyses in time domain. Positive sequence electro-mechanical transient programs, namely PSSE in [10], Power World in [11] and PSLF in [12] are generally used to study the dynamic performance of transmission systems, which are assumed to be balanced.

iii) Steady state: This power system model refers to the time frame from 1 year to 1 minute. The steady state model primarily studies load-flow, protection and short circuit capacity. Power flow studies the production cost models, voltage regulation and power transfer. This steady state model is governed by algebraic equations such as power balance equations, Kirchhoff laws, etc. in the phasor domain. Unbalanced phasor domain power flow programs, namely CYMEDIST (CYME Distribution System Analysis Tool) [13] and OpenDSS (Open Distribution System Simulator) in [14], [15] can perform both snapshot and quasi-static analysis.

The distribution network is characterised by its dispersed and diverse nature. Simulation of such a vast distribution network using EMTP-type programs is computationally challenging for detailed modelling of the large number of distribution network elements such as power delivery elements (lines, transformers, shunt capacitor banks) and power conversion elements (generators and loads). Above all, such EMTP-type programs require a considerable amount of time to solve the differential equations. On the other hand, the positive sequence electromechanical transient programs are not suitable for modelling a typical distribution network due to its inherent unbalanced nature. For these reasons, the primary study of this research work relies on steady state analysis of the distribution network by modelling and analysing it in phasor domain.

OpenDSS in [16] is chosen as a preferred phasor domain unbalanced power flow simulation tool. The adequate application of this tool for DG impact studies were highlighted in [17], [18]. Phasor domain analysis of the AC system was first introduced by Steinmetz in 1893 [19], [20]. This revolutionary approach has allowed engineers to calculate the steady state behaviour of the AC system using an elementary algebraic set of equations rather than a time dependent quantity which requires calculus. A quasi-static time series analysis is a preferred choice because it permits distribution network analysis for periods of a day, week or months. This quasi-static time series simulation provides a series of steady state solutions by eliminating any dynamic effects in each solution. The quasi-static analysis solves multiple network algebraic equations for different operating conditions. It can involve variation in load profiles and/or PV generation profiles, and its record voltages at each node over time and computes short circuit capacity of the distribution network.

1.3 Aim of the Research

The main aim of this research is to investigate the active planning and operation of increased PVDG integration in LVDN through steady state power system analysis. To address this aim, three research objectives will be discussed in detail in this thesis. They are the methodology in quantifying the steady state technical impacts, the impacts of the existing regulatory policies towards the DSO revenue and measures to alleviate voltage fluctuation. The research objectives are:

1. To investigate statistically the impacts due to increased integration of PVDG in the existing distribution network. This impact study will include customers' voltage profiles, voltage unbalance at 3 phase nodes and voltage sag due to a random single line to ground faults.
2. To study the impact of net metering in conjunction with the volumetric tariff structure on DSO's revenue and investigate how to improve such impacts by considering capacity-based tariff structure.
3. To investigate the existing autonomous coordinated voltage control techniques of grid-tied PV inverters in alleviating the voltage fluctuation.

1.4 Thesis Outline

The thesis is divided into 6 chapters. The first chapter introduces briefly the impacts on the performance of the LVDN due to increased integration of PVDG and the choice of the phasor domain unbalanced power flow tool. Chapter 2 includes a detailed literature review of the steady state technical and economic impacts due to PVDG integration in a LVDN followed by the existing connection guidelines and

methodologies. Chapter 2 concludes by proposing the research objectives by identifying the research gaps from the literature review. A probabilistic approach in quantifying the impacts due to increased integration of PVDG in LVDN is discussed in Chapter 3. Chapter 4 presents the impact on DSO's revenue due to net metering in conjunction with the volumetric tariff under the increased integration of PVDG in LVDN. Chapter 4 further investigates ways to improve such impacts on the DSO's revenue by considering a capacity-based tariff in designing network tariff structure. Enhanced autonomous coordinated voltage control techniques for grid-tied PV inverter are proposed in Chapter 5. Conclusion and potential future work are presented in Chapter 6.

Chapter 2

Literature Review

This chapter discusses the present state of the art of DG (distributed generation) integration into the power system. It includes general impacts on the power system performance followed by a detailed discussion on the technical and economic impacts due to the PVDG (photovoltaic distributed generator) integration in LVDN (low voltage distribution network). The technical impacts are voltage fluctuation, increases in the short circuit level and losses. The economic impacts focus on net-metering in conjunction with volumetric tariff structure. A short summary of the network tariffing structure is also presented. Present connection guidelines and methodologies are also included. The chapter ends with formulating the research objectives by identifying the research gaps.

2.1 General Impact Studies

DG impacts on power distribution systems were studied in [21]–[26]. These contributions began with the definition of DG in [22] and its associated drivers, challenges and opportunities [24]. More importantly, Barker *et.al* [21] presented the hierarchical order in relation to DG. First, it impacts on the basic electrical parameters of the LVDN such as power flow modification, voltage profile fluctuation, quality of voltage profile such as harmonics, flicker, unbalances, voltage stability and dynamics and contribution to short circuit current and power. Second, it impacts on the design, planning and network operation of the LVDN such as protection planning and modification of the network monitoring and planning. Finally, if the reverse power

flow from PVDG exceeds the loading capacity of the substation transformers, the insulation inside the transformer can age prematurely.

A technical document from EPRI in [27] has shown that the feeder response to PVDG is unique to the individual feeder's characteristics. The basic feeder characteristics include voltage level, load, feeder topology, power delivery elements (lines, transformers, capacitors, etc.), power conversion elements (loads, generators, storage, etc.), control operating criteria and switched/controllable elements. Fundamentally, ERPI's technical document in [27] concluded that for any specific feeder, the increased integration of PVDG will impact on the followings:

1. the voltage (overvoltage, voltage deviation and voltage unbalance);
2. loading (thermal and demand);
3. protection (PVDG fault current contribution towards the total fault current leading to malfunctioning of breaker/fuse coordination, sympathetic tripping and anti-islanding);
4. power quality (such as resonance, distortion);
5. the control algorithms of the capacitor bank, voltage regulator and transformer tap changers.

Resolving these impacts entails extra tasks for DSOs (Distribution System Operators) in maintaining the secondary aims of the power system. This involves an extra investment on DSO's capital and operational expenditures. A report from EU Commission Smart Grid Task Force in [28] suggested the necessity to incentivise system operators such as DSOs in fulfilling the primary aims of the power system under increased integration of PVDG. This means that DSOs should develop adequate

tools to assess any technical challenges that arises under the high integration level of PVDG. Again, the DSOs are regulated entities where their costs and revenues are remunerated from the network tariff structure set by the NRA (national regulatory authority). Gareth *et al.* [29] concluded the requirement of a proper distribution network pricing scheme to reflect proper costs and benefits to incentivise the DG developers and DSOs in promoting the higher integration of DG. Adversely, a report from EU Distribution System Operators in [30] has shown the implementation of a volumetric network tariff structure in distribution customers could impact the DSO's income and investment planning abilities under increased integration of PVDGs. The regulatory impact on the incentive for DG integrating for DSOs was thoroughly studied by A.Picciariello *et al.* [31] and it was concluded that there is an essential requirement for new regulatory strategies to hedge against potential DSO disincentives to integrate DG. By virtue of the dispersed and diverse nature of the LVDN, the above impacts can be further escalated due to temporal and spatial behaviour of different demographic areas [32], [33]. In the following paragraphs the steady state impacts as a manifestation of increased PVDG in an LVDN are discussed in detail.

2.2 Steady State Technical Impacts

In normal condition without PVDG, voltage rise may be observed in a distribution system during light load condition if the capacitor banks (fixed or switched) are left energised [34]. A fixed capacitor bank installed downstream of the voltage regulator may pose coordination issues with voltage regulation in the case of load-center compensation technique of line drop compensation (LDC) [35]. With the voltage spread approach of LDC technique, this issue can be mitigated. During bidirectional power flow, reverse mode operation of the voltage regulator is essential to set its tap

setting. Often, a voltage override feature is deployed to protect against overvoltage caused by incorrect LDC settings or under unusually high loads. Due to the inherent intermittent nature of solar insolation, the salient impacts of increased PVDGs integration are reverse power flow and voltage fluctuation [36]. Significant integration of PVDGs could lead to voltage rise at the downstream of the distribution feeder [37]–[39]. Voltage rise in such a context occurs when the injected PVDG current is higher than the upstream current. Without proper setting of the dead band of the off-load tap changer (OLTC) in the presence of significant PVDGs, voltage rise may further be aggravated [40]. Integration of PVDG may impact the operation of these devices depending on their operational settings, location and load level [41].

Under normal operation without any PVDG integration, any requirement of reactive power by the downstream loads (considering the threshold limit of the reactive power supplied from the sub-transmission is exceeded) is sensed by the capacitor switch bank (CSB) located upstream. The CSB is activated to provide the required reactive current which flows downstream of the feeder [42]. But under high penetration of PVDG on the downstream, such normal action of capacitor banks may further aggravate the voltage limits due to reverse power flow from PVDGs. Similarly, the step voltage regulator (SVR) has a line drop compensation (LDC) to estimate the line voltage drop, and performs voltage correction based on line current, line resistance and reactance parameters, and load side voltages. Such LDC senses the direction of real power flow to perform correct voltage regulation. But with significant penetration level of PVDGs, the SVR will detect the wrong direction when reverse power flow occurs [42]. Impacts on the traditional distribution network voltage regulators such as OLTC, line voltage

regulator (LVR), CSB and LDC due to intermittent solar insolation were studied in [43]–[45].

So far, some of these devices have been modified to accommodate bidirectional power flow, such as reconfiguration of the control setting of the voltage regulators and substitution of breaker protection relays or reclosers [46]. But, under the increased integration of PVDGs further readjustment will be necessary, such as disabling the reverse flow sensing in LVR, increasing the current setting of the transformer directional overcurrent protection and innovative fuse-recloser or fuse-relay coordination. Depending on the type and location of the fault, protection schemes such as fuse saving, fuse clearing, fuse-fuse coordination, fuse-recloser coordination and relay-fuse coordination may be affected [47].

Given the dispersed and diverse nature of LVDN, the DSOs do not have full knowledge of the aforementioned impacts could affect their network. Kateraei *et al.* [36] mentioned two essential impact studies relating to the steady state and dynamic state. Therein, the steady state study is used by distribution system engineers in analysing the worst case and the probable case scenarios through load flow studies. Relating steady state study of the power system, voltage fluctuation, an increase in network losses, thermal loading and increases in the short circuit level are the most critical threats and challenges for any specific feeder [3], [27]. From the above discussion, alleviating voltage fluctuation and quantifying the increase short circuit level becomes a necessary measure to maintain the secondary aim of the DSO. In the following section voltage fluctuation, short circuit level and losses due to PVDG integration in a distribution network are discussed in detail.

2.2.1 Voltage Fluctuation

When the injected PVDG current is higher than the upstream current, voltage rise issues are observed and consequently a manifestation of reverse power flow phenomena [48]–[50]. Detailed analysis of voltage fluctuation in two buses radial network system is presented in Appendix A: Voltage fluctuation. Traditional voltage fluctuation control devices such as OLTC, LVR, and CSB are not primarily designed to mitigate the fluctuations in voltage caused by the intermittent primary energy resource (solar insolation) [43], [51]. Nonetheless, as discussed by Agalgaonkar *et al*. [44], an optimal reactive power coordination strategy based on the load and irradiance forecast data can be employed to reduce the duty associated with the operation of OLTC and LVR. Furthermore, as proposed by Jung *et al*. [52], coordinating techniques can be deployed to overcome voltage fluctuations through the synergetic operation of automated voltage regulators and capacitors in conjunction with PVDG inverters. Flexible ac transmission system (FACTS) devices can also alleviate operational frequency of these devices. Zhang *et al*. [53] deployed dynamic voltampere reactive (VAR) compensation to mitigate the voltage fluctuations. The reduced frequency operation of OLTC, LVR, CSB, and LDC without the support of FACTS devices, can be supplemented through smart functionality on the PVDG grid tied inverter (GTI) to alleviate the voltage fluctuation. Such smart functionality of the GTI monitors the voltage within its vicinity and responds to an appropriate VAR requirement by the distribution network [54]. With the advanced control capability of smart GTI as seen in [55], which has essentially FACTS functionality to a limited extent, the requirement of additional devices is eliminated, and the uncertainty error caused by irradiance and load forecast, as discussed earlier, is much less influential.

So far, reactive power control (RPC) methods have included Q(U) control (reactive power as a function of the local voltage), PF(P) control (PF as a function of the PVDG active power), and PF(U) control (power factor as a function of the local voltage). On the other hand, active power curtailment (APC) method includes P(U) control (active power as a function of the local voltage). The VAR management for alleviating the voltage fluctuation primarily depends on the volt-ampere (VA) capacity of the PVDG GTI, upstream transformer loading, and any associated line and transformer losses. From a European perspective, the German grid code as discussed in [56] and [57], respectively, recommends the active involvement of PVDG GTI to alleviate the voltage fluctuation at the POC (point of connection) as a technical requirement for the connection to medium-voltage (MV) and low-voltage (LV) networks.

A further alternative to the German grid code is a technique proposed in E. Demirok *et al.* [58] that alleviates voltage fluctuation for an LV balanced network by controlling the PF of the GTI through continuous monitoring of active PVDG power(P) and the voltage(U) within its vicinity [PF (P, U)]. On the other hand, this approach imposes higher upstream transformer loading compared with the other techniques in [58] such as Q(U) and PF(P). Normally, the P(U) control is limited by the VA rating of the PVDG GTI; however, in reality, the PVDG output power fluctuates and could exceed its VA rating. According to Collins *et al.* [59], instantaneous fluctuating PVDG power can be employed to monitor the VA rating of PVDG GTI by utilizing dynamic maximum reference as a control technique for P(U) control along with the Q(U) to alleviate the voltage fluctuation for an Australian long rural MV feeder network. Nevertheless, such an approach comes with higher curtailment losses, which must be

considered, even if the methodology performs well in alleviating resultant voltage fluctuations. In the work of Liu *et al.* [60], local linear control is investigated to substitute the real power into reactive power when the output power fluctuates thereby mitigating any voltage fluctuation. There, they investigated methods of selecting the control parameter through sensitivity minimization and violation optimization. The limitation of such an approach is that there is no valid result if the number of buses in the distribution system is large (i.e., more than five buses).

In a typical European LVDN (three-phase four-wire), the conglomeration connection of single-phase PVDG system (mostly rooftop) and different loads could create an unbalance in the LVDN. This is mainly due to a neutral point shifting of the three-phase voltages occurring while injecting active power and injecting or absorbing reactive power by the PVDG inverter. Exploiting the RPC in such unbalanced network is challenging, yet Weckx *et al*. [61] suggested that by tuning the control parameters optimally, which are grid and time dependent, the local controllers of active and reactive power could potentially reduce the voltage fluctuation without shifting the neutral point of the three-phase voltage. This was achieved by optimal injection or absorption of reactive power in one phase to avoid excessive voltage in other phases. Moreover, as described in R. Caldon *et al.* [62], the operation of Q(U) control, in conjunction with the injection of correction current, mitigates the voltage fluctuation and reconfigures the unbalanced network to a balanced network. Therein, both single-phase and three phase inverters are used to achieve this approach. Thus, the voltage unbalance mitigation procedure in conjunction with the operation of the RPC techniques is equally important to alleviate the voltage fluctuation.

PF(P) control is implemented as a function of PVDG active power, which depends on irradiance and temperature. Whenever high irradiance coincides with high peak demand, the voltage rise may not exceed the overvoltage limitation and the requirement of such a technique will be unnecessary. Furthermore, it regulates all the PVDG GTI participating in the public network irrespective of the voltage profile. The Q(U) controller on the other hand exchanges reactive power when the solar PVDG sources are not the primary source of the voltage fluctuation. Although this method directly uses the instantaneous information of the local voltage, which is a consequence of the PVDG power production, and the activity of the load demand is in its vicinity. Again, Q(U) control may not react to critical voltage fluctuation at the far end feeder when it is embedded to the rooftop PVDG GTI located near the distribution transformer (DT). Furthermore, PF(U) controller also exchanges reactive power when the solar PVDG source is generating active power. From S.B Kjaer *et al.* [63], a stable operation of PF(U) is evaluated in the solar PV inverter. However, the droop control of PF(U) and Q(U) is different as the former uses PF and the latter uses reactive power. However, under equal grid impedances and generation of active power, the two functions can be made to generate an equal amount of reactive power.

Samadi *et al*. [64] also evaluated a different technical aspect of recent German grid code called an active-power-dependent standard characteristic curve, Q(P). There, they utilize the voltage sensitivity matrix to calculate the exact required reactive power in each node. A strategy to support grid stability in the event of frequency–voltage variation was reported in the work of Serban *et al.* [65]. Here, they considered electrical energy storage to extend the existing standards for grid support. However, they have not discussed the extended grid support under internode activity and

contingency disturbances at distribution system level. However, if combinations of coordinating algorithms among the existing voltage control techniques are of any additional advantage has not been addressed in detail [58] and [59]. For this reason, the research objective entitled, "*To investigate the existing autonomous coordinated voltage control techniques of grid-tied PV inverters in alleviating the voltage fluctuation*. " is proposed in section 2.5 Research Objectives.

2.2.2 Short Circuit Level

The maximum short circuit rating at any connection point in the distribution network is specified by the Distribution Code [66] in Ireland. For any new connection, the short circuit studies determine the maximum short circuit level at that connection. In general, protection system planning, and the analysis of fault and pre-fault conditions are standard procedures in determining the circuit breakers rating and setting of the protective relays in the power system. In the case of a distribution network with DG, the fault level is determined by the short-circuit contribution of the upstream grid together with the DG. Further, in the case of medium and low voltage distribution networks, the short-circuit impedance of the HV/MV or MV/LV transformers determines the contribution of the fault current in the upstream grid [67]. Detail analyses on the short circuit level is presented in Appendix B: Short Circuit Analyses.

Usually, the short-circuit impedance of such transformers are selected as low as possible to enhance the voltage regulation and the general power quality of the distribution network [67].From A. Ballanti *et al*. [68], the influence of higher DG concentration in LV network towards MV distribution network was reported. There are

two important reasons that could potentially cause deterioration due to further penetration of PVDG in MV networks. Firstly, most of the short circuit capacity of the MV network is close to its design fault level, that leaves small margin for acceptable deterioration due to further PVDG integration [67] and, secondly, due to higher penetration of PVDG in LVDN, the fault level of the upstream grid may increase which may directly impacts the protection and switch gear equipment [69]. For these reasons, as a thumb rule, fault analysis is mandated before any interconnecting new entrant PVDG in the distribution network. Both symmetrical and unsymmetrical fault analysis are equally important, but the initial study always begins with symmetrical fault analyses. Usually, the distribution system engineer provides the fault level at the connection point and the X/R ratio of the source impedance before connecting any DG.

PVDGs are integrated into the electrical distribution network through power electronic (PE) converters. But such PE converters lack inertia due to the absence of rotating mass. It does not respond in a manner similar to synchronous or asynchronous based DG in carrying the fault current based on electro-magnetic characteristics. Above all, PE converters have the flexibility in controlling the response time during fault conditions. Yet, different control techniques of PE converter such as voltage control and current control techniques may affect the fault contribution differently. For instance, according to M.E. Baran *et al.* [70] the fault contribution is higher during the transient period of the first 5–10 cycles when the control technique of a PE converter is based on voltage control. Meticulous analysis of the fault level before anticipating any number of PVDGs within the LVDN is one of the most important planning procedures. Through such planning procedure, the necessary rating of the interrupting devices and setting of the protection relays can be configured for stable operation during any

contingencies. IEC Standard 60909 provides extensive short circuit analysis. Further application of this standard in fault level studies of MV and LV radial distribution networks in the presence of DG was reported in [67].

2.2.3 Network Losses

The risk of component overload and the losses in the grid are both related to the RMS value of the current. The risk of overload is related to the highest values of the current, whereas the losses depend on all values, but with higher values contributing more than smaller values [71]. Most PVDGs are connected in the vicinity of the load consumption. As a result, the power flow from the upstream network is reduced, which ideally lowers the component loading and the losses in the feeder. This allows for extra capacity of the feeder to host additional PVDGs. A certain amount of the PVDG integration could reduce the risk of overloading at the higher voltage levels and feeder losses. The feeder characteristics, the rating of PVDGs along with its production profile and the diversified load consumption pattern allow for the detail study of the impacts of component overloading and feeder losses due to PVDG integration. In distribution networks, most of the network losses are load-dependent i.e. occur due to line copper losses (I^2R) [72]. Thus, any associated loss reduction cost will be a quadratic function of the network user's contribution towards the line current. Another characteristic of the distribution network is that it has a higher resistive component (R) than the reactive component (X) i.e. $R/X >> 1$. Quezada *et.al* in [73] claimed the consensus idea of DG improving the network losses is not always true. In that paper, it presents an approach to compute annual energy losses variations when different penetration and concentration levels of different DGs are connected to a distribution network. Finally, the paper recommends that DG units with reactive power control provide a better

network voltage profile and lower losses. In particular for PV study, A.G. Marinopolous *et al.* [74] proposes a new correlation index that connects the sizing and the siting of a PV unit with the respective impact on Joule losses of a radial distribution feeder. Through this index, the DSO can evaluate the contribution of a new PV unit interconnection to the annual Joule losses of a line beforehand, and thus perform a better cost allocation.

2.3 Economic Impacts

Renewable non-firm distributed generation (DG) integration in the low voltage distribution network (LVDN) is inevitable if the EU 20-20-20 targets are to be achieved [75]. Statistically, accommodating such non-frim DG in the LVDN presents both technical and economic challenges to the distribution system operators (DSOs). The Council of European Energy Regulators (CEER) [76] discusses a methodology to define the future core role of the DSOs into three categories, which are i) core regulated activity ii) activity allowed under conditions and with justification and, iii) not allowed, competitive non-DSO activity. To foster such roles, incentivising DSOs for the anticipated activities are much needed to meet the EU 20-20-20 goal [28]. On the other hand, DSOs are regulated companies where the revenues are remunerated from a regulated tariff set by the national regulatory authorities (NRA).

Regulation authorities estimate DSO's allowed revenues primarily based on their operational cost, depreciation, the rate of return on their assets, capital expenditure on network expansion and additional fair profit [77]. As per A.Picciariello *et al.* [31], the regulated DSO's capital and operational aspects are shown in Figure 2.1. Herein, both

capital and operational revenues are regenerated from the regulated tariff which is then passed to the end customers.

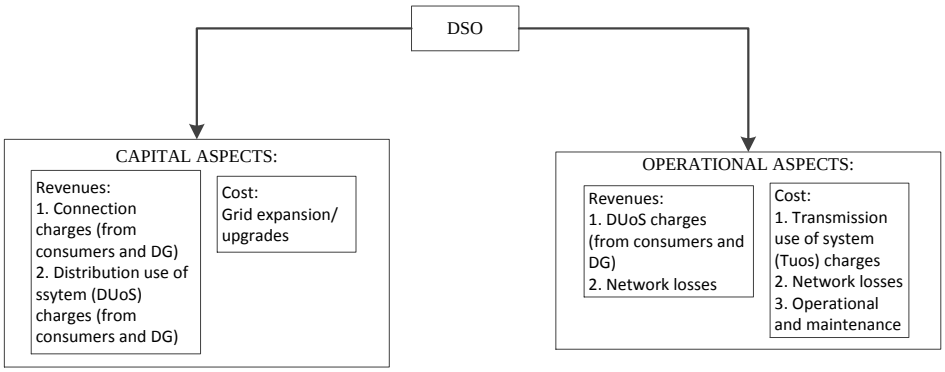

Figure 2.1 : Overview of DSOs revenues and expenditures

In practice, the electric grid is defined by high fixed costs and low variable costs [78]. Until now, the regulated distribution network tariffs imposed on the residential consumers of LVDN are largely based on the volume of energy consumed i.e. kWh for a predefined period of one or two months [79]. On the other hand, the associated infrastructure and network expansion costs are levied as flat charges to all the network users. In principle, the cost of the network depends on the topology and capacity of the given network. But the influence of adopting volumetric tariff may likely offset the exact cost incurred in facilitating the network to all the users [30].

The transition towards energy efficient and low carbon targets may drastically change the normal electricity consumption pattern which may reduce the volume of energy consumed by the individual consumers. Such reduction in volumetric energy may impact the DSO in balancing their incurred cost and returned revenue if the adopted tariff is based on the volumetric charges [30]. Above all, the situation will be highly severe if more network users defer the on-peak demand charges (usually at daytime) by their own embedded generation. This means that their overall volumetric

electricity bill will be even lower. Interestingly, the unmanaged heat pumps and electric vehicles will result in higher energy consumption resulting in revenue uncertainty to the DSO's business [30]. Besides, the volumetric tariff does not incentivise the network users in shifting their peak demand or limiting their peak consumption. Undoubtedly, as a higher number of network users change their normal consumption pattern due to the above-discussed reasons, special attention needs to focus on understanding how to sustain stable revenue with fair marginal profit for the DSO in providing their core network services. In fact, the network grid is a shared infrastructure where the cost incurred in providing the network service to one user depends on the services provided to other users and their approaches to network utilisation [78]. Further concerning issues would arise in sharing the network cost among various network users from the benefits they receive from the network or the cost they levied to the DSO. But the challenge is in identifying how much each network users would cost for their network usage.

The practice of net metering allows the PVDG installed consumer (prosumer) to pay only the distribution charges for the volume of energy consumed during the unavailability of their self-generated power. This will certainly reduce the electricity bill primarily because of the reduction in volumetric distribution charges [80]. At present, most of the prosumers receive two incentives: one from reduced electricity bills because of net-metering combined with volumetric charges and the other from a feed-in-tariff from selling their self-generated electricity. To sustain stable revenue, the DSO may increase the charges per kWh consumed by the network users (both consumer and prosumer) to balance the reduced charges from net-metering. Conversely, the normal consumers will end up paying the increase charges because of

prosumer activity leading to cross subsidisation between normal consumers and prosumers. To overcome such cross subsidisation and recovery of distribution cost, some countries (Spain and Germany) adopted a solution called “self-consumption fee” [80]. Yet, such a solution discourages PV development. Above all, to overcome cross-subsidising between different customers and to recover DSOs network services, DG may charge the cost incurred in the connection fee, distribution-use-of-system (DUoS) and losses in distribution network due to its presence [81].

The regulatory impact on the incentive for DG integration for DSO was thoroughly studied by Picciariello.A *et.al* in [31] and it was concluded that the requirement for new regulatory strategies to hedge against potential DSO disincentives to integrate DG is essential. Above all, under high penetration of DG in LVDN, the current practice of volumetric charges in conjunction with net-metering is likely to cross subsidise the normal customers and the prosumers or DG installed customers [80]. Recently, CEER [82] highlighted the guidelines of good practice for network tariff in the presence of intermittent DG in the LVDN.

The critical technical impacts due to high penetration of photovoltaic distributed generation (PVDG) in the LVDN are voltage fluctuation, thermal/network losses and increase in short circuit current [83]. Such impact studies on utilities are essential during the early stage of PVDG integration if the regulatory policy has to consider a higher non-firm DG share. Such impact studies were reported in M.A.Akbari *et al.* [84] and A.Navarro *et al.* [85]. But correlating the uncertain impact metrics with the DSO revenue was not discussed to this end. To address this, the research objective entitled,

"*To study the impact of net metering in conjunction with the volumetric tariff structure on DSO's* revenue " is proposed in section 2.5 Research Objectives

2.3.1 Network Tariff Structure

Regulatory bodies supervise the fundamental design of the electricity tariffs where the DSOs are remunerated for their incurred network cost along with the fair profit from the network users. In principle, the regulatory body provides consensus guidelines in designing the network tariff. As per EU directives[1], the ratemaking principle can be classified into three prominent principles which are also discussed in A.Picciariello *et al.* [78] and J.Reneses *et al.* [86]. They are:

i. Sustainability principles

a. Guaranteed universal access to electricity to all the network users.

b. The entire cost recovery from the incurred cost of the network services.

ii. Economic efficiency principles

a. Productivity efficiency is the least cost imposed to the network users for the network services provided by DSO.

b. Allocation efficiency is the cost imposed on the network users per how much they value the service they receive

c. Cost Causality is the type of charge that accurately accounts how much each network user contributes to the network costs.

d. Equity charge is the method of charging the same customer for the usage of the same services.

[1] All EU countries must comply with the Directives 2003/54/EC for electricity tariff ratemaking accounting primarily the non-discriminatory and cost-reflective approach.

iii. Customer protection principles

a. Transparency avails all the network users of the methods and results of the allocated network tariff through their respective electricity bills

b. Simplicity accredits the methods and the results from the allocated network tariff should be simple enough to understand by every network user.

c. Stability means reducing any regulatory uncertainty through stable short-term network tariff and gradual changes towards long term network tariffing.

DSOs are inherently natural monopolies and therefore their revenues and business are supervised by the NRA (National Regulatory Authority). NRAs estimate their allowed revenues primarily based on their operational cost, depreciation, the rate of return on their assets, capital expenditure on network expansion and additional fair profit. A report from EDSO in [87] highlights different network tariffs depending on the geography, time of use, fixed and variable elements, payment liability, type of service and type of consumer. With respective to the low voltage distribution network (LVDN), the EURELECTRIC in [79], [88] and Picciariello *et al.* [78] suggest three network tariffing structures. They are fixed, volumetric and capacity charges respectively.

i. Fixed charge *(price/period)*: Fundamentally, the electric grid is defined by high fixed costs and low variable costs [78]. The long-run cost of operating the distribution grid is allocated mostly as a fixed charge [79]. This cost includes network losses, network peak demand and connection cost. Such cost does not reflect the electricity consumption or any cost causality.

ii. *Volumetric charge (price/kWh/period)*: The distribution network tariffs in LVDN are mainly based on the volumetric tariff to cover the variable cost incurred while transporting the electrical energy [79]. But, the volumetric charges could vary depending on the time of the day within the month and could incur charge as a flat tariff or as a time-of-use with different pricing depending on the on and off peak periods [88]. It is highly adopted in LVDN because the tariff structure is simple, affordable for small users and sufficient to provide DSO's CAPEX and OPEX charges. But such charges are not the most cost reflective because the network transportation cost is mostly capacity based.

iii. Capacity charges (price/kW/period): Capacity charges imposed on the maximum power used during a certain period for an instance during the on-peak period. It could cover flat, variable and time-of-use charges respectively [87], [88]. They are briefly discussed below:

a. *Flat*: Typical capacity and charges are fixed equally for all the network users and imposed per the meter reading.

b. *Variable*: Contract based different capacity charges for each network user. With the advent of smart meters, the more observed maximum capacity charge can be billed to the low voltage consumer in contrast to their contracted capacity charge.

c. *Time-Of-Use*: Variable charges which depend on the time of use. This tariffing structure requires smart meter for bilateral communication.

2.4 Connection Guidelines and Methodologies

In the UK and the Republic of Ireland , the guidelines for renewable DG connection are provided by the Energy Networks Association (ENA) in [89] and Electricity Supply

Board (ESB) in [90] respectively. Both these two guidelines adopt the European Norm (EN) 50438[2] standard which entails the requirements for micro-generation plants to be connected in parallel with public low voltage distribution networks [91]. In the UK, as per ER G83/2[3] guidelines, up to and including 16 Amperes per phase connection in low voltage distribution for small scale generations are set as a mandatory requirement. Similarly, in the Republic of Ireland, the micro-generation can be connected either in single phase or three phases. According to conditions governing the connection and operation of micro-generation set by ESB in [90], single phase micro-generation connection up to and including 25 Amperes (main fuse) in low voltage of nominal 230 V is the requirement. Again, for three phase connections, a micro-generation unit up to and including 16 Amperes at low voltage of nominal 230/400 V is permitted. Connection guidelines for other European countries are provided in EN 50438. However, different connection policies, charges and methodologies have been employed to date and are discussed briefly in the following paragraphs.

2.4.1 Connection Policy and Charges

Primarily renewable DGs are connected into two categories of voltage levels. They are a) medium and high voltage in sub-transmission and transmission level respectively and, b) low voltage at distribution level. The large-scale renewable based power plants (LSRPP) are usually connected to a higher voltage and their presence in the sub-transmission and transmission level is quite noticeable [3]. The LSRPP has also a better steady state voltage profile and power quality. Also, LSRPP has higher connection charges as compared to DG in distribution level [81]. Medium and high voltage

[2] EN 50438 is superseded by EN 50549 -1 as per Requirements for Generations.
[3] ER G83 is superseded by EREC G98

customers are usually mandated with the capacity type of tariff[4] which is either time-of-use or contract based [79]. LSRPP could be subjected to a capacity tariff which includes explicitly the connection fee and use of the system charges.

In a regulated distribution business, the third party open access allows all customers to access transparently and unbiasedly the electrical distribution network for purchase and sale of energy [77]. Respective network cost incurred while providing such facilities by the network operators are imposed to the network users through the regulated network charges. Traditionally, connection charges are paid one time, whereas use-of-system charges are paid periodically to cover the total network utilisation cost during the regulated period. The connection charges of DGs in LVDN are relatively lower than the LSRPP [81]. Generally, DG connection charges are divided into shallow and deep charges [81], [92]. In general, the connection charges to the distribution network are the same for all the network users connected at the same voltage level. Particularly, in LVDN, the connection charges of DG could differ depending on the location and time of connection. This is called 'connection policy', which provides two distinctive types of connection charges [81], [86] and are given in the following points.

i. *Shallow charges*: These are the charges incurred to connect the DG to the nearest distribution network. The DG installed customers contribute to such a grid service connection. Shallow charges exclude any reinforcement cost that might occur during DG integration to the network. Instead, these incurred costs are reflected as use-of-system charges or deep charges.

[4] Capacity tariff: Maximum amount of energy that can be withdrawn or feed in at the connection point at any given time (measured in watt).

ii. *Deep Charges*: On the other hand, in a saturated LVDN, any new DG connection may exceed the network acceptable deterioration level. Under such a condition, the DG owner may impose deep connection charges to improve the network DG hosting level. The deep connection charges comprise of a service connection and relevant upstream grid reinforcements in supplying the contracted capacity. For instance, the connection of the new entrant DG may increase the short circuit level of the distribution network which may result in replacing the protection and switchgear at the upstream voltage level. It may also entail enlarging a substation, reinforcing a line and replacing other distribution operation and control equipment. If the new entrant DG owner is required to pay such high deep connection charges, then it may likely hinder further integration of DG into a saturated LVDN system. Such increases in short circuit level is due to the contribution of all the DGs present in the network. In the case of DG proliferation in LVDN, socialising the relevant reinforcement cost will discourage cross-subsidizing between the DG owners and encourages the higher integration of DGs. Through this approach, the network operator's investment can be recovered through use-of-system charges rather than the connection fee. With respect to large DG connected at MV and HV level, the discussed approach may be exception.

2.4.2 Connection Methodology

Traditionally, the technical issues are assessed by the network operators for the connection of new entrant DG installations. This approach is usually termed as 'first-come-first-served' and could potentially sterilize or saturate part or all of the distribution network from further new entrant DG integration [93]. This usually happens due to poor siting of DG resulting in early sterilization (i.e. restricting from further development of DG due to technical constraints) of the network. Network

reinforcement could alleviate such a situation with extra expenses. But such approaches require planning and time, leading to uncertainty. The ideal approach is to leverage the existing network infrastructure to assess the maximum DG integration that will not exceed the acceptable deterioration limit of the network. This requires methodologies such as long-term planning to optimally assess the maximum capacity of DG. For DG connection in transmission and sub-transmission network, studies in [94]–[96] performed optimal power flow in determining the optimum capacity limitation. In the case of LVDN, due to its inherent heterogeneous characteristic, the methodologies described above cannot be applied. Eurelectric in [97] commented that there is no one-size-fits-all solution because distribution networks are rather heterogeneous in terms of grid equipment and DG density at different voltage levels. Every distribution network should be assessed individually in terms of its network structure (e.g. customers and connected generators) and public infrastructures (e.g. load and population density).

There exist different methodologies to connect DGs which require different levels of effort and innovation such as advanced design and planning, monitoring and management tools. As the level and the diversity of effort and innovation increases, the level of DGs capacity will increase proportionately. This progressive evolution is shown in Figure 2.2 where, the evolution of more dynamic and advanced distribution systems will evolve from i) passive network via ii) reactive network integration to iii) active network integration.

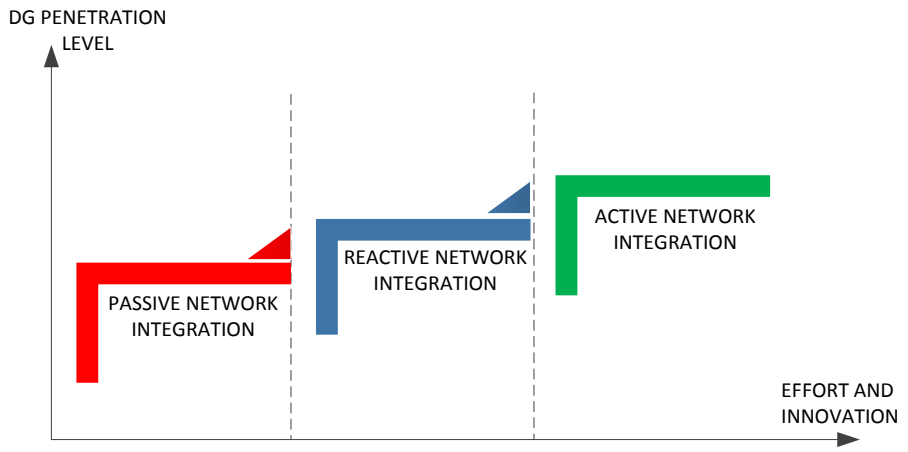

Figure 2.2 : Three-Step Evolution of Distribution Systems [97]

i. *Passive network integration*: This approach adopts the traditional development strategy 'fit and forget' for DG integration by resolving all the issues in the planning stage such as voltage control, transformer tap setting, protection plan, etc. Such an approach allows all the connected DG to integrate into the grid with full rated capacity or firm grid connection mode. DSOs only intervene if there are any contingencies within the LVDN or the entire power system. During such scenarios DGs are disconnected until the entire system is restored to its normal operating state.

   a. Advantage: Low flexibility in monitoring, controlling and managing which is necessary during network operation.

   b. Disadvantages: Such an approach may lead to over-sizing of the LVDN and subsequently sterilizing the network when the density of DG integration increases. Passive integration requires network reinforcement to accommodate higher density of DG integration, making this approach less economical.

ii. *Reactive network integration*: This approach adopts a strategic, operational methodology where any contingency issues (such as congestion, voltage violation, etc.) in LVDN due to DG integration are resolved during the operational stage. It

motivates the consideration of as much as DG integration at the planning stage as possible with less restriction in a non-firm grid connection mode. Some countries with a high density of DG integration have already adopted such an approach. Due to inappropriate planning of rooftop-PV integration, high curtailment of PV feed in power may occur. It ultimately hampers the remuneration periods for the subsidies and incentives from government and regulatory bodies.

a. Advantage: More flexible control of DG under any contingencies such as reactive and active power control, better coordination between load and DG; DG and OLTC (on-load-tap-changer) / LDC (line drop compensator). Allows higher integration of DG than passive integration.

b. Disadvantage: This approach could restrict many hours per years of DG injections (i.e. DG curtailment) leading to loss of business if proper restriction fees are not paid. Due to lack of optimal integration practice in the planning stage, such an approach could sterilize a portion of the network making to new DG interconnection challenging. One example is the poor siting of DG leading to limitations in further DG accommodation in the network. Such an approach could potentially defer new DG integration until network reinforcement is completed, again, making this approach unfavourable for long term planning.

iii. *Active network integration*: The traditional passive and reactive DG integration seeks to mitigate any technical challenges through prompt responses such as through DG disconnection or curtailment of DG feed-in power. The active network integration optimally interacts between planning, access, connection and operation to improve DGs hosting capacity as non-firm DG integration. Some of the active integration enablers are the current technology in network observation and control along with the advancement in data analysis and ICT (information, communication

and technology). Active integration foresees the optimum flexibility of LVDN to accommodate higher DGs by deferring the network sterilization in a secure, reliable and the most economical way. The network reinforcement could be deferred until the moment when it becomes more cost-effective than the on-going cost of procuring services from DGs. However, active network integration often challenges the system planner and the regulator in particular. For instance, active network integration requires a detailed planning procedure that requires a large amount of input parameters. Such input parameters could be the exhaustive studies of the likely impacts due to increased PVDG integration. Temporal and spatial characteristics are often associated with such exhaustive impact studies. Later, the execution of these planned solutions through an operational procedure in the control stage could encounter further uncertain difficulties. After observing such likely impacts, further active planning procedure includes optimization techniques as per the suggestion from the IEEE task force on DG planning and optimization [17]. Compounding with the intermittent nature of solar and the uncertainty of DSO's investment and revenue, an active integration methodology of PVDG in LVDN could be a challenging task in fulfilling concurrent objectives such as decarbonisation and sustainability of network operators' business. Acknowledging such primary challenges are the key motivations of this research.

2.4.3 Active planning approach

Currently, most PVDGs are integrated either in passive or reactive approach. Both passive and reactive integration approaches suffer potential deterioration of the LVDN and subsequently create the requirement of oversizing the LVDN [97]. Again, the reactive integration approach may have resolved some of the critical issues at the

operational stage, but difficulties persist in coping with the curtailment of energy from PVDG and the associated network losses. To overcome such potential deterioration of the network, an active planning approach can be envisaged for the given specific network. Such active planning approaches include an exhaustive assessment of the risk associated with increased integration of PVDG in the LVDN. Increasing integration of non-firm single phase PVDG in LVDN may degrade the power quality of supply, possibly beyond general limits [3].

Notably, the increased integration of PVDG impact the level of transients due to large current variations, on observed voltage fluctuation due to intermittent sources as seen in [83], on phase unbalance due to dispersed integration of single phase PVDG and on voltage sags due to increased short circuit currents [98]. According to M. Bollen *et al.* [3], there are two types of power quality (PQ) impact metrics which are distinguished by the method of measurement. They are i) PQ variations which are recorded at predefined instants and ii) incidents triggering cascaded PQ events in the network. These two PQ impact metrics can be further categorised into two PQ indices as described in [98], namely site and system indices. For each index and for each PQ impact metric, the risk associated with integrating large numbers of dispersed PV generations can be assessed [99].

The PQ variations are small variations in voltage and current waveforms which primarily occur in the normal operating condition of the power system [3], [98]. For instance, PQ variations include long and short voltage fluctuations, unbalances and harmonics. Accumulated PQ variations could lead to premature aging of the LVDN assets such as transformer insulation, tap changers etc. as seen in [100], whereas very

high levels of variation may lead to equipment failure [101]. The PQ events are characterised by large and sudden deviations from the normal voltage waveform. Voltage sags and transients are known PQ events [100]. Further PQ events can be classified into normal which are expected events and abnormal events [3]. Normal events are due to power system switching occurrence during transformer and capacitor energisation. Abnormal events are more concerned with the integration of distributed generation such as PVDG. For instance, short circuits and earth faults are considered as abnormal events. About 70% of the faults in a distribution network are unsymmetrical single to line ground (SLG) faults and is considered one of high risked abnormal events [102]. Such abnormal events lead to severe voltage sags [100]. Under such abnormal events, large reactive power flows are required during voltage recovery after the faults. But this requirement of large reactive power may lead to high inrush current from the capacitance which may lead to blowing of the fuses or other sensitive power electronic components [100]. Voltage sag is a multi-dimensional phenomenon that includes measuring voltage sag and detecting them [103].

The need for probabilistic studies in determining the impact of PV generation in LV networks was highlighted in M. Bollen *et al.* [3] and A.Keane *et al.* [17]. A report from EPRI [27] recommends a stochastic approach in determining the PV hosting capacity in a distribution network. The stochasticity was mainly on the position and size of the PV generation while the steady state impact was performed deterministically i.e., considering worst case scenarios such as maximum recorded PV generation with minimum recorded load profiles. As specified by M. Bollen *et al.*[3], the long-term measurement data is valuable in determining the steady state impact in a power distribution feeder. Further, EN 50160 in [104] presents the voltage characteristic in a

probabilistic manner such as the 95% level over a given time, the voltage magnitude should be within a given limit.

Above all, a specific customer with a PV installed may not coincide with the worst-case scenarios. Consideration of worst-case scenarios may strictly restrict the estimated PV hosting capacity. For this reason, a combination in stochasticity of the PV location, size, and generation profiles together with the demand load profiles will represent a probabilistic scenario-based study. A similar study was reported in A. Navarro *et al.* [85] where the authors performed probabilistic impact assessment from the low carbon technologies in an LV distribution system. Therein, the authors leverage Monte-Carlo simulation. Along the same vein, Klonari *et al*. [105] utilizes smart meter data to performed probabilistic estimation of PV hosting capacity. But A. Navarro *et al.* [85] considered only voltage variation due to varying PV generation as a PQ impact study.

A probabilistic power flow analysis was studied by Z.Ren *et al.* [106] where the probability distributions of power flow responses are estimated using a non-parametric fixed bandwidth kernel density estimation. The choice of bandwidth highly influences the kernel density estimation as seen in [107] and therefore, the choice of constant bandwidth may not represent an appropriate probability distribution for power system responses. A new probabilistic technical impact assessment was studied by M.A. Akbari *et al.* [84]. But, M.A. Akbari *et al.* [84] again lacks the stochasticity in the peak PV generation value and profile together with PVDG location. A Monte-Carlo based PV hosting capacity was reported in A.Dubey *et al.* [108] but considers the hourly stochastic analysis of PV and load profile by taking the time periods of the day when PV generation is likely to be high. Further, A.Dubey *et al.* [108] lacks the temporal and

spatial characteristic of both PV generation and load demand profiles. Consideration of the high amount of PVDG integration in an existing LVDN requires statistical information on its impact on the operation of a power system. The distribution network is highly dispersed and diverse and often characterised as a heterogeneous system [97]. To discuss the statistical analyses for active planning approach, the research objective entitled, "*To investigate statistically the impacts due to increased integration of PVDG in the existing distribution network* " is proposed in section 2.5 Research Objectives

2.5 Research Objectives

The main aim of this research is to investigate the active planning and operation of increased PVDG integration in LVDN through steady state power system analysis. To address this aim, three research objectives will be discussed in detail in this thesis which were proposed earlier in sub-section 1.3 Aim of the Research. In brief, they are the methodology in quantifying the steady state technical impacts, the impacts of the existing regulatory policies towards the distribution system operator (DSO) revenue and measures to alleviate the voltage fluctuation.

1. ***To investigate statistically the impacts due to increased integration of PVDG in the existing distribution network***

The need of an active planning approach discussed in section 2.4.3 Active planning approach presents that the temporal and spatial characteristics of both load demand and PV generation profiles are important to perform a stochastic random process study through a Monte-Carlo simulation. The objective is to quantify the likely impacts of the operation of the power system by considering two PQ impact metrics namely PQ variations and PQ events which are further assessed in terms of two PQ indices, namely site and system indices. Chapter 3 presents the detail study of this aim.

2. ***To study the impact of net-metering in conjunction with the volumetric tariff structure towards DSO's revenue***

Referring to the literature review of sub-section 2.3 Economic Impacts, correlating the uncertain impact metrics with the DSO revenue was not discussed to this end. The objectives of this research are i) to analyse the uncertain impacts of higher penetration of PVDG on DSO core activity, and ii) to evaluate the potential revenue of the DSOs in the presence of PVDG. For this specific study, operational aspects considered are PVDG impacts on i) network losses ii) voltage fluctuation and, iii) transformer loading. Chapter 4 investigates into these objectives in greater details.

3. ***To investigate the existing autonomous coordinated voltage control techniques of grid-tied PV inverter in alleviating the voltage fluctuation.***

From the literature review of sub-section 2.2.1 Voltage Fluctuation, the combinations of coordinating algorithms among the existing voltage control techniques are of any additional advantage has not been addressed in detail. The objective of this research is to enhance PVDG penetration by combating critical voltage fluctuation with the help of combining a few coordinating algorithms. The importance of this research will lie in implementing two different algorithms in a real suburban Dublin LVDN without exceeding the VA rating of the converters. PF, node voltage (U), and active power (P) are the three critical pieces of information for each node. The realisation of such coordinating algorithms is discussed in depth in Chapter 5.

Chapter 3

Probabilistic approach in quantifying the steady impacts

This chapter discusses the probabilistic approach in quantifying the steady state impacts by analysing risk assessment of power quality variations and events that may arise due to high photovoltaic distributed generation (PVDG) integration in a low-voltage distribution network (LVDN). Due to the spatial and temporal behaviour of PV generation and load demand, such an assessment is vital before integrating PVDG at the existing load buses. Two power quality (PQ) variations such as voltage magnitude variation and phase unbalance together with a PQ abnormal event i.e. voltage sag due to random SLG (single line to ground) faults are considered as the PQ impact metrics. These PQ impact metrics are assessed in terms of two PQ indices, namely site and system indices. In this work, the temporal and spatial characteristics of both load demand and PV generation profiles are leveraged to perform a stochastic random process study through a Monte-Carlo simulation. This aims to quantify the likely impacts of the operation of the power system by considering the two PQ impact metrics. The succeeding aim is to further assess the impact observed from the Monte-Carlo simulation against the extreme-case scenarios. Here the extreme-case scenarios are i) maximum demand with no generation and, ii) no demand with maximum generation. This research work is disseminated as a journal publication[5] which can be

[5] S. Pukhrem, M. Basu, and M. F. Conlon, "Probabilistic Risk Assessment of Power Quality Variations and Events under Temporal and Spatial characteristic of increased PV integration in low voltage distribution networks," IEEE Trans. Power Syst., vol. 33, no. 3, pp. 3246-3254, 2018.

found in List of Publications

This chapter is subdivided into 5 sections. Section 3.1 describes the specification of the distribution network and the assumption made in this work. Section 3.2 summarizes the impact metrics considered. Section 3.3 presents the PQ impact studies. Probabilistic analysis and conclusion are presented in Sections 3.4 and 3.5, respectively.

3.1 Network Description and Assumption

3.1.1 Network Description

The original IEEE European LVDN [109] is considered as a test bed for this study and is shown in Figure 3.1. It has a Dy (delta-star) sub-station transformer of 800 kVA rating and consists of 905 three phase nodes. This distribution network represents a typical 4 wire 3 phase low-voltage distribution network common in European countries. The original test bed had 55 single-phase domestic customers. Out of the 55 customers, phases A, B, and C accommodate 38.2%, 34.5% and 27.3% of the loads respectively [110]. These 55 customers could be potential prosumers i.e. installed with PVDG at their premises.

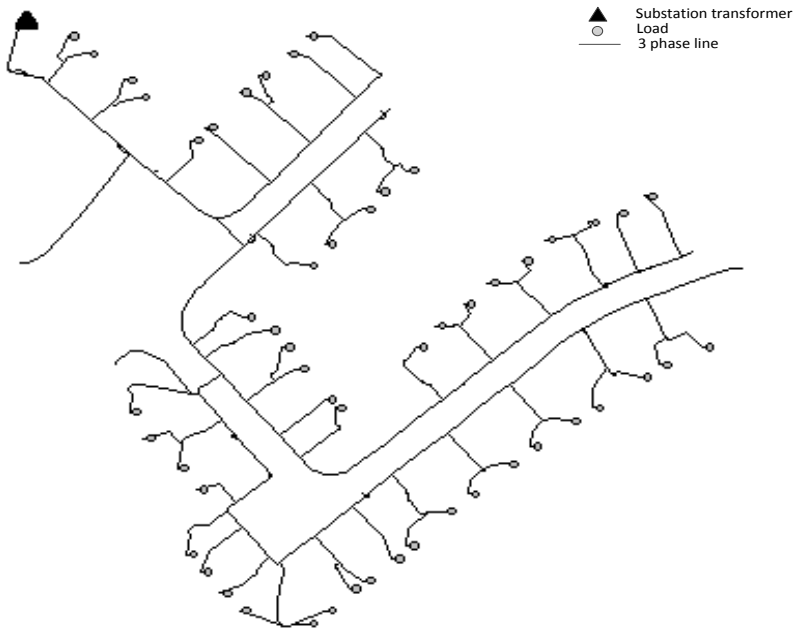

Figure 3.1 : One-line diagram of the European low voltage test feeder

3.1.2 Assumptions

For this study, latitude of UK demographic region is chosen. In order to assess the impacts of solar PVDG in conjunction with seasonal load profile of domestic customer to the LVDN performance, the sunniest month i.e. June and the circa 200 days of seasonal load profiles are chosen. This assumption will assess the impacts of solar PVDG during summer in various seasonal loading of the domestic customer.

From the Whitworth Meteorological Observatory in [111], a 5-minute resolution of 30 sunny days representing the month of June from the year 2015 is considered for the PV generation profiles and is shown in Figure 3.2. As an example, it can be seen from Figure 5, the per unit solar generation at 12 noon on 15th of June is between 0.1 and 0.2, whereas, the per unit solar generation at 12 noon on 11th of June is in between 0.9 and 1.

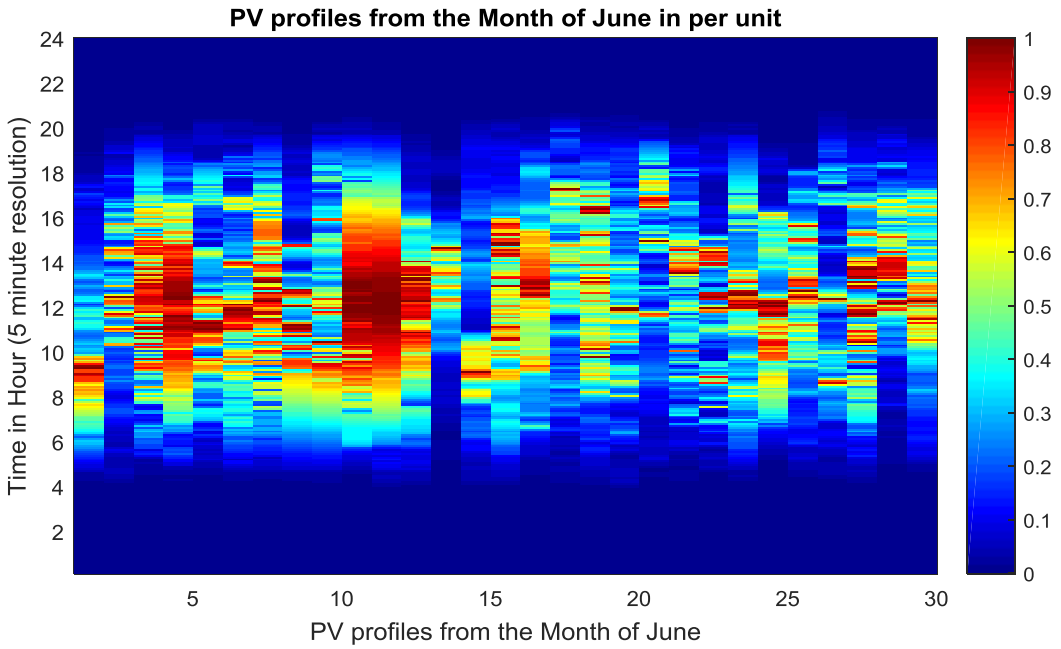

Figure 3.2 :Checkerboard plot of the PV profiles for the month of June 2015 in per unit

Similarly, a pool consisting of 200 load profiles with 5-minute resolution, which reflects the temporal behavior of load consumption pattern from the Low Carbon Technology (LCT) project in [112] is considered as the domestic load profiles and is shown in Figure 3.3. From Figure 3.3, typically it can be seen that the per unit load consumption is between 0–0.3 for the duration between midnight to 3 am. Again, starting from 6 pm until midnight, most of the houses consume more electricity showing a generic load consumption pattern. Each of the 55 customers are assumed to have a 0.95 lagging power factor whereas the PVDG is assumed to export power at unity power factor. The peak PV generation levels are randomly varied between 1 and 5 kW in steps of 1 kW. Similarly, the peak load demands are randomly varied between 1 and 10 kW in steps of 1 kW. The IEEE EU LVDN is characterised by the spatial and temporal behavior of the load demand. Together with the temporal behavior of PV generation, various stochastic scenarios can be analysed. Furthermore, the consideration of randomness in defining the peak PV generation, peak load demand

and location of PV generation provides stochasticity in performing a probabilistic risk assessment. Here, the PV generations are allowed to connect only to the existing load buses i.e., 55 load buses in total. A quasi-time series power flow OpenDSS [16] for every 5 minutes is chosen as the preferred simulation tool. The implementation of the probabilistic study is performed in a co-simulation platform between MATLAB and OpenDSS.

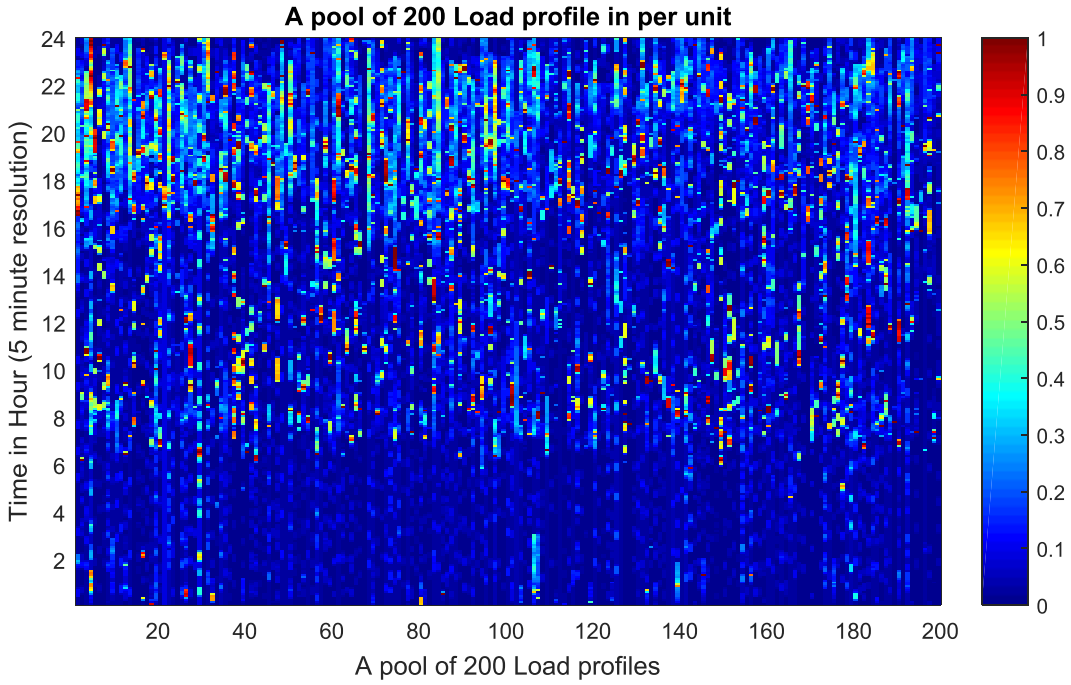

Figure 3.3 : Checkerboard plot of the load demand for the 200 days representing a temporal behaviour in per unit

3.2 Impact Metrics

In this work, overvoltage and voltage unbalance due to the stochastic integration of increased PVDG are considered as PQ variations whereas voltage sag due to random SLG faults is taken as a PQ events. Two PQ indices, namely site and system indices are considered here. The single site index refers to any particular PQ impact metrics at the point of connection of PVDG to the utility grid. The system index refers to a segment or the entire distribution system. Normally, the system index represents a value of a

weighted distribution [98]. In this work, a segment of the distribution network observed by the monitoring device located at the secondary terminal of Dy sub-station transformer is assumed to provide the PQ system indices. Here, the system indices are "special" site indices at the secondary terminal of the Dy sub-station transformer since the chosen system indices are not derived from site indices.

3.3 PQ Impact Studies

3.3.1 Probabilistic Study

For each PQ impact metrics namely variations and events, a probabilistic study considering both temporal and spatial factors is performed. Figure 3.4 represents the Monte Carlo simulation to assess PQ variation metrics. Herein, both PVDG and load demand are characterized by each respective pool of profiles. The location of each load bus is obtained in order to connect new PVDG randomly in the existing load buses. A penetration level, ***n***, is defined at the beginning of the Monte Carlo simulation. So, when the number of PVDG installed customer (prosumer) i.e., N_pv is 11, then penetration level ***n*** is equal to 20%. The penetration level is incremented by 20% up to 100% for every 100 different stochastic scenarios[6] (see the Appendix C: Statistical Analyses). Each stochastic process designated by 'MC' is characterised by re-defining the existing loads and connecting new PVDGs randomly in the existing load buses for each penetration level. In total, there are 500 different stochastic processes. The existing loads are re-defined in two ways, peak load values and load demand profiles. The peak load demand values for each 55 customers are randomly varied from 1 to 10

[6] Appendix C2: Confidence intervals and level

kW and has a rectangular/normal distribution [101]. Similarly, the corresponding load demand profile is randomly selected from the pool of 200 load profiles and also has a rectangular distribution. The rectangular distribution is defined by its probability density function (pdf) ‘f(x)’ and has a uniform value between the lower bound ‘a’ and the upper bound ‘b’. The pdf is given by.

$$f(x)= \frac{1}{b- a} \tag{3.1}$$

$$\text{where } a \leq x \leq b$$

The connection of new PVDG is allowed only to the buses where loads already exist in the LVDN. For each penetration level ‘n’, the customer (prosumer) that wishes to install PVDG is determined by ‘N_pv’ permutation of total load buses i.e., ‘L’ through an ordered sampling without replacement [113]. This type of sampling is designated by ‘$P^{L}_{N\_pv}$ ’, and is given by

$$P^{L}_{N\_pv} = L* (L-1) * \ldots.* (L-N\_pv+1) \tag{3.2}$$

where,

L = Total load buses

N_pv = No. of prosumers

$P^{L}_{N\_pv}$ = Permutation without replacement

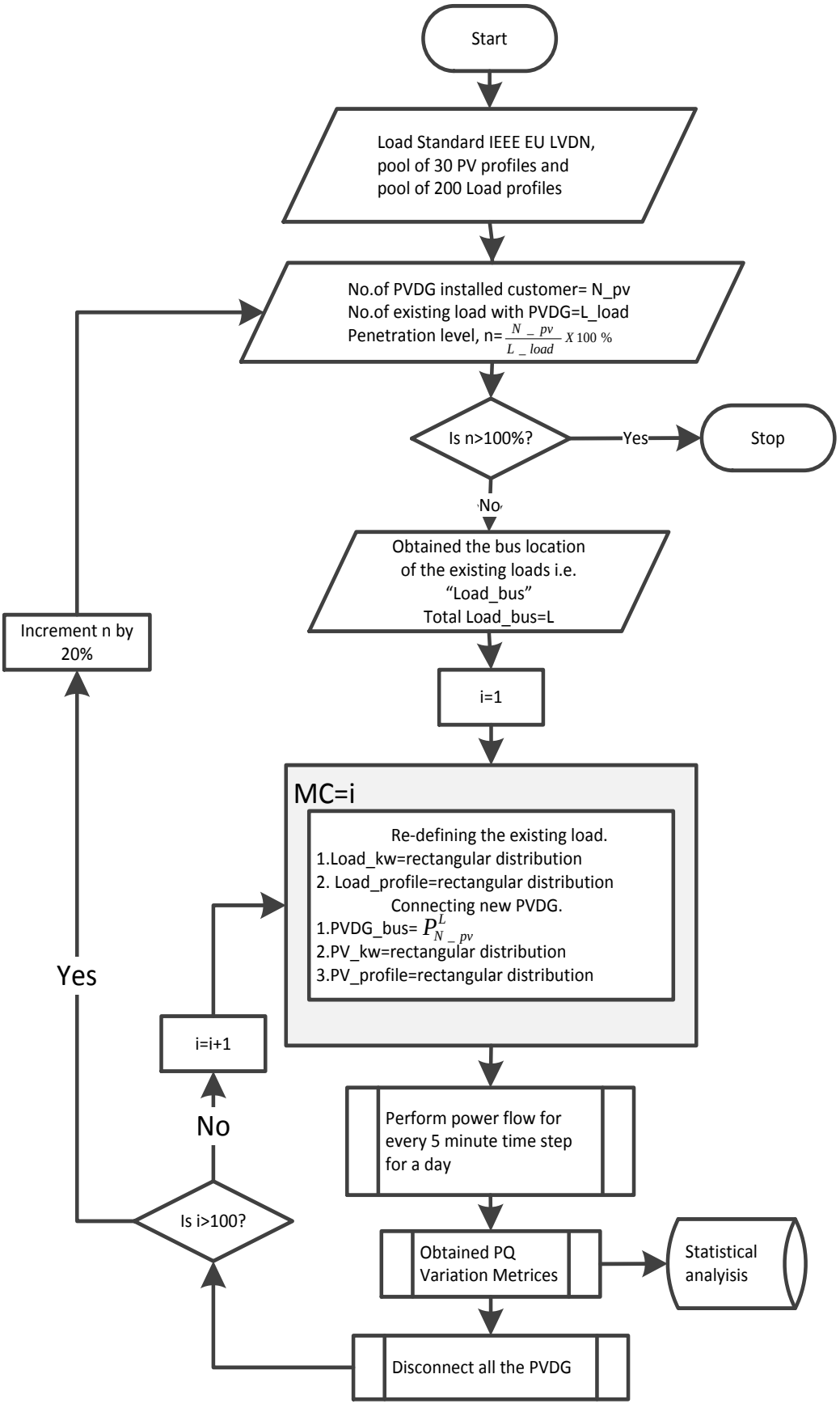

Figure 3.4 : Monte-Carlo simulation to assess PQ Variation Metrics

The peak PVDG generation ('PV_kW') values randomly vary from 1 to 5 kW and have a rectangular distribution given by (3.1). Similarly, the corresponding PVDG generation profile is randomly selected from the pool of 30 PV profiles and has a rectangular distribution. A phasor mode power flow is solved in OpenDSS for every 5 minutes through the MATLAB COM[7] interface. Finally, the PQ variation metrics are obtained from the power flow for further statistical analyses. Before proceeding to the next Monte-Carlo simulation, i.e., when MC = i + 1, all the installed PVDGs are disconnected and the same process of re-defining and connecting new PVDG in the LVDN is repeated. The EN 50160 in [104] is adopted to measure the voltage magnitude variation i.e., the voltage magnitude should be within ±10% of the nominal voltage for 95% of a defined period (typically one week) and voltage unbalance i.e., the unbalance should be less than 2% for 95% of a defined period (typically one week).

[7] Appendix D: COM Interface between MATLAB and OpenDSS

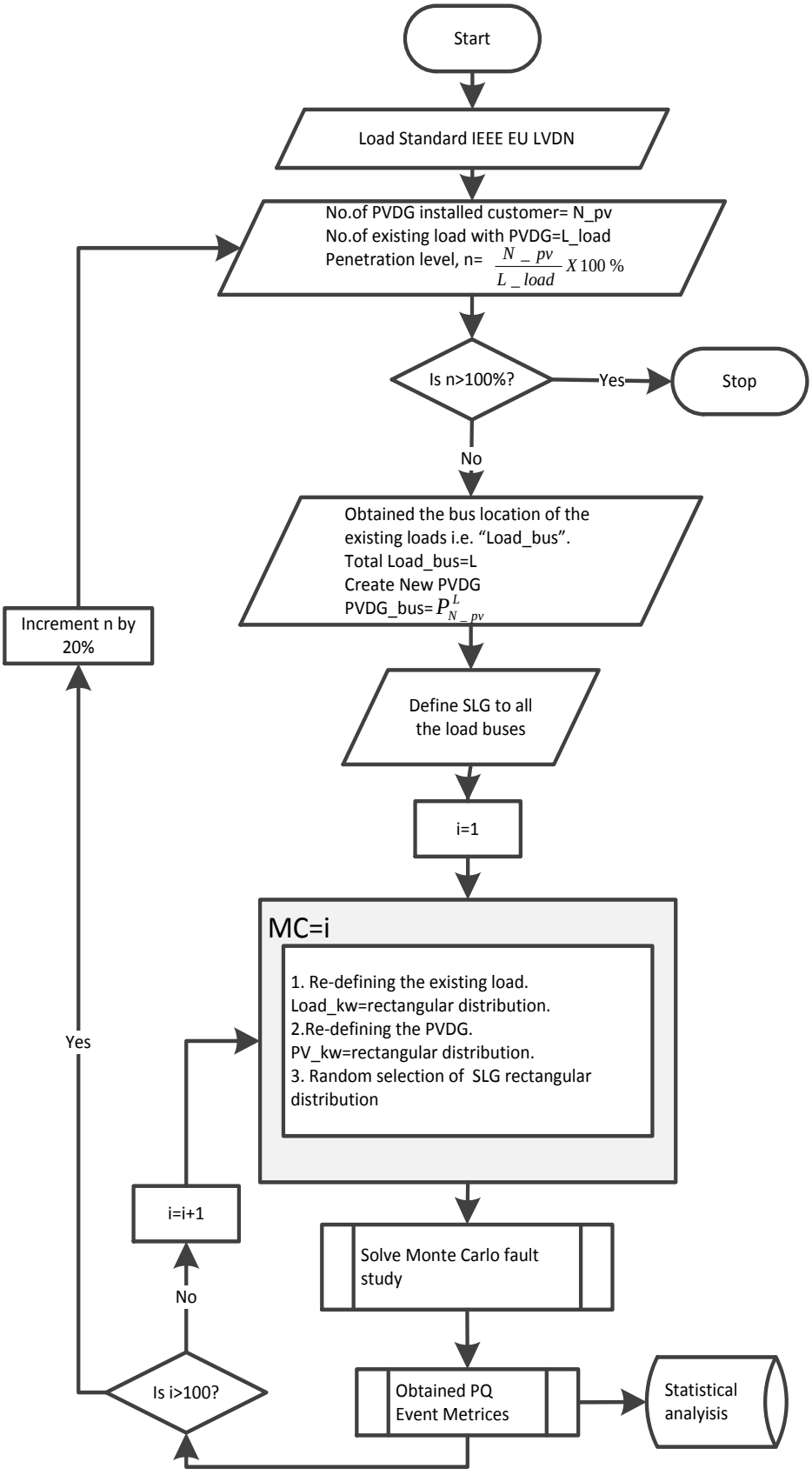

Figure 3.5 : Carlo simulation to assess PQ Event Metrics

Figure 3.5 represents the Monte Carlo simulation to assess PQ event metrics. A penetration level, n, is defined at the beginning of the Monte-Carlo simulation. The penetration level is incremented by 20% up to 100% for every 100 different stochastic scenarios. The location of each load bus is obtained to connect new PVDG randomly in the existing load buses. As discussed earlier, for each penetration level, 'n', the new PVDG connection to the existing load bus is performed by 'N_pv' permutation of 'L' through an ordered sampling without replacement. A list of SLG (single-line-to-ground) faults is defined for all the load buses which will later select one randomly at a time for each Monte-Carlo fault study. Voltage drop, and recovery are associated with applying and clearing the fault but observing the voltage sag depends on the method of monitoring the sag [100].

Herein, both PVDG and load demand are characterized by their peak value in order to assess the voltage sag at the system and site (where loads are connected) due to SLG faults. Each stochastic process, MC, is characterised by re-defining the peak values of the existing loads and PVDGs for each penetration level followed by performing a random SLG fault. In total, there are 500 different stochastic processes. The peak values of each load randomly vary between 1 to 10 kW and have a rectangular distribution. Similarly, for each penetration level, the peak value of each PVDG is also randomly varied between 1 to 5 kW and has also rectangular distribution. The random selection of each SLG fault from the 55 SLG faults is again represented by a rectangular distribution. A Monte-Carlo fault study is performed in OpenDSS [16] and finally, the PQ event metrics are obtained for further statistical analyses. The fault study mode in OpenDSS selects a random fault object from the list

of faults and disables the current fault object before the next Monte-Carlo fault study proceeds.

Only the minimum magnitude of the voltage sags for a recorded duration (i.e., sampled either for one cycle or for half cycle) due to the SLG fault will be monitored in this fault study analysis. The remaining voltage will adopt to quantify the voltage sag during SLG fault events [100]. So, the term ‘deep sag’ and ‘shallow sag’ will be used here. A deep sag is a sag with a low magnitude of remaining voltage whereas the shallow sag is a sag with a large magnitude of remaining voltage. Voltage sag duration, phase angle jumps during the unsymmetrical faults and point-on-wave, waveform distortion, or the transients at the start and end of the events are not considered for this study. It is further considered that, due to the assumption of monitoring the voltage sag as a minimum magnitude, an overshoot immediately after the sag will be observed.

3.3.2 Extreme Case Scenarios

Consideration of extreme-case scenarios will enable a comparison of the results obtained from the probabilistic study in further assessing the PQ impact metrics due to increased PVDG integration. For the PQ variation metrics, two extreme case scenarios are considered, namely, ‘*Extreme case 1*’ and ‘*Extreme case 2*’ which is presented in Table 3.1.

Table 3.1 : Extreme Case Scenarios for PQ variation metrics

Case	PVDG	Load
Extreme Case 1	1.100% penetration level of PVDG together with maximum recorded PV generation profile from 30 days sunny days. 2.All the 55 customers (prosumers) have 5 kW (upf) PVDG installed in their premises.	Minimum recorded load profiles or zero load demand
Extreme Case 2	0% penetration level of PVDG or no PVDG installed	1. All the 55 customers have peak load demand of 10 kW 2. Maximum recorded load demand profiles from the pool of 200 load profiles

The maximum recorded PV generation and load demand profiles from their respective pools are shown in Figure 3.6. Similarly, for PQ event metrics, two extreme case scenarios are considered, namely, '*Extreme case 3*' and '*Extreme case 4*' which is presented in Table 3.2.

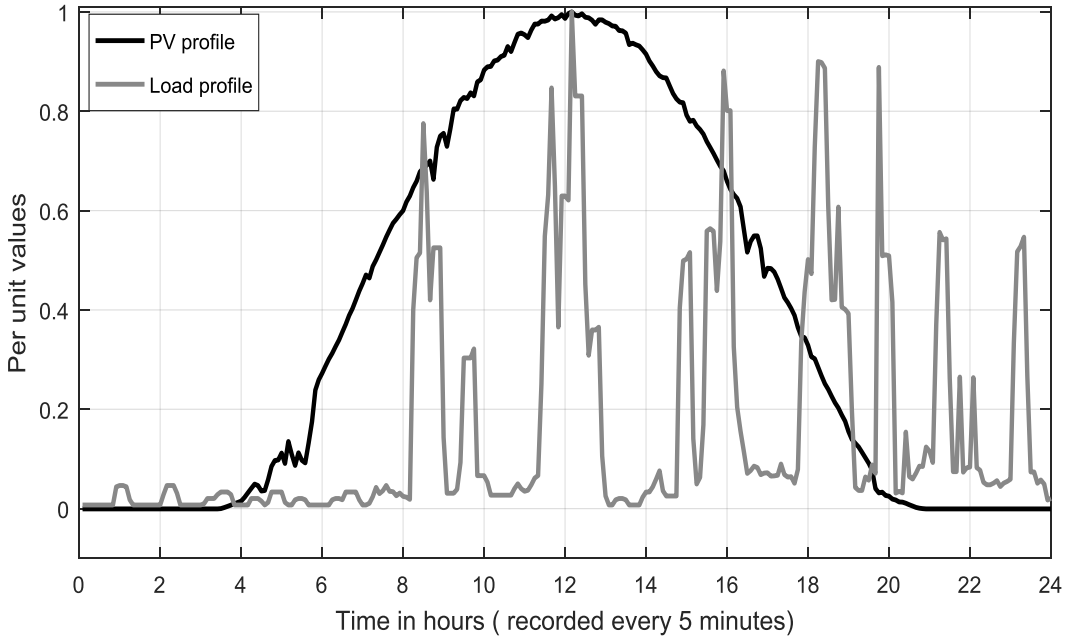

Figure 3.6 : Maximum recorded PV generation and load demand profiles

Table 3.2 : Extreme Case Scenarios for PQ event metrics

Case	PVDG	Load
Extreme Case 3	100% penetration level of PVDG or all 55 prosumers with peak generation of of 5 kW at upf	Zero load demand
Extreme Case 4	0% penetration level of PVDG or no PVDG installed	All the 55 customers have peak load demand of 10 kW

3.4 Probabilistic Analysis

3.4.1 PQ Variations Metrics and Indices

From the Monte Carlo simulation, cumulative distribution functions (CDFs) can be computed for each case study and for each PQ variation metrics and indices[8] (See Appendix C: Statistical Analyses). For overvoltage metrics, voltage in per unit represents the random variable *x* and F(*x*) represents the CDF of *x*. In total, there are 8 CDFs for each penetration level. The corresponding CDF enables to determine the probability of occurrence overvoltage at the site for each case study (Please refer See Appendix C1: Calculation of CDF and Complementary CDF).

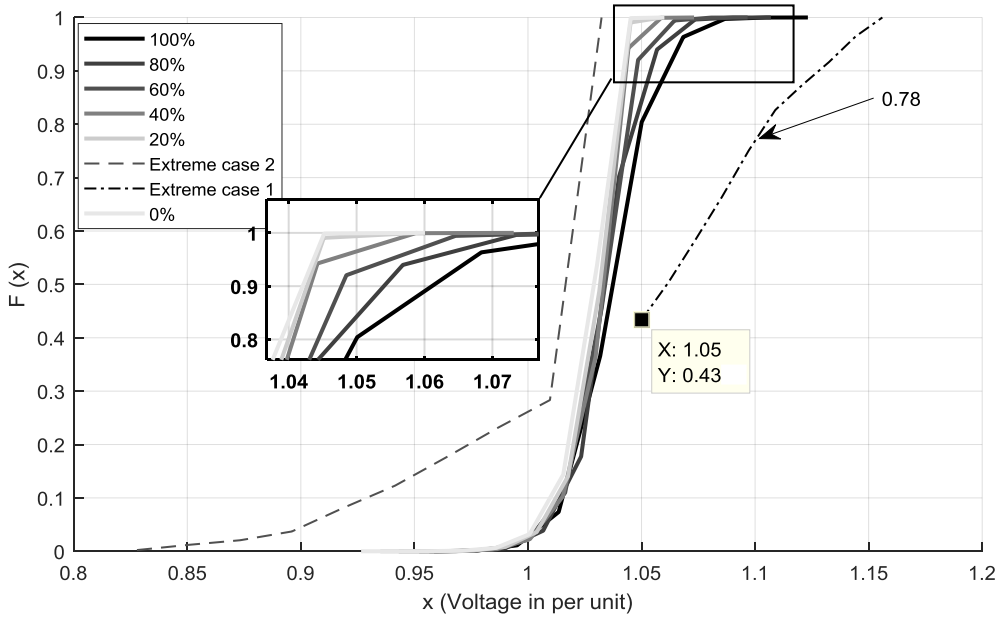

Figure 3.7 : CDF of site indices for overvoltage metric

From Figure 3.7, the probability of occurring overvoltage i.e., 1.1 p.u. at the site is 0.78 approximately for '*Extreme case 1*'. Further, it can be seen that the CDFs of all the penetration levels stay within the two extreme case scenarios. Again, from Figure

[8] Appendix C1: Calculation of CDF and Complementary CDF

3.7 the CDFs of case studies, namely 60%, 80% and 100% penetration levels together with '*Extreme case 1*' show that there is a probability of occurrence of overvoltage by a certain percentage of the customers. This is explained in Figure 3.8.

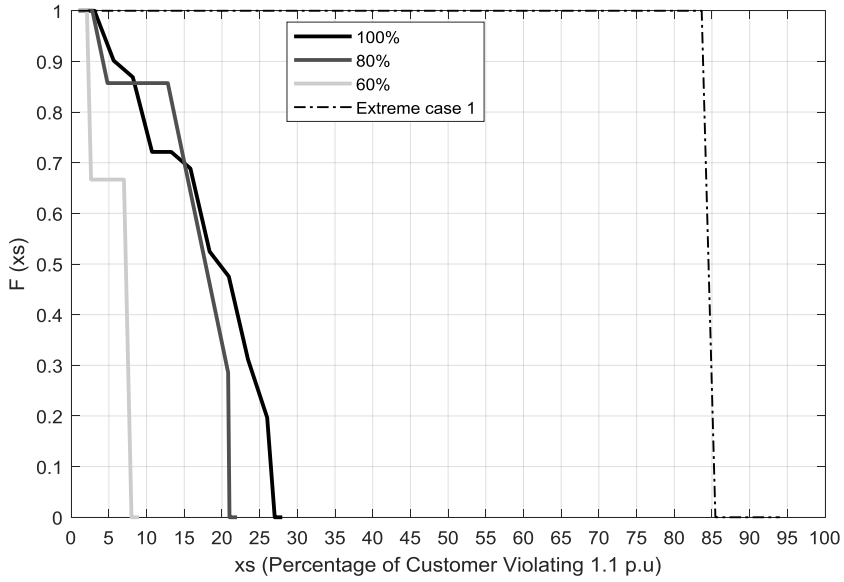

Figure 3.8 :CCDF of % of customer violating overvoltage

Referring to Figure 3.8, the percentage of customers violating 1.1 p.u. represent the random variable *xs* and F(*xs*) represents the complementary CDF (CCDF) evaluated at *xs* in four case studies, namely 60%, 80% and 100% penetration levels together with '*Extreme case 1*'. The CCDF allows the representation of how frequent a random variable exceeds a particular limit. From Figure 3.8, the probability of 20% of customers violating 1.1 is 0.5 in the case of 100% penetration level, 0.35 in the case of 80% penetration level and 1 in the case of '*Extreme case 1*'. Again, the probability of maximum percentage, i.e., 85% (approximately) of the customers violating 1.1 p.u. is 0.8 in the case of '*Extreme case 1*'. Whereas, the probability of maximum percentage, i.e., 25% (approximately) of the customers violating 1.1 p.u. is 0.2 in the case of 100% penetration level. But less than 5% of customers are likely to experience overvoltage in all the four cases. Thus, these CCDF trails show that as the penetration level increases,

there is a higher probability of percentage of customers observing overvoltage. It can be seen in Figure 3.7 that, the probability of occurrence of minimum voltage, i.e., 1.05 p.u. is about 0.43 for '*Extreme case 1*'.

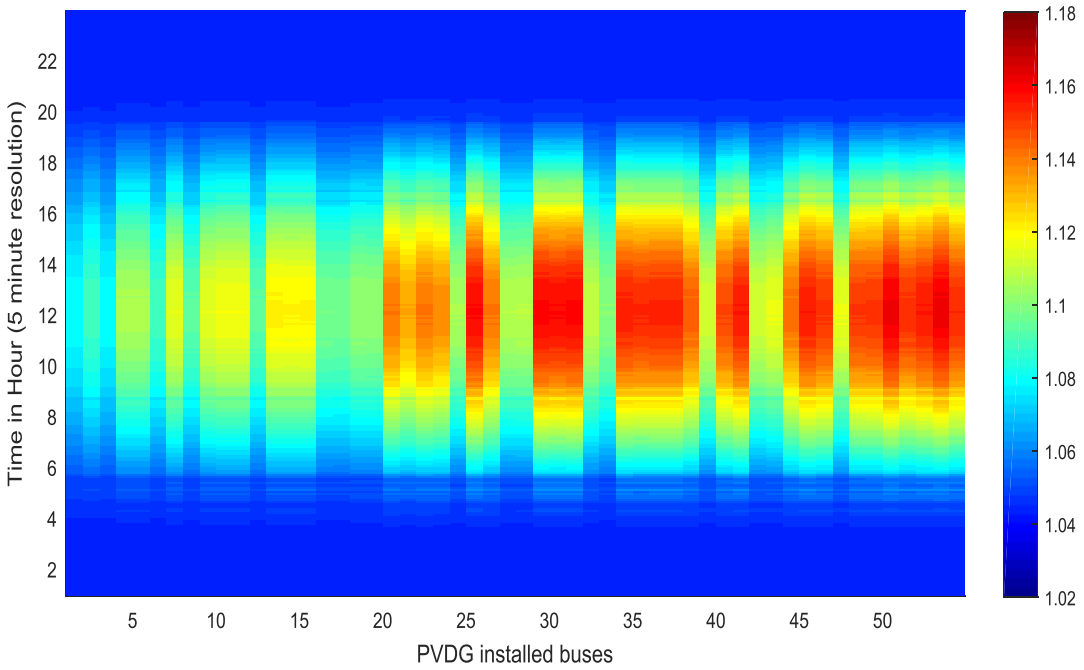

Figure 3.9 : Voltage checkerboard plot of all 55 customers in p.u for 'Extreme case 1' study.

This can be further seen in Figure 3.9 that most of the customers have a minimum voltage in between 1.04 p.u. to1.06 p.u. Figure 3.9 represents the checkboard plot for the voltages observed in all 55 nodes. This particular plot is made for *'Extreme case 1'*. It can be observed here that under *'Extreme case 1'*, voltage profile starts to increase down the feeder. From midday till afternoon maximum voltage rise can be observed from node 25 onwards. Similarly, in the case of overvoltage system indices, voltage in per unit represents the random variable X and F(X) represents the CDF of X. In total, there are 8 CDFs for each penetration level. The corresponding CDF enables to measure the probability of occurrence of overvoltage at the system for each case study. From Figure 3.10, the probability of occurrence of overvoltage (i.e.1.1 p.u.) at the system is 0 for all the 8 cases. But the probability of occurrence of minimum voltage of

1.04 p.u. is 0.4 in the case of '*Extreme case 1*'. This can be further seen in Figure 3.11 that the minimum voltage for all the three phase voltages at substation transformer is about 1.04 p.u. in the case of '*Extreme case 1*'. For each index, the unbalance factor is computed and quantified against the standard, i.e., the voltage unbalance factor should be less than 2% for 95% of a defined period (typically one week).

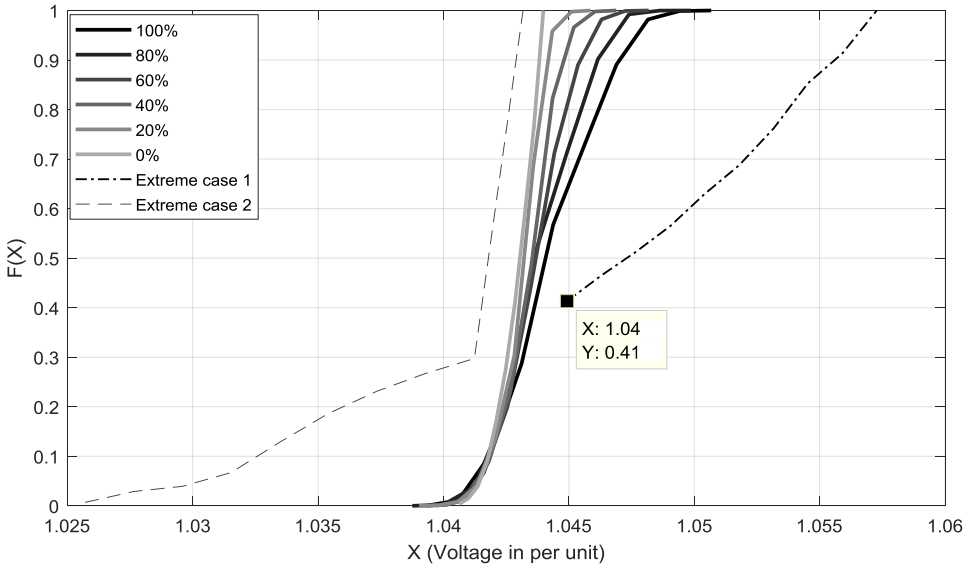

Figure 3.10 : CDF of system indices for overvoltage metric

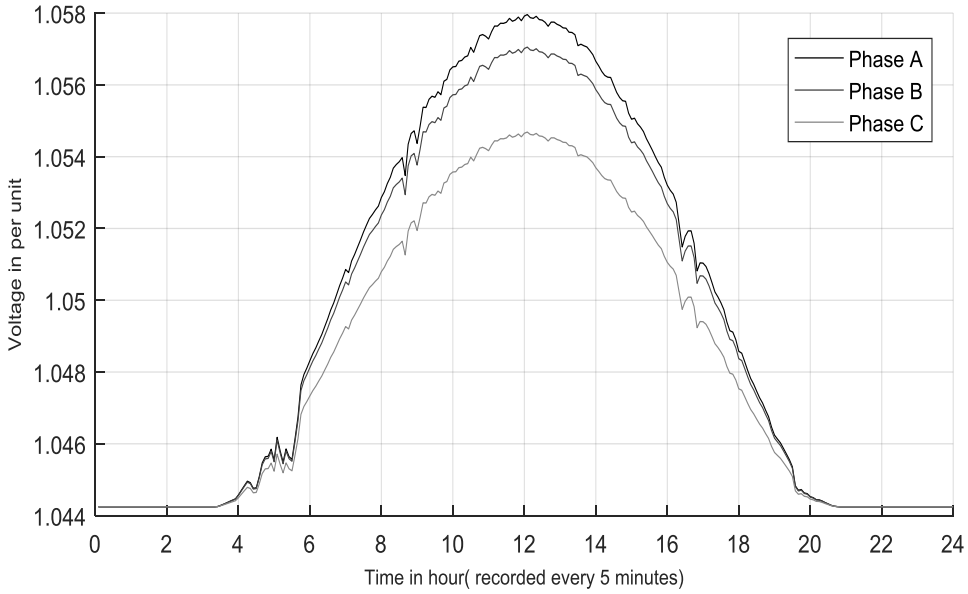

Figure 3.11 : Three phase voltages at substation transformer

The unbalance site indices are computed at the three-phase node where the customers connect their single-phase service cable. Therefore, there are 55 three phase nodes to consider for site voltage unbalance. To quantify the percentage of occurrence of voltage unbalance that exceeds a defined threshold limit, a cumulative plot of voltage unbalance factor versus percentage of occurrence (i.e., duration) are shown in Figures 3.12 and 3.13.

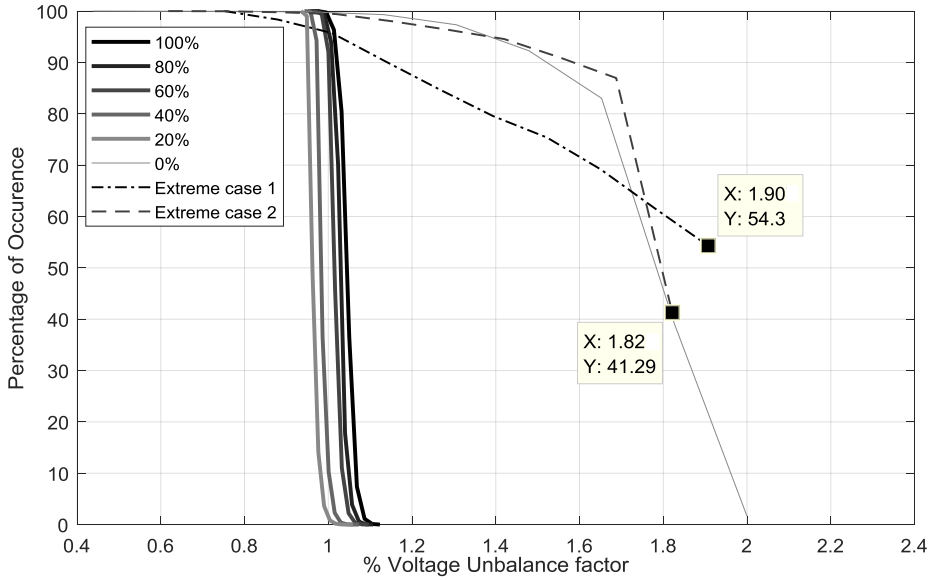

Figure 3.12 : Percentage of site voltage unbalance factor

These graphs are essentially a CCDF. Figure 3.12 shows the site voltage unbalance factor for 8 different cases. It can be seen here that the percentage of occurrence of the voltage unbalance factor of almost 1.8 is 60% in the three cases, namely, 0% penetration level, '*Extreme case 1*' and '*Extreme case 2*'. This increase in voltage unbalance at 0% penetration is expected due to unbalanced loading in the LVDN. However, '*Extreme case 1*' and '*Extreme case 2*' are the extreme conditions and stays within the limit. The percentage of occurring maximum voltage unbalance factor of 1.90 is 54.3% in the case of '*Extreme case 1*'. And, the percentage of occurring maximum voltage unbalance factor of 1.82 (in %) is 41.29% in the case of '*Extreme*

case 2'. The unbalance factor primarily depends on the loading in each phase. It can be recalled that out of the 55 customers, phases A, B and C accommodate 38.2%, 34.5% and 27.3% of the loads respectively, showing a certain level of balance loading and is shown in Figure 3.12 as 0% penetration. A further observation from Figure 3.12 shows that the integration of PVDG reduces the voltage unbalance factor. This is primarily due to the phase cancellation between the phases or in words the PV integration increases the positive sequence components since it injects positive sequence component into the network. But as the PVDG penetration increases from 20% to 100%, the voltage unbalance factor starts to increase by a small factor. The percentage of occurring maximum voltage unbalance factor of about 1 to 1.2 (in %) is 100% of all the 8 cases. This means that most of the time the voltage unbalance factor at each three phase nodes will be within 1–1.2 (in %) meaning it will stay within the limit. Overall, it can be concluded here that, PVDG integration alleviates voltage unbalance in the LVDN. This is primarily due to the phase cancellation between the phases as the local loading is met by the local generation.

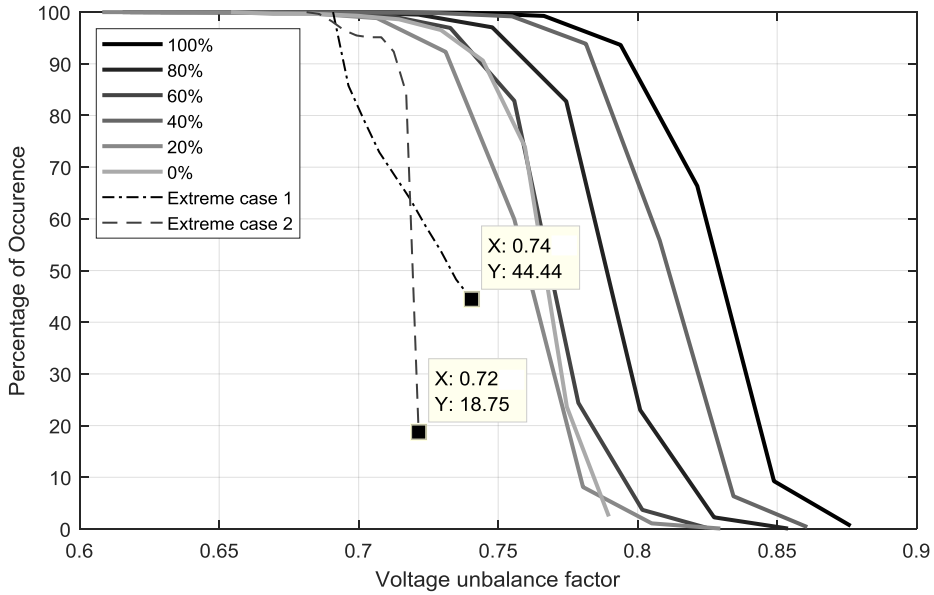

Figure 3.13 : Percentage of site voltage unbalance factor

The system index voltage unbalance factor is shown in Figure 3.13. The unbalance factor is within the limit for all the 8 cases. Similarly, here, as the penetration of PVDG increases from 0% to 100%, the voltage unbalance increases by a small factor. The percentage of occurring minimum voltage unbalance factor of 0.74 (in %) is 44.44% in the case of '*Extreme case 1*'. And, the percentage of occurring minimum voltage unbalance factor of 0.72 (in %) is 18.75% in the case of '*Extreme case 2*'. Further, the percentage of occurring maximum voltage unbalance factor of about 0.7 to 0.75 (in %) is 100% of all the 8 cases. This means that most of the time the voltage unbalance factor at the transformer will be within 0.7 to 0.75 (in %). Overall, the voltage unbalance at the transformer will be within the limit in all the 8 cases.

3.4.2 PQ Events Metrics and Indices

From the Monte Carlo simulation, cumulative distribution functions (CDFs) can be computed for each case study and for each PQ event metrics and indices. As discussed earlier, the observed voltage sags will be represented as a percentage of the remaining voltage in the Monte-Carlo fault study. For the voltage sags site index, the remaining voltage represents the random variable y and F (y) represents the CDF of y. The corresponding CDF enables the measurement of the probability of observing a certain percentage of remaining voltage for a particular case study. A higher percentage of remaining voltage means it is a shallow sag i.e., low fault current or towards the 100% of the y axis in Figure 3.14. Whereas, a lower percentage of remaining voltage means it is a deep sag i.e., high fault current or towards the 0% of the y axis in Figure 3.14.

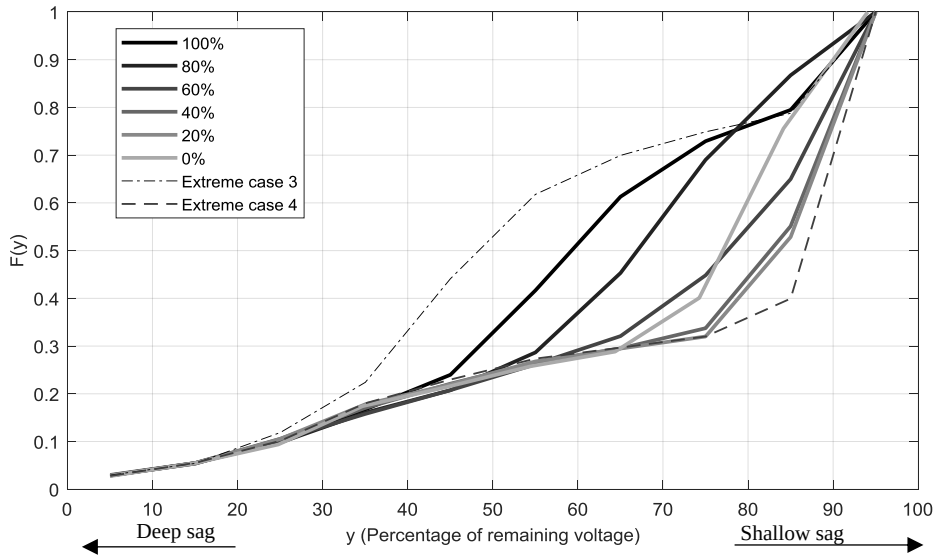

Figure 3.14 : CDF of site indices for voltage sag

From Figure 3.14, for the case of up to 40% of remaining voltage, all the case studies have the same CDF except the '*Extreme case 3'*. Starting from 45% of remaining voltage, the F(*y*) gradually increases as the penetration of PVDG increases with '*Extreme case 3*' showing the highest probability of occurring the remaining voltage ranging between 30% to 80%. That means '*Extreme case 3*' has the highest probability of seeing lower percentage values of remaining voltage i.e., deep sag (high fault current). When F(*y*) = 0.4, '*Extreme case 4*' shows high percentage of remaining voltage around 85% which mean a shallow sag. Again, the '*Extreme case 4*' shows the highest probability of occurrence of high percentage of remaining voltage i.e., shallow sag. From this analysis, it can be concluded that the presence of PVDG together with load demand contributes to the fault current at the load buses leading to voltage sag. As the penetration of PVDG increases, higher probability of occurrence of lower percentage of remaining voltage or deep sag is observed. But depending on the type of generator model, voltage sags might be different. Here, according to the Monte Carlo fault study, the PV generator is switched into a dynamic mode by converting it into the Thevenin's equivalent and finally to Norton's equivalent [16].

Similarly, for voltage sags system index, the remaining voltage represents the random variable *z* and F (*z*) represents the CDF of *z*. The corresponding CDF enables the measurement of the probability of observing a certain percentage of the remaining voltage for a particular case study.

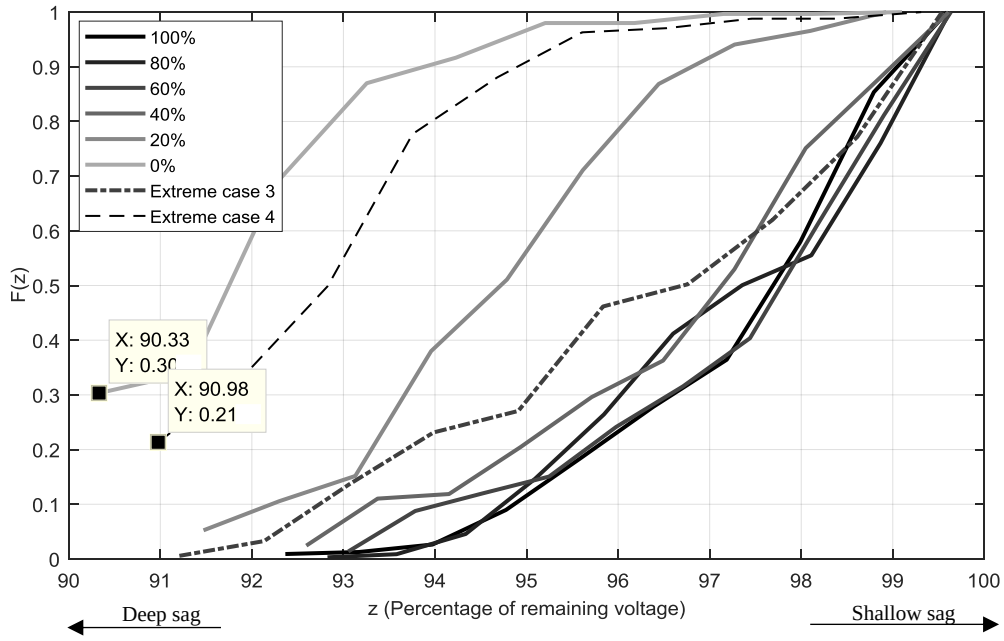

Figure 3.15 : CDF of system indices for voltage sag

From Figure 3.15, the CDFs of 40%, 60%, 80% and 100% penetration levels together with '*Extreme case 3*' follow the same profile or relatively similar slope. This profile signifies that all the CDFs correspond to shallow sag which means low fault current at the point where these voltage sags are measured i.e., at the secondary side of Dy transformer. This is true because the integration of DG along the feeder will reduce or lower the fault current contribution at the beginning of the feeder i.e., substation Dy transformer for fault beyond the DG location [3]. This means that if the fault occurs beyond the DG location down the feeder, the fault current seen at the upstream feeder will be lower. Due to the random integration of PVDG and random occurrence of SLG fault, the fault current seen at the upstream feeder or secondary side of a substation transformer is low. With the increased random integration of PVDG, the fault current

seen at the upstream feeder can be even lower and this is one of the cases observed in Figure 3.15. For the case studies, 0% of penetration level, 20% of penetration level and '*Extreme case 4*' are concerned, the F(*z*) increases as the percentage of remaining voltage increase. This is because the fault current seen by the upstream feeder is as expected since there is less or no PVDG contribution towards the fault current. With 20% of penetration level, the F(*z*) is lower as compared with 0% of penetration and '*Extreme case 4*'.

3.5 Conclusion

This study proposes the consideration of two PQ impact metrics and indices as a means to measure the likely impacts of increased PVDG integration under spatial and temporal behaviour of both PV generation and load demand. For each PQ impact metrics, 8 different cases were considered, namely, PVDG penetration levels at 0%, 20%, 40%, 60%, 80%, and 100%, a maximum generation with zero demand and maximum demand with zero generation. A Monte Carlo simulation is chosen as a tool for such stochastic process. From the results, site overvoltage shows a likely impact that will persist as the PVDG integration increases. The probability of the maximum percentage of customer violating 1.1 is higher in the case of '*Extreme case 1*' (i.e., maximum generation with zero demand) than in the case of 100% penetration level. At the 100% penetration level, the maximum percentage of customer violating 1.1 p.u. is 25% and the probability of occurrence is 0.2. Further about 20% of customers will violate 1.1 p.u. at the 100% penetration level and the probability of occurrence is 0.5. However, less than 5% of the customers will observe overvoltage in four case studies, namely 60%, 80% and 100% penetration levels together with '*Extreme case 1*', whereas, the system overvoltage stays within the limit.

In terms of site voltage unbalance, integration of PVDG reduces the voltage unbalance as compared with no PVDG integration or low penetration level. This is mainly due to the phase cancellation. This increase in voltage unbalance at 0% penetration is expected due to the unbalanced loading in the LVDN. Overall, the site and system voltage unbalance stay within the limit for all the 8 different cases. In the case of site voltage sag, as the penetration of PVDG increases, higher probability of occurrence of lower percentage of remaining voltage or deep sag is observed. However, the system voltage sags are quite different from that of the site. The probability of occurrence of lower remaining voltage or deep sag reduces as the penetration of PVDG increases. This is because PVDG integration reduces the fault current seen at the upstream feeder. In conclusion, the increased integration of PVDG poses some threat to the performance of the power system. From the probabilistic study, overvoltage poses the highest threat, whereas voltage unbalance stays within the limits. Further, increased integration of PVDG will contribute towards fault current leading to deep sag at the site. This probabilistic approach can be used as a tool to identify the likely impacts due to PVDG integration at the existing load buses. This will enable quantifying the likely impacts against the extreme-case scenarios.

In the following Chapter 4, the impact of net-metering in conjunction with the volumetric tariff structure towards DSO revenue will be discussed in detail followed by the consideration of capacity-based tariff structure.

Chapter 4

Impact of the net metering and volumetric tariff

Due to the intermittent nature of solar energy, together with the temporal and spatial behaviour of domestic customers, increasing penetration of PVDG could lead to uncertainty related to the core activity of the DSOs and recovery of revenue. Analysing the likely impacts of increased PVDG has brought about the need for studies to determine if regulatory policy has to consider a higher non-firm PVDG share. DSOs are regulated by the national regulatory authorities (NRA) and their revenue is generated from the tariff structure set by the NRA (see sub-section 2.1.3). To this end, most EU LVDN domestic customers are charged per volume of energy consumed, whereas, most of the DSO costs are directly proportional to the capacity of the LVDN. With increasing penetration of PVDG in LVDN, DSOs could likely face a time-lag in recovering their revenue. To address such likely impact scenarios, two methodologies are studied in this section. The first method aims to analyse the uncertain impacts of higher penetration of PVDG on DSO core activity such as voltage fluctuation. Second method aims to evaluate the DSO potential annual revenue under high PVDG integration. This research work is disseminated as a publication[9] which can be found in List of Publications. The IEEE EU low voltage network in [109] has been considered as a test bench for this study and is shown in Figure 3.1. This test bench has a substation transformer of 800 kVA rating consisting of 905 three phase nodes with 55 single phase domestic customers.

[9] S. Pukhrem, M. Conlon, and M. Basu, "The relationship between PVDG technical impacts and DSO revenue : An approach to foster a higher share of non-firm PVDG integration," in CIGRE Symposium, 2017.

4.1 Uncertain Impact Analysis

A 5-minute resolution yearly solar profile of the year 2015 obtained from the Whitworth Meteorological Observatory [111] and is considered for the PV generation profiles. Similarly, a 5-minute resolution load profile from Low Carbon Technology (LCT) project [112] is considered as the domestic load profile. From the yearly data, the month of June has the highest PV generation profile and for this reason, it is utilised for the potential extreme impact studies which is shown in Figure 3.2.

Further, a pool consisting of 200 load profiles with 5-minute resolution were created from the LCT project which reflects the temporal behaviour of load consumption pattern which is shown in Figure 3.3. Each 55 customers are assumed to have 0.95 lagging power factor whereas the PVDG is assumed to export power at unity power factor. No energy storage system is used to buffer the daily PVDG production.

Referring to Figure 4.1, after defining the representative LVDN and the pool of PVDG and load demand profiles, further assumptions for the impact analysis are as follows. For each 55 customers, the peak load demand varies in two modes i.e. between 1 and 4 kW and between 5 and 8 kW respectively. Similarly, PVDG is installed in three levels of penetration (high, medium and low). These customers with installed PVDG are potential prosumers. For each penetration level, the PVDG peak production at each installation is further classified into two modes i.e. between 1 and 3 kW and between 3 and 5 kW respectively. Finally, the PVDG and load demand profiles are randomly selected from their respective pools. Subsequently, the load flow is computed for each three modes of PVDG penetration levels, two modes of peak load demand and

two modes of PVDG peak production. In total, there are 12 separate simulations for this impact analysis.

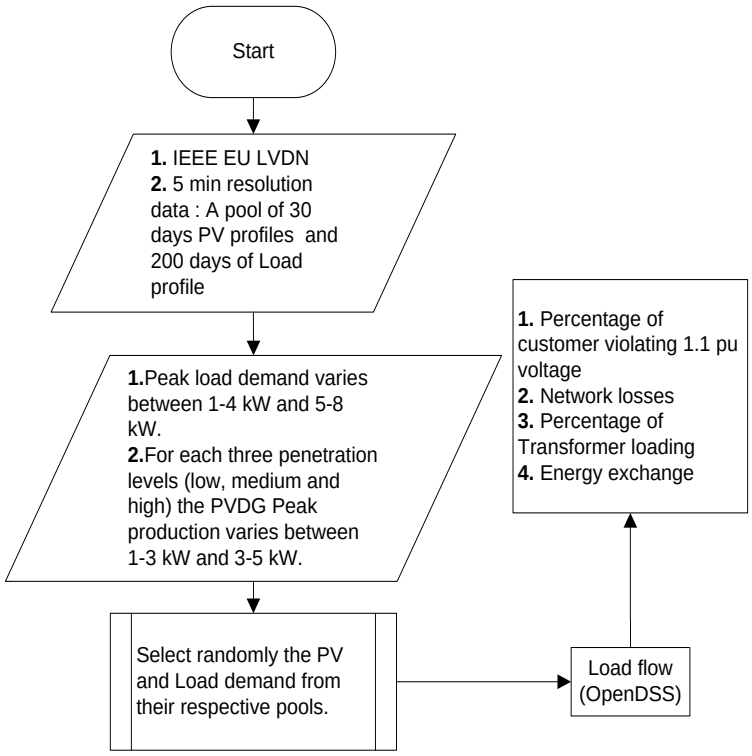

Figure 4.1 : Flowchart for impact analyses

The different possible combinations of three PVDG penetration levels together with the variation in peak PV generation and peak load demand are described in Table 4.1. The case study "M" stands for zero PV penetration level with peak load demands varying from 1-8 kW.

Table 4.1 : Designation of 13 possible studies

Designation	**A**	**B**	**C**	**D**	**E**	**F**	**G**	**H**	**I**	**J**	**K**	**L**	**M**
Penetration level	Low	Low	Low	Low	Med	Med	Med	Med	High	High	High	High	No PV
Variation in peak PV generation (kW)	1-3	1-3	3-5	3-5	1-3	1-3	3-5	3-5	1-3	1-3	3-5	3-5	0
Variation in peak Load demand (kW)	1-4	5-8	1-4	5-8	1-4	5-8	1-4	5-8	1-4	5-8	1-4	5-8	1-8

Table 4.2 represents the comparative analysis of different distribution of generation and loads accounting for 3 impact analyses. It is observed from Table 4.2, that the studies “K” and “L” violates over voltage regulation (i.e. 1.1 per unit voltage) by 54.54 % and 41.82 % of the total customers respectively due to high penetration of PVDG with high peak generation.

Table 4.2 : Comparative analysis of the 13 different studies accounting 3 impact analyses

Combination Study	Percentage of customer violating 1.1 pu voltage	Average network losses for a day in kVA	Percentage of peak loading w.r.t the substation transformer rating i.e. 800 kVA
A	0	0.16	16.48
B	0	6.58	50.80
C	0	0.32	15.25
D	0	1.38	51.18
E	0	0.20	17.98
F	0	0.97	49.12
G	0	0.39	20.29
H	0	2.28	43.02
I	9	0.47	21.73
J	0	0.99	43.28
K	54.54	0.63	28.49
L	41.82	2.08	66.70
M	0	2.19	51.88

It can be further noted from Table 4.2, that the study “B” has the highest average network losses i.e. 6.58 kVA whereas, the study “L” has the highest percentage of peak loading i.e. 66.70%. Detailed comparative analysis can be further studied by referring to Table 4.2. Figures 4.2 and 4.3 represent the boxplot of active and reactive power losses in the network under the 13 different combination studies. It can be noted that study “B” shows highest kW and kVAr losses similar to Table 4.2. This is because, as described in Table 4.2, study “B” corresponds to low PVDG penetration level together with low peak production i.e. between 1 and 3 kW and high load demand of peak value varying between 5 and 8 kW. Other additional factors could be the temporal behaviour of PVDG production, and the load demand profiles. It is interesting to note that, all the studies except study “B” show relative network losses similar to the study “M”.

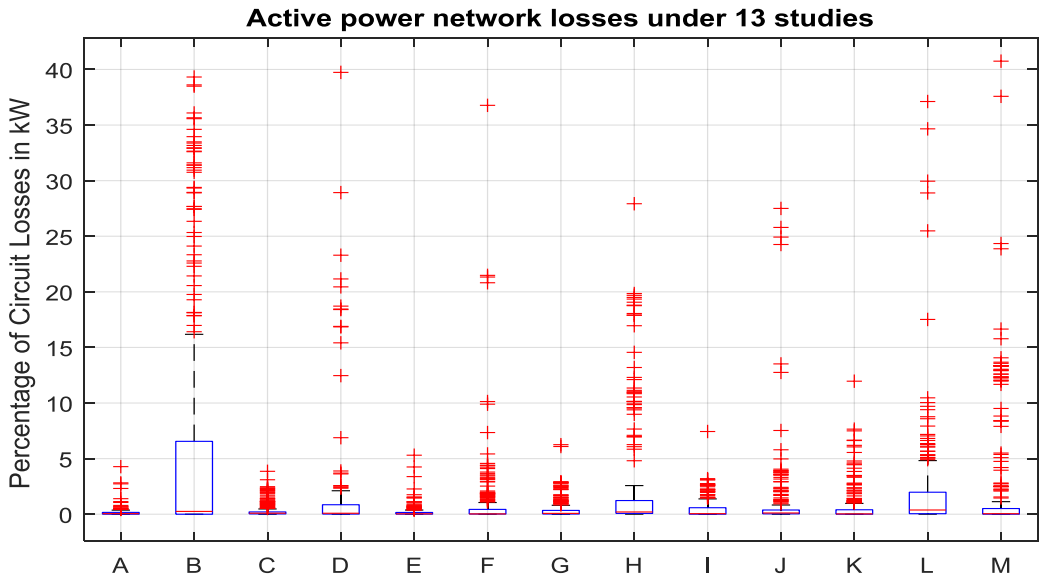

Figure 4.2 : Boxplot of the kW network losses under 13 studies.

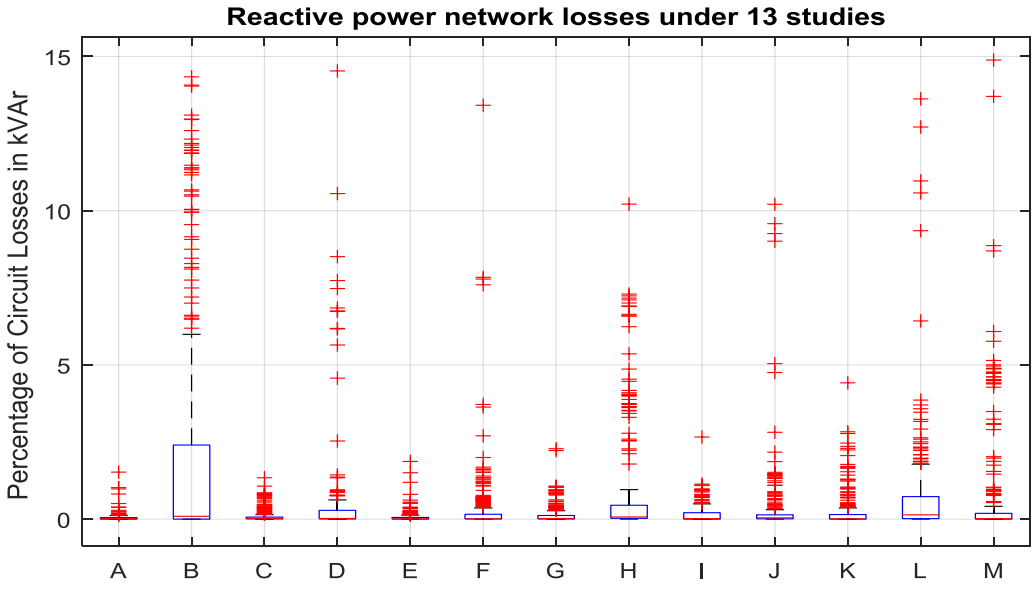

Figure 4.3 : Boxplot of the kVAr network losses under 13 studies.

Again, Figures 4.4 and 4.5 represent the boxplot of kW and kVAr exchange at the substation transformer under the 13 different studies. It can be noted here that all the studies except studies “B” and “M” experience reverse active power flow. Study “L” presents the highest average reverse active and reactive power flow. This is because, study “L” corresponds to high penetration level of PVDG together with high peak generation and high load demand as describe in Table 4.1.

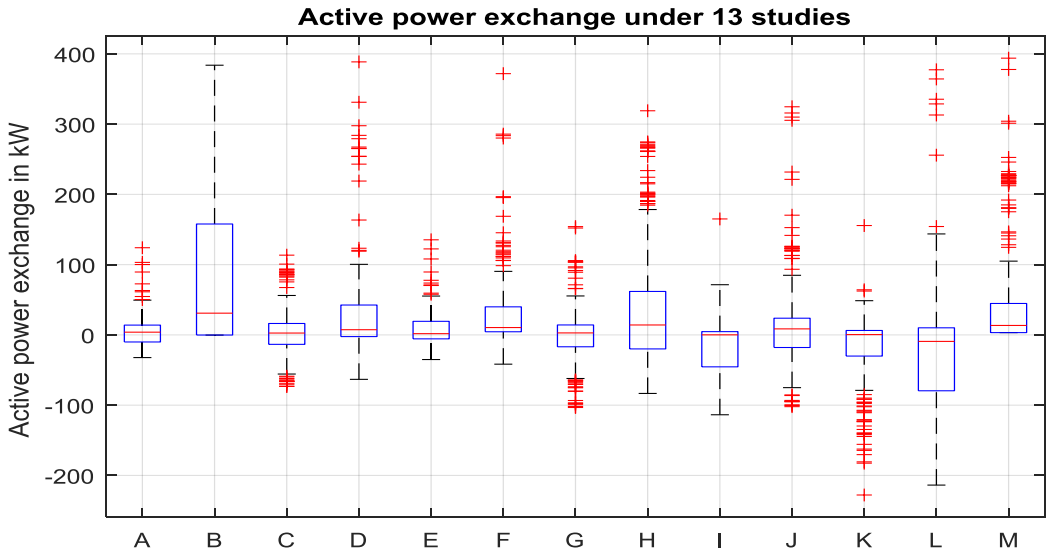

Figure 4.4 : Boxplot of the kW of Active power exchange under 13 studies

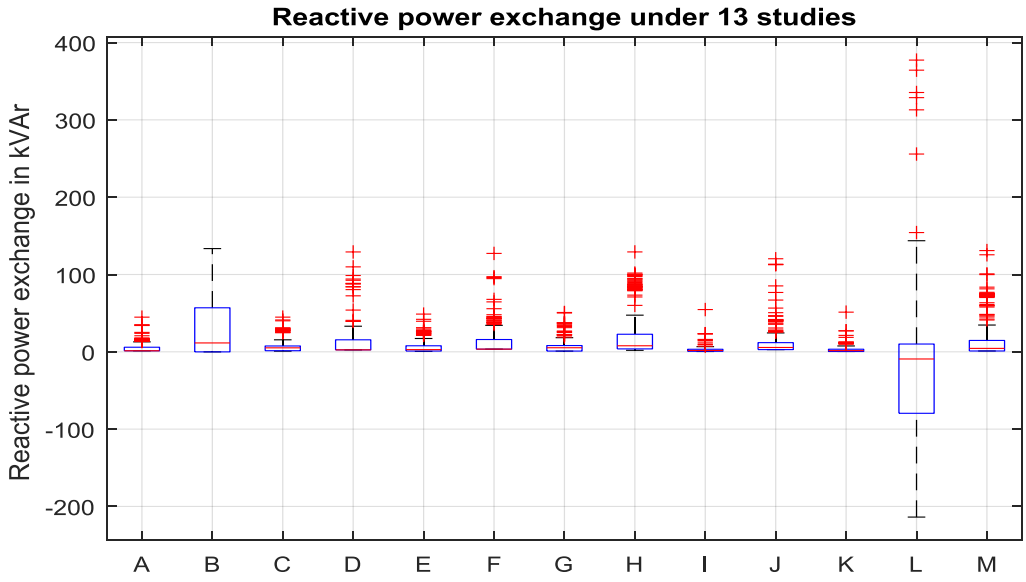

Figure 4.5 : Boxplot of the kVAr of reactive power exchange under 13 studies

4.2 Potential Revenue Evaluation

In evaluating the annual revenue, a time resolution of 1 hour is considered by averaging the 5-minute resolution data from both solar PVDG and load demand which is shown in Figure 4.6. Here, the behaviour during winter of high latitude demographic regions (low irradiation and high energy demand) is observed. A volumetric tariff in

conjunction with net-metering is assumed for revenue evaluation. Further, it is also assumed that there are no feed-in-tariffs, taxes and VAT in the calculation of revenue.

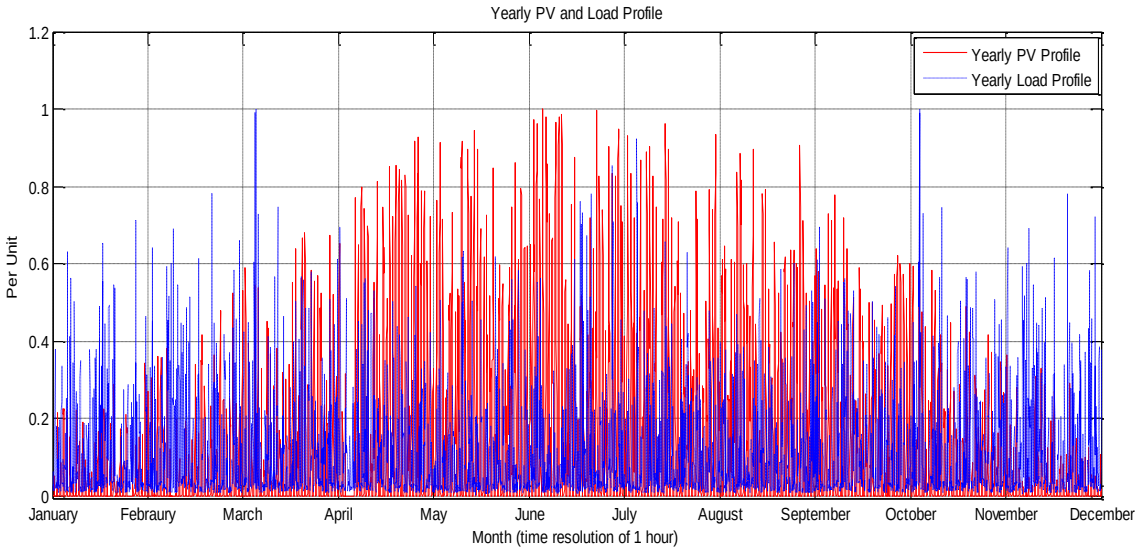

Figure 4.6 : Yearly PV and Load profile in per unit for the year 2015

With respect to Figure 4.7, after defining the representative LVDN and the annual PVDG and load demand profiles, further assumptions for the revenue analysis are considered as follows. In this case, a high PVDG penetration level is assumed, i.e. all 55 customers installed PVDG in their premises. For each 55 customers, the peak load demand varies in the range between 5 and 8 kW. Similarly, the PVDG peak production can be varied in two modes i.e. between 3 and 5 kW and between 6 and 8 kW respectively. Two separate load flows are computed with and without PVDG. In order to maintain consistency in determining the revenue, the annual peak load demand profile is kept the same level for both load flow studies with and without PVDG. In total, there are 3 separate simulations for this evaluation of revenue. Finally, the obtained energy exchanges are utilised to compute the electricity price without taxes and levies. The computed electricity price is further separated into two categories: energy supply cost and network cost. In practice, the network cost comprises of a fixed charge (i.e. EUR/day, month or year) and a variable charge depending on the volume

of energy consumed by the customer (i.e. EUR/kWh). The revenue of the DSO i.e. the network cost is calculated for four different countries with similar demographic regions. They are Denmark (DK), The Netherlands (NL), Ireland (IE) and United Kingdom (UK).

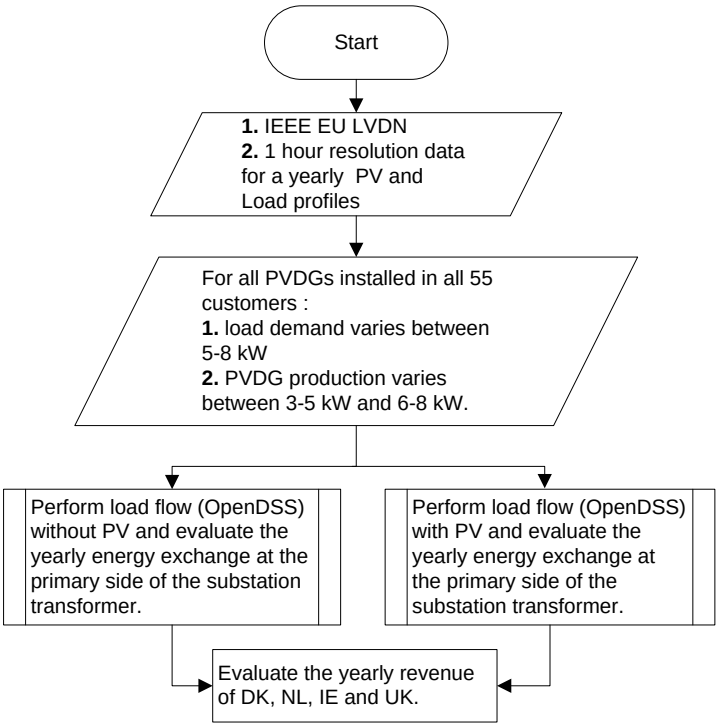

Figure 4.7 : Flowchart for annual revenue evaluation

After defining the yearly temporal pattern of PVDG and load demand, further random allocation of the peak values of both PVDG and load is defined. Three different combination studies can be considered for this revenue evaluation. They are shown in Table 4.3.

Table 4.3 : Three different combination of peak values of both PVDG and load demand

Designation	**Range of peak value of PVDG in kW**	**Range of peak value of load in kW**
X i.e. medium penetration	3-5	5-8
Y i.e. high penetration	6-8	5-8
Z i.e. No_PV	0	5-8

The simulation results show about 53 % and 93% of the total customers violates the over voltage regulation for the studies “X” and “Y” respectively. Further, about

57% and 121% of the energy drawn from the utilities were seen as reverse power flow events at the substation transformer for both the studies “X” and “Y” respectively. The total annual energy (in kWh) flow to the load for each study “Z”, “X” and “Y” are 318355.77, 233906.57 and 217769.44 respectively. These energy flows are utilised in the following part to calculate the electricity price for the respective countries. It can be observed that, in the case of studies “X” and “Y”, the energy flow is decreased by 20-30% compared to study “Z”. More comparative analyses for all the three distributions are presented in Table 4.4.

Table 4.4 : Yearly comparative analysis of the three studies accounting 4 impact analyses

Study	**Total annual energy flow to the load in kWh**	**Annual Maximum Demand seen at the transformer**	**Percentage of customer violating 1.1 pu voltage**	**Average network losses for a day**		**Percentage of peak loading w.r.t the substation transformer rating i.e. 800 kVA**	**Percentage of reverse power flow with respect to the energy drawn from the utilities**
				kW	**kVAr**		
Z	318355.77	390.62	0	0.82	0.30	51.67	0
X	233906.57	390.78	52.72	0.96	0.35	51.69	57.38
Y	217769.44	390.87	92.72	1.72	0.63	51.70	120.60

Electricity prices in the four countries (DK, NL, IE and UK) were obtained from EuroStat[10]. Table 4.5 describes the disaggregated electricity price data for household consumers for the year 2015 in EUR/kWh. Here, distinctive prices for energy supply, network cost and associated taxes and levies are shown for each of the four countries. From Table 4.5, it is seen that the network cost varies in each of these countries. Denmark charges highest taxes and levies but it has the lowest cost of energy supply. On the other hand, the UK charges lowest taxes and levies, but it has the highest cost of energy supply. Overall, the observation concludes that Denmark bears the highest

[10] http://ec.europa.eu/eurostat/statistics-explained/index.php/Electricity_price_statistics

percentage of network cost in the price of electricity if the taxes and levies are excluded, whereas, Ireland charges the highest network cost price.

Table 4.5 : Disaggregated price data for household consumers, 2015 (in EUR/kWh)

Composition of the electricity prices for household consumers (in EUR/kWh)					**Share in price without taxes and levies (in %)**	
Country	Total	Energy Supply	Network Cost	Taxes & Levies	Energy & Supply	Network cost
Denmark	0.30	0.03	0.05	0.21	40.6	59.4
Netherland	0.18	0.06	0.05	0.06	55.9	44.1
Ireland	0.24	0.13	0.06	0.04	66.6	33.4
UK	0.21	0.15	0.05	0.01	75.9	24.1

From the annual energy flow to the load as given in Table 4.4, yearly revenue for all the four countries is computed for the three studies which are presented in Table 4.6. Here the network cost in EUR/kWh is multiplied by the total annual energy exchange in kWh. Annual revenue generated from the study "Z" is considered as the reference revenue for comparing with the revenue for the other two studies. It can be observed that the penetration of PV peak generation is inversely proportional to the revenue of the DSO. The revenue generated can be directly attributed towards the percentage of reduction in energy flow to the load from the utility. From the above discussion, energy flow reduces by 20-30% in the case of studies "X" and "Y" respectively, compared to the reference case study "Z". These percentages of reduction in energy flow attribute to the same percentage of reduction in revenue. This representative loss in the revenue is due to two reasons.

Table 4.6 : 2015 annual share in price without taxes and levies for four different countries

Countries	**Energy Supply in Euro**			**Network cost in Euro**		
	"Z" i.e. Without PVDG	**With PVDG**		**"Z" i.e. Without PVDG**	**With PVDG**	
		"X"	**"Y"**		**"X"**	**"Y"**
Denmark	12098	8888	8275	17828	13099	12195
Netherland	21967	16140	15026	17510	12865	11977
Ireland	42341	31110	28963	21011	15438	14373
United Kingdom	50300	36957	34408	15918	11695	10888

Firstly, the charging of the domestic customer is mainly through high percentage of volumetric consumption with low fixed charge [79]. Whereas, the electric grid operation cost is primarily defined by high fixed charge and low variable charge [114]. The long-run cost of operating the electric grid is allocated mostly as a fixed charge which includes network losses, peak capacity of network, connection cost and network reliability. Secondly, due to the application of the net-metering system, the volume of energy consumption reduces due to PV generation. This could reduce the overall electricity bill of the prosumers leading to a decrease in the DSO's network cost. To sustain stable network cost, the NRA may impose higher fixed charges or higher charges per energy or volume of kWh consumed by the network users (both consumer and prosumer) to balance the reduced charges from net-metering. Conversely, the normal consumers will end up paying the increased charges because of prosumer's activity leading to cross subsidisation between normal consumers and prosumers. Further amendments on these two aspects are necessary for sustainable revenue generation for the DSO without cross-subsidising different types of customers.

4.3 Capacity based tariff structure

Referring to Table 4.6, the reference revenue is observed to drop by almost 20% and 30% for studies "X" and "Y" respectively with respect to the reference revenue 'Z'. As discussed earlier, this revenue was generated by considering a volumetric tariff in conjunction with net-metering. In order to reflect a correct price signal without cross subsidising between different customers and at the same time generating sustainable revenue for the DSO, a cost causation-based power/capacity distribution network tariff was discussed in [115], which can be further explored. As the intermittent PVDG penetration increases within the LVDN more capacity based charges will be inevitable

by identifying the challenges posed to the customer, retailer and DSO [116]. Whether such capacity-based network tariff will be able to incentivise the DSO in maintaining their core activity under increased penetration of PV is further discussed in [117].

The application of capacity-based tariff structure could concurrently recover the sunk cost of the DSO and alleviate the cross-subsidisation is the following part of this investigation. The main idea of the following analysis is not to design an optimal tariffing structure but rather to justify whether the consideration of capacity-based tariff structure in the previous tariff i.e. Volumetric tariff in conjunction with net metering could incentivise the DSO without cross-subsidisation. Here, the capacity charges can be imposed on the maximum power used during a certain period of time for an instance during the on-peak demand period. From the network operator point of view, the reinforcement of the network is directly related to the total diversified peak demand of the network over a certain period such as a year.

The objective of the capacity-based tariff structure is to reflect the peak demand that contributes to the stress on the network. A simple explanation of capacity-based tariff structure is explained here. According to EDSO in [30], the two different consumers with different contracted capacity[11] presented in Figures 4.8 and 4.9 has the same volume of consumption or generation over a day, however, with capacity based tariff structure they will pay differently in using different levels of grid capacities. Customers 1 and 2 contribute maximum used capacities of 5 kW and 7.5 kW respectively. This further illustrates that irrespective of the volume of energy which

[11] Maximum used contracted kW capacity with the corresponding price.

passes through the distribution network, customers with different levels of stress on the grid will have this reflected through capacity-based tariff structures.

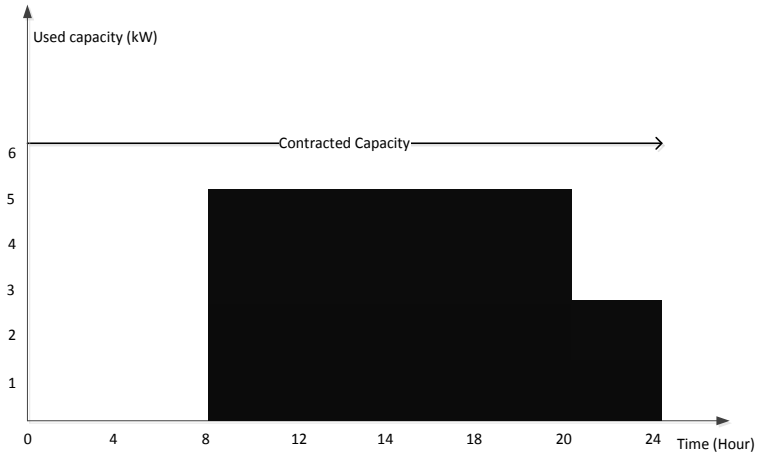

Figure 4.8 : Customer 1

Volume of energy consume/generated: 5kW*****12h + 2.5 kW *****4h = 70 kWh
Contracted capacity: 6 kW and Maximum used capacity: 5kW

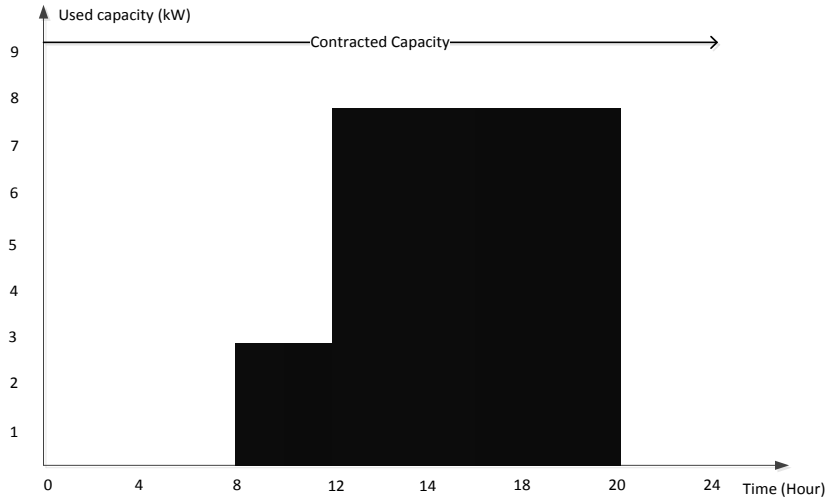

Figure 4.9 : Customer 2

Volume of energy consume/generated: 2.5kW*4h + 7.5 kW*8h = 70 kWh
Contracted capacity: 9 kW and Maximum used capacity: 7.5kW

In this analysis, the capacity based tariff is determined by dividing the revenue by the sum of the customers highest peak loads [118]. The price of power may typically be

2–4 €/kW per month, and the price (€/kW) is a constant and the same for all customers [118]. Only the network cost will be considered in calculating the final revised revenue. From sub-section 4.2 Potential Revenue Evaluation, it was assumed that all 55 customers installed PVDG in their premises. For each of the 55 customers, the PVDG peak production varied in two modes i.e. i) Study 'X' which varies the peak production of PVDG between 3 and 5 kW and ii) Study 'Y' which varies the peak production of PVDG between 6 and 8 kW respectively. Only studies 'X' and 'Y' are considered to apply the capacity-based tariff structure.

From Table 4.4, total hourly peak demand of all the 55 customers for studies X, Y and Z measured at the secondary side of the distribution transformer are 390.87 kW, 390.78 kW and 390.62 kW respectively. In the previous section 4.2 Potential Revenue Evaluation, it was assumed that the annual peak load demand profile was kept the same for both load flow studies with and without PVDG for all the 55 customers where the only variable was the peak demand which varies from 5-8 kW.

Table 4.7 determines the capacity-based tariff structure based on the above assumption. In the case of Ireland, the annual network cost for study 'X' is 15437.83 Euro (see Table 4.6) and the maximum total mean hourly load demand for study 'X' is 390.77 kW (see Table 4.4). Following the above assumption, the annual capacity tariff for all 55 customers will be (15437.83/390.78) *55 = 2172.78 Euro/kW and the monthly capacity tariff for each customer will be (2172.78/12)/55=3.29 Euro/kW per month.

Table 4.7 : Capacity based tariff under PVDG integration

Countries	Capacity Tariff per year for all 55 customers		Capacity Tariff per month for all 55 customers	
	With PVDG		With PVDG	
	"X"	"Y"	"X"	"Y"
	Euro/kW	Euro/kW	Euro/kW	Euro/kW
Denmark	1843.61	1715.99	2.79	2.59
Netherland	1810.69	1685.35	2.74	2.55
Ireland	2172.78	2022.42	3.29	3.06
United Kingdom	1646.08	1532.14	2.49	2.32

The revised annual network cost comprises of the volumetric and capacity tariff in conjunction to net-metering. In the case of Ireland, the revised annual network cost for all 55 customers for study 'X' will be 15437.83 (see Table 6) + 2172.78 (see table 7) = 17610.61 Euro.

Table 4.8 further shows the comparison between the revised annual network cost (i.e. volumetric and capacity tariff in conjunction to net-metering) and the reference network cost i.e. study 'Z' (see Table 4.6, volumetric tariff with no PVDG) along with the previous network cost (see Table 4.6, volumetric tariff in conjunction to net metering).

Table 4.8 : Comparison of the tariffing structure for the year 2015

Countries	Reference Network Cost i.e study 'Z' without PVDG	Previous Network Cost With PVDG		Revised Network Cost With PVDG	
		'X'	'Y'	'X'	'Y'
	Euro	Euro	Euro	Euro	Euro
Denmark	17827.92	13098.77	12195.09	14942.38	13911.09
Netherland	17509.57	12864.86	11977.32	14675.55	13662.67
Ireland	21011.48	15437.83	14372.78	17610.66	16395.21
United Kingdom	15917.79	11695.33	10888.47	13341.41	12420.61

The revised network cost shows the drop by almost 16% and 21% for studies "X" and "Y" respectively with respect to the reference network cost. It can be observed that in the case of the revised network cost, there is a 4% and 9% increase in the total

network cost with respect to the previous network cost for studies ‘X’ and ‘Y’ respectively. It can further be concluded that the increase in the revenue is higher for study “Y” i.e. high penetration of PVDG than study ‘X’ i.e. medium penetration of PVDG.

The above analysis was calculated by assuming a solar irradiation and load profiles of a high latitude demographic regions as shown in Figure 4.6 where the behaviour during the winter session shows low irradiation and high load demand. Since the capacity-based tariff structure mainly focuses on the peak usage of the network, all the 55 customers contribute to the stress on the network during winter peak demand. The increased revenue in the revised network cost may could potentially incentivise the DSO in mitigating any over voltage issue which arises due to high penetration of PVDG as observed from Table 4.4 that almost 93% of the domestic customers violates the 1.1 per unit limit under high penetration of PVDG.

4.4 Conclusion

Being an intermittent source, increased penetration of PVDG is likely to pose uncertain challenges to the DSO. Above all, due to the temporal and spatial behaviour of loading and generation in the distributed network, it could even exacerbate the challenges in maintaining the core activity of the DSOs which is to provide stable and reliable electricity to all customers. This work has explored the factors through a series of studies and presented an insight into some of the impacts that could pose apparent threats for DSOs. Two-time resolutions were studied in this work. Firstly, for the impacts study, 5-minute resolution was considered. It was observed from Figure 4.4 that there is frequent reverse power flow under various studies. Also, over-voltages are

likely to be observed under high penetration of PVDG in the domestic premises (see Table 4.2). It is also interesting to note that with increased penetration of PVDG, the average network loss is quite similar to the network losses observed without PVDG. Secondly, for yearly simulation, 1-hour resolution was chosen. It was observed from Table 4.4 that, with high penetration of PVDG, almost 93% of the domestic customers will violate the 1.1 per unit (i.e. 10% of the nominal value) over voltage regulatory limit in a year. Above all, at high PVDG penetration, almost 120% of the energy drawn from the utility will be exported as reverse power to the upstream sub-transmission network in a year. However, on an average, the network losses and transformer loading are almost equivalent to the condition without PVDG in the LVDN.

The annual network cost of the DSO with respect to the reference revenue (i.e. the network cost generated without PVDG) gradually declines as the penetration of PVDG increases in the case of volumetric tariff structure in conjunction to net metering. Consideration of capacity based tariff structure together with the volumetric tariff in conjunction with net metering improves the annual revised network cost (i.e. by 4% and 9% increase in the total network cost with respect to the previous network cost for studies ‘X’ and ‘Y’ respectively) which could incentivise the DSO in mitigating the voltage rise issue arises due to high penetration of PVDG as observed from Table 4.4 that almost 93% of the domestic customers violates the 1.1 per unit limit under high penetration of PVDG.

It is evidenced from the previous Chapter 3 and this chapter that as the penetration of PVDG increases in an LVDN the occurrence of overvoltage is inevitable. In the

following Chapter 5, an enhanced method to alleviate this observed overvoltage will be discussed in detail.

Chapter 5

Enhanced autonomous coordinated voltage control techniques

An enhanced voltage management technique is presented in this Chapter where the co-ordination of two local PVDG inverter control techniques are leveraged to increase the PVDG integration from 35.65% to 66.7% of distribution transformer (DT) of 500 kVA. This research work is disseminated as journal publication[12] which can be found in List of Publications

5.1 Network specification and recorded data

Here Figure 5.1 represents the 31 PVDGs integration in the sub-urban Dublin LVDN. Again, in this study all the 74 residents receive the same solar irradiance which is obtained from the Whitworth Meteorological Observatory in Manchester, UK of the year 2013 [111]. A similar procedure to convert the irradiance observed from meteorological data into single phase PV generator profiles is adopted as described in [85]. The typical single phase domestic customer PVDG generator and load profile data having a resolution of 5 minutes was acquired from [112].

[12] S. Pukhrem, M. Basu, M. F. Conlon, and K. Sunderland, "Enhanced Network Voltage Management Techniques Under the Proliferation of Rooftop Solar PV Installation in Low-Voltage Distribution Network," IEEE J. Emerg. Sel. Top. Power Electron., vol. 5, no. 2, pp. 681–694, 2017.

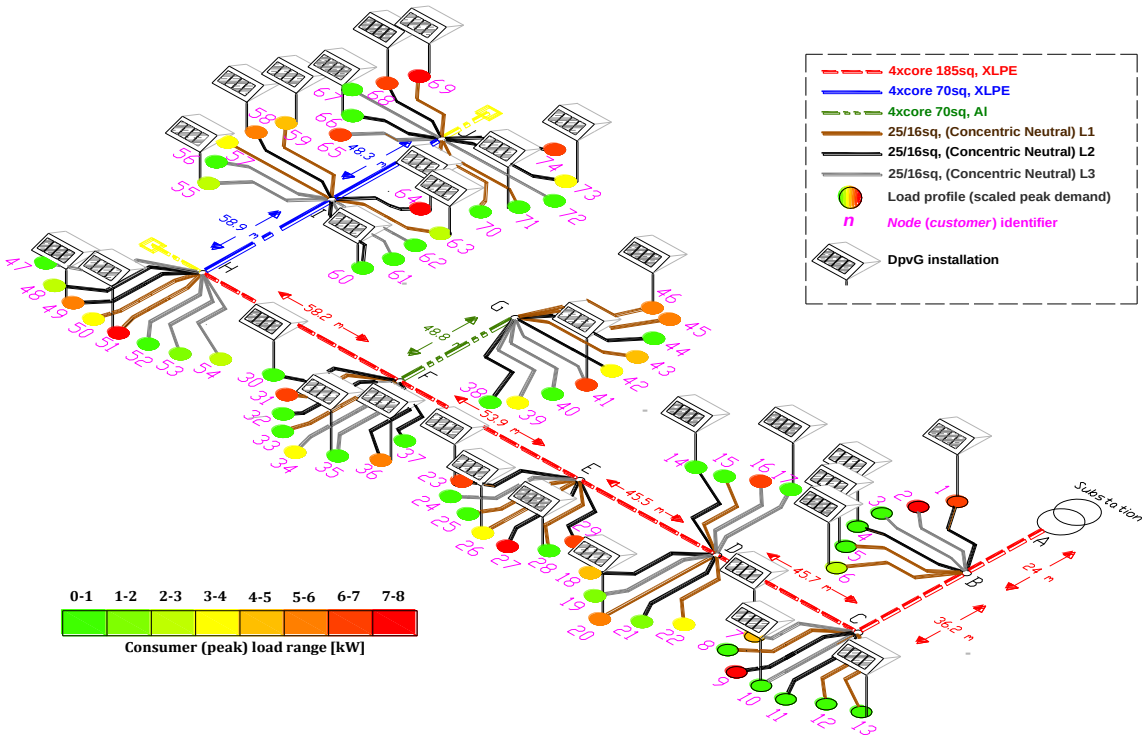

Figure 5.1 : LVDN illustrating the connection of rooftop 31 PVDGs installation

Figure 5.2 illustrates both the load and PVDG profiles. The PVDG output is considered over the course of a single day. It is further assumed that all the 74 residents have similar residential load profiles representative of typical single-phase domestic customers with different peak demands.

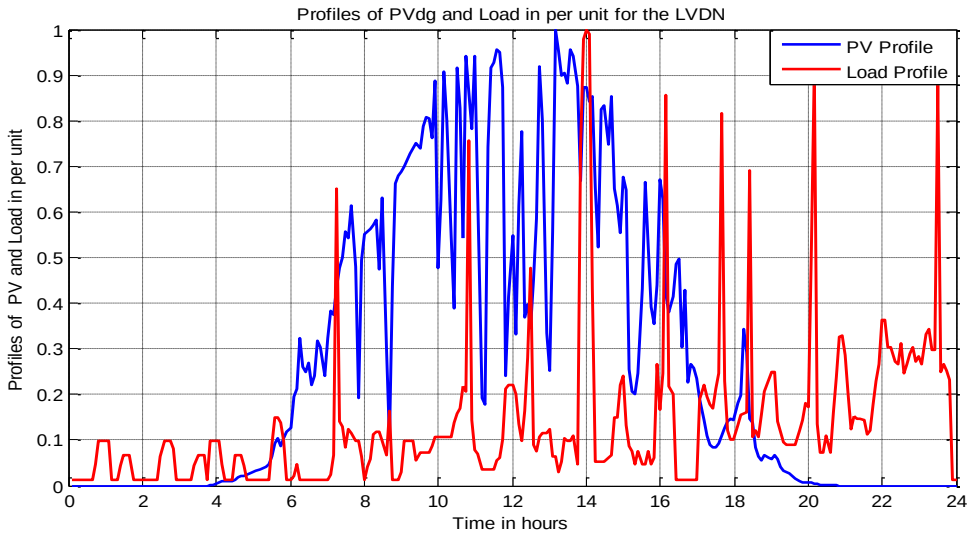

Figure 5.2 : Recorded PVDG and Load profile in per unit

Table 5.1 summarizes the load and PVDG distributions where two types of PVDG penetration scenarios are considered, namely with 31 and 58 PVDG installations, which represent a penetration level of 35.65 % and 66.70% of the DT 500 kVA rating respectively. Due to significant integration of 58 PVDG out of 74 domestic customers, the manifestation of overvoltage is observed in the downstream nodes starting from node 55 to node 74 which is shown in Figure 5.3.

Table 5.1 : Customer peak load demand and PVDGs installation distribution

Peak load distribution in kW	**% of customer connecting the load (out of 74)**	**% of customer installing PVDG (out of 31)**	**% of customer installing PVDG (out of 58)**
$0 < Peak_{load\ demand} < 1$	47.3	48.39%	39.66%
$1 < Peak_{load\ demand} < 6$	33.8	29.03%	37.93%
$Peak_{load\ demand} \geq 6$	18.9	22.58%	22.41%

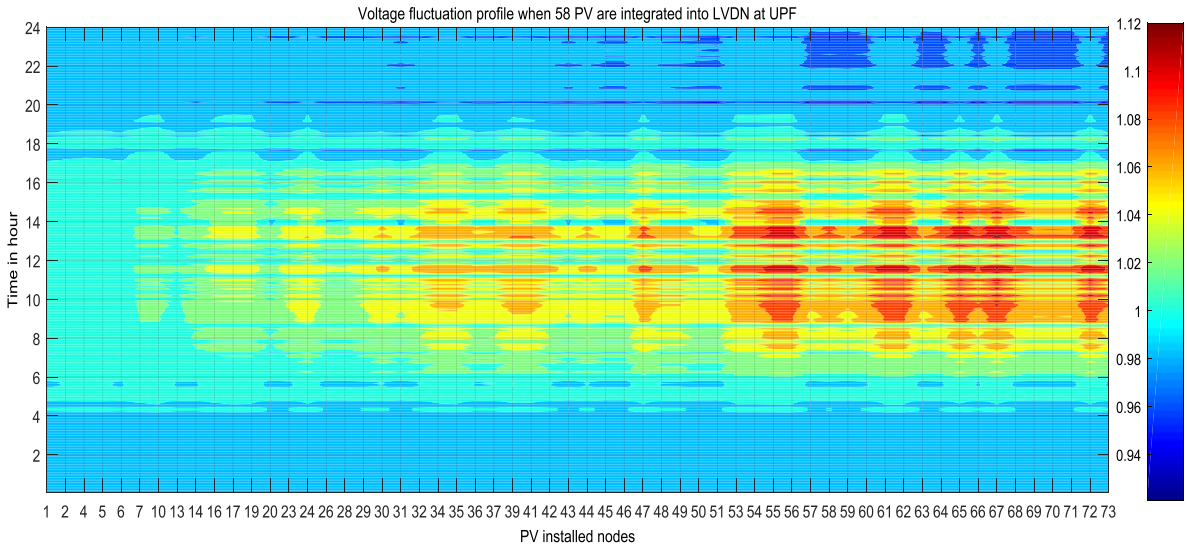

Figure 5.3 : Contour plot for Voltage fluctuation profile in each 58 PVDG installed nodes

5.2 Summary of the existing droop control

Here, the three best known local droop control techniques i.e. PF(P), Q(U) and PF(U) are simulated and their advantages and disadvantages. PF (P) control (power factor as a function of the PVDG active power) is implemented as a function of PVDG active power which depends on irradiance and temperature. Whenever high irradiance coincides with high peak demand, the voltage rise may not exceed the overvoltage

limitation and the requirement of such a technique will be unnecessary. Furthermore, it regulates all the PVDG GTI (Grid-Tied-Inverter) connected to the public network irrespective of the voltage profile. The Q (U) controller (reactive power as a function of the local voltage) on the other hand exchanges reactive power when the solar PVDG sources are not the primary source of the voltage fluctuation.

This method directly uses the instantaneous information of the local voltage which varies as a consequence of the PVDG power production and the activity of the load demand in its vicinity. Again, Q (U) control may not react to critical voltage fluctuations at the far end feeder when it is embedded to the rooftop PVDG GTI located near the distribution transformer (DT). Furthermore, PF (U) controller (power factor as a function of the local voltage) also exchanges reactive power when the solar PVDG source is generating active power. However, the droop control of PF (U) and Q (U) are different as the former uses power factor and the latter uses reactive power. But under equal grid impedances and generation of active power, the two functions can be made to generate an equal amount of reactive power. Samadi *et al*.in [64] also evaluated the different technical aspects of the recent German grid code called an active power dependent standard characteristic curve, Q (P). In that document, the authors utilize the voltage sensitivity matrix to calculate the exact reactive power required in each node. However, if combinations of coordinating algorithms among the existing voltage control techniques are of any additional advantage, these have not been addressed in detail.

5.3 Design of Coordinating Algorithms

The objective of this study is to enhance PVDG penetration by combating critical voltage fluctuation with the help of combining a few coordinating algorithms. The importance of this sub-section lies in implementing two different algorithms in a real suburban Dublin LVDN without exceeding the VA rating of the converters. Power factor (PF), node voltage (U) and active power (P) are the three critical informations for each of the nodes. No communications between nodes are necessary. The significant contribution of this work is to introduce two novel co-ordination of the existing local droop controllers and further proposing a methodology to limit the frequent switching between the two droop controllers. The two coordinating techniques are: 1) power factor as a function of both instantaneous node voltage and active power, 2) reactive and active power as a function of instantaneous node voltage. Through these two coordinating techniques higher PVDG could be integrated without affecting the DSO's core activity.

The design of these coordinating algorithms is discussed in the following paragraphs. Whenever any node voltage in LVDN exceeds the critical voltage limit i.e.1.1 p.u. and simultaneously the available VAR levels are exhausted, the coordinating algorithms extend the voltage support controllability of each of the PV GTIs. The first coordinating algorithm combines two RPCs (Reactive Power Control) namely, PF (U) and PF (P). As discussed earlier, PF (U) is a function of instantaneous node voltage and can only support voltage until the GTI VA rating is reached. GTIs closer to DT are unable to support voltage fluctuation at the far end when it is embedded with PF (U). In such cases, another RPC such as PF (P) could be effective as it can regulate all the GTIs in the LVDN irrespective of the nodal voltages. The

procedure for such a coordinating algorithm is as follows. Initially, all PV GTIs are embedded with PF (U) where it maintains the voltage support mechanism up to the PV GTI VA rating. Once any node voltages excess the first voltage limit (1.08 p.u.) and simultaneously the VAR option is exhausted, the voltage support technique will switch from PF (U) to PF (P). Subsequently, the corresponding required PF (Ux) for such node voltage (> 1.08 p.u.) is calculated using the droop curve, equations, and parameters as given in Table 5.2. Using this new PF (Ux) as one of the droop parameters, the voltage support technique switches to PF (P) where it controls the PF of all PV GTIs irrespective of the voltage information. Moreover, when the node voltage is less than 1.08 p.u., the voltage support technique reverts back to PF (U) from PF (P). Thus, through such a coordinating technique the voltage support in LVDN can be achieved when the PV penetration increases.

The second coordinating algorithm works in a similar manner, but it combines one RPC namely, Q (U) and one APC (Active Power Control), namely P (U). As mentioned earlier in the introduction, Q (U) could be inefficient as a voltage support mechanism for the far-end node when the VAR exchange is restricted to the VA rating. Therefore, APC such as P (U) could assist in voltage support in a similar situation. The procedure for the analogous coordinating algorithm is as follows.

Table 5.2 : Different coordinating techniques and their corresponding droop characteristics

Techni-ques	Droop curve	Droop Equations	Droop parameters
PF(U) & PF(P)	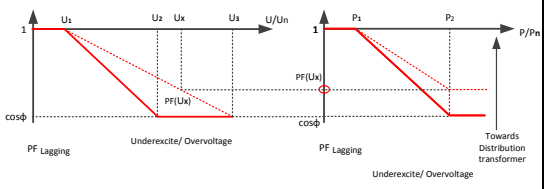	$PF(U,P) = \begin{cases} cos\Phi_{UPF} & ,U \le U_1 \\ -1+(cos\Phi+1)\left(\frac{U-U_1}{U_2-U_1}\right) & ,U_1 < U \le U_2 \\ PF(Ux) = -1+(cos\Phi+1)\left(\frac{U-U_1}{U_3-U_1}\right) & ,U > U_2 \\ -1+(PF(Ux)+1)\left(\frac{P-P_1}{P_2-P_1}\right), & P_1 \le U \le P_2 \\ cos\Phi & ,U > U_3 \end{cases}$	$U_1 = 1.04$ $U_2 = 1.08$ $U_3 = 1.1$ $P_1 = 1$ $P_2 = 0.5$ $cos\Phi = [0.9]$ lagging $cos\Phi_{UPF} = 1$
Q(U) & P(U)	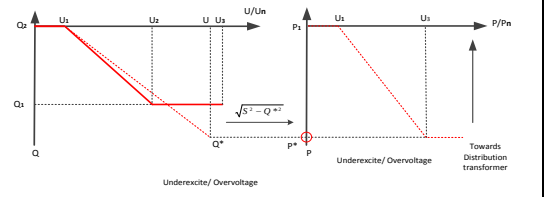	$Q(U) = \begin{cases} Q_2 & ,U \le U_1 \\ Q_3 = \left[Q_2+(Q_1-Q)\left(\frac{U-U_1}{U_2-U_1}\right)\right] & ,U_1 < U \le U_2 \\ \text{Change the droop curve to } P(U) & ,U > U_2 \end{cases}$ $P(U) = \begin{cases} Q^* = Q_2+(U-U_1)\left(\frac{Q_1-Q_2}{U_3-U_1}\right) & ,U > U_2 \\ P^* = \sqrt{S^2-Q^{*2}} & \\ P_1+(U-U_1)\left(\frac{P^*-P_1}{U_3-U_1}\right) & ,U_1 \le U \le U_3 \\ P^* & ,U > U_3 \end{cases}$	$Q_1 = -Pn\sqrt{\frac{1}{(cos\Phi)^2}-1}$ $Q_2 = 0$ $U_1 = 1.04$ $U_2 = 1.08$, $U_3 = 1.1$ $P_1 = 1$ $cos\Phi = [0.9]$ lagging

All the PV GTIs are embedded with Q (U) at the beginning. When any node voltages exceed the first voltage limit (1. 08p.u) and simultaneously the VAR support is exhausted, the voltage support technique will switch from Q (U) to P (U). Furthermore, the corresponding Q* to support the voltage when the node voltage is greater than 1.08 p.u. is calculated using the droop curve, equations, and parameters as given in Table 5.2. Using this new Q*, the corresponding P* is calculated and assigned as one of the droop parameters for the voltage support technique P (U) where it controls the active power (P) of all PV GTI in terms of the instantaneous voltage information. Additionally, once the node voltage is less than 1.08 p. u, the voltage support technique will revert back to Q (U) from P (U). Thus, through such a coordinating technique, equivalent LVDN voltage support is achievable by assigning the required Q* for voltage support and thereby curtailing the minimum required P. Hence, through these two coordinating algorithms, effective voltage support can be achieved by overcoming each individual controllability limitation.

The procedure to execute the voltage management technique in the LVDN is as follows. Initially, all the LVDN parameters (line parameters, the distance between each node and buses, bus data information), PVDG and load profiles are accumulated to perform a quasi-time series power flow analysis using the OpenDSS program for every 5 minutes. The implementation of power flow in a co-simulation platform between MATLAB and OpenDSS is realised to implement these co-ordinating algorithms. Initially, all the PVDG and load demand are equipped with UPF. The power flow will stop only when the total time reaches 1440 minutes which corresponds to 24 hours. For every 5-minute time step, the instantaneous voltage profile at each of the PVDG installed nodes (node '*p*') are monitored '$\left(V_{t_n}\right)_p$' where '*p*' denote a particular PV installed node and 't_n' is the instantaneous time. If $(V_{t_n})_p \leq V_j$ is satisfied where V_j =1.04 p.u, each PVDG GTIs will stay in an idle stage i.e. their PF will be UPF. Otherwise, if $V_j < \left(V_{t_n}\right)_p \leq V_k$ is satisfied where $\mathbf{V_k}$=**1.08** p.u, then the '*Q*' or '*PF*' limiter algorithm is activated. '*Q*' or '*PF*' limiter algorithm is given in steps a-e. Due to rapid fluctuation of irradiance; the '*Q*' or '*PF*' limiter algorithm is necessary to mitigate frequent switching between two droop characteristics.

a. Compute the static 'Q' or 'PF' from the droop characteristics from Table 10.
b. Find the absolute difference between the previous i.e. $\left(Q_{t_{n-1}}\right)_p$ or $\left(PF_{t_{n-1}}\right)_p$ and present i.e. $\left(Q_{t_n}\right)_p$ or $\left(PF_{t_n}\right)_p$ values of 'Q' or 'PF'. In other words, $\Delta Q = \left|\left(Q_{t_n}\right)_p - \left(Q_{t_{n-1}}\right)_p\right|$ or $\Delta PF = \left|\left(PF_{t_n}\right)_p - \left(PF_{t_{n-1}}\right)_p\right|$.
c. If both $\left(V_{t_n}\right)_p > \left(V_{t_{n-1}}\right)_p$ i.e. difference between the present and past instantaneous node voltage and $\Delta Q < \varepsilon_1$ or $\Delta PF < \varepsilon_2$ conditions are

simultaneously satisfied, then assign the new required 'Q' or 'PF' as the present static value calculated from the droop equation.

d. If $\left(\boldsymbol{V_{t_n}}\right)_{\boldsymbol{p}} > \left(\boldsymbol{V_{t_{n-1}}}\right)_{\boldsymbol{p}}$ is satisfied and $\boldsymbol{\Delta Q} < \varepsilon_{\mathbf{1}}$ or $\boldsymbol{\Delta PF} < \varepsilon_{\mathbf{2}}$ is not satisfied, then the required 'Q' or 'PF' is calculated as follows: $\left(\boldsymbol{Q_{t_n}}\right)_{\boldsymbol{p}} = \left(\boldsymbol{Q_{t_{n-1}}}\right)_{\boldsymbol{p}} + \boldsymbol{\Delta Q}/\delta$ or $\left(\boldsymbol{PF_{t_n}}\right)_{\boldsymbol{p}} = \left(\boldsymbol{PF_{t_{n-1}}}\right)_{\boldsymbol{p}} + \boldsymbol{\Delta PF}/\delta$.

e. However, if $\left(\boldsymbol{V_{t_n}}\right)_{\boldsymbol{p}} > \left(\boldsymbol{V_{t_{n-1}}}\right)_{\boldsymbol{p}}$ is not satisfied,then, the required 'Q' or 'PF' is calculated as follows: $\left(\boldsymbol{Q_{t_n}}\right)_{\boldsymbol{p}} = \left(\boldsymbol{Q_{t_{n-1}}}\right)_{\boldsymbol{p}}$ or $\left(\boldsymbol{PF_{t_n}}\right)_{\boldsymbol{p}} = \left(\boldsymbol{PF_{t_{n-1}}}\right)_{\boldsymbol{p}}$.

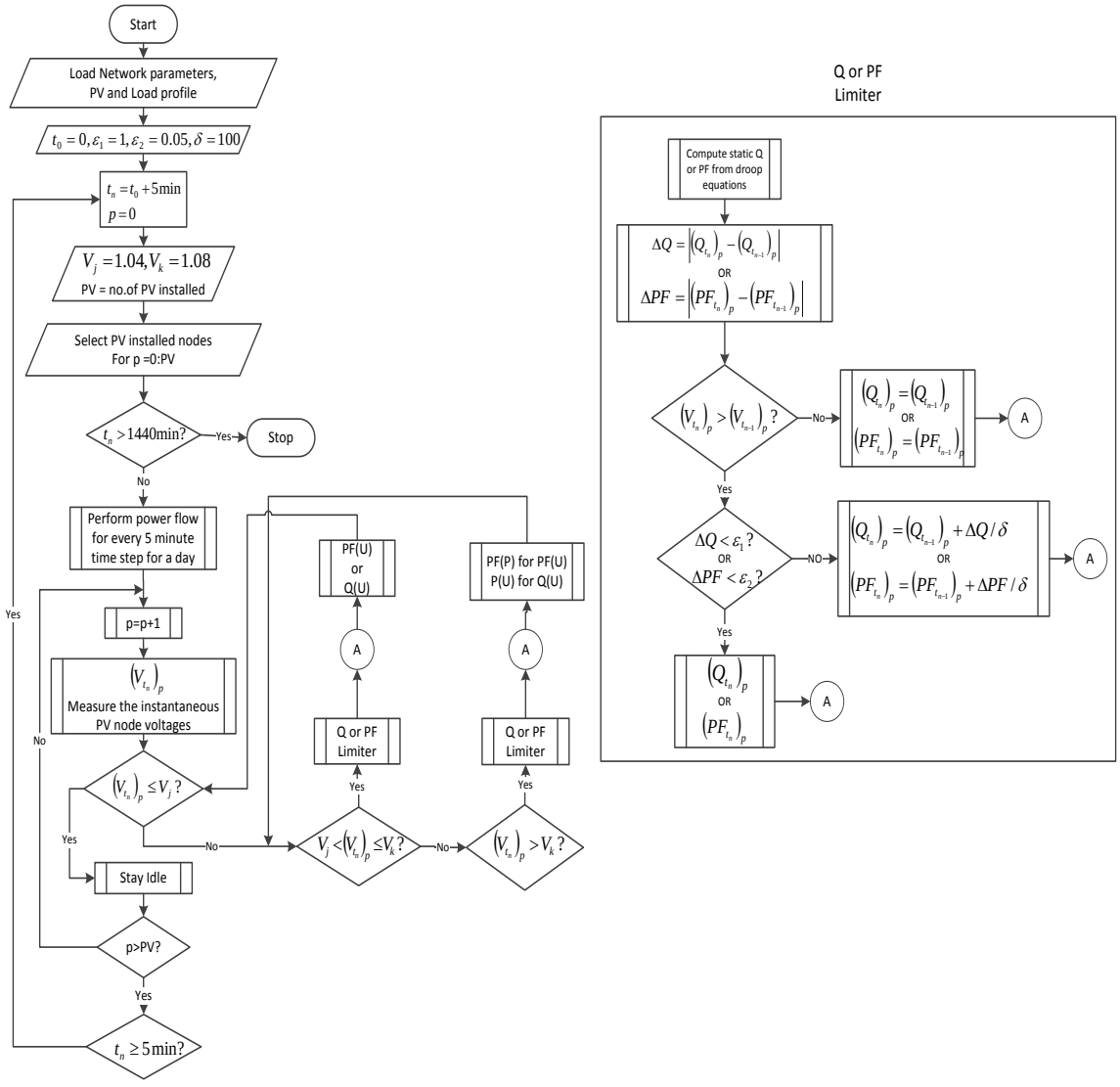

Figure 5.4 : Coordination algorithm

After the ‘Q’ or ‘PF’ limiter algorithm is activated, the required ‘Q’ or ‘PF’ for Q (U) or PF (U) voltage control is assigned to all the PVDG GTI without exceeding the VA rating of the GTIs. However, if $\boldsymbol{V_j < \left(V_{t_n}\right)_p \leq V_k}$ is not satisfied and simultaneously $\boldsymbol{\left(V_{t_n}\right)_p > V_k}$ then the ‘Q’ or ‘PF’ limiter algorithm is activated thereby computing the necessary corresponding PF (Ux) or Q* from the $\boldsymbol{\left(V_{t_n}\right)_p}$ as the extreme measure. Subsequently, the droop characteristic changes from Q (U) to P (U) or PF (U) to PF (P). Finally, depending on $\boldsymbol{\left(V_{t_n}\right)_p}$ value if $\boldsymbol{V_j < \left(V_{t_n}\right)_p \leq V_k}$ is satisfied, the droop characteristic reverts back from P (U) to Q (U) or PF (P) to PF (U) only after passing through ‘Q’ or ‘PF’ limiter. The process continues until the simulation time (1440 minutes) is over for the entire PV installed node. The entire flow of the process is shown as a flowchart in Figure 5.4. In the following part of this study, different RPCs and two coordinating algorithms are simulated to validate their performance. Herein, $\varepsilon_1, \varepsilon_2$ and δ are obtained by a heuristic method. These values have a direct influence on the performance of the network voltage management control.

5.4 Simulation results and discussions

Figure 5.5 shows the statistical variation in the voltage unbalance at node “J” of the distribution network presented in Figure 5.1. Again, typically, the standard level requirement is that the unbalance is less than 2% for 95% of a defined period (typically one week). It can be seen that the standard is met in this case.

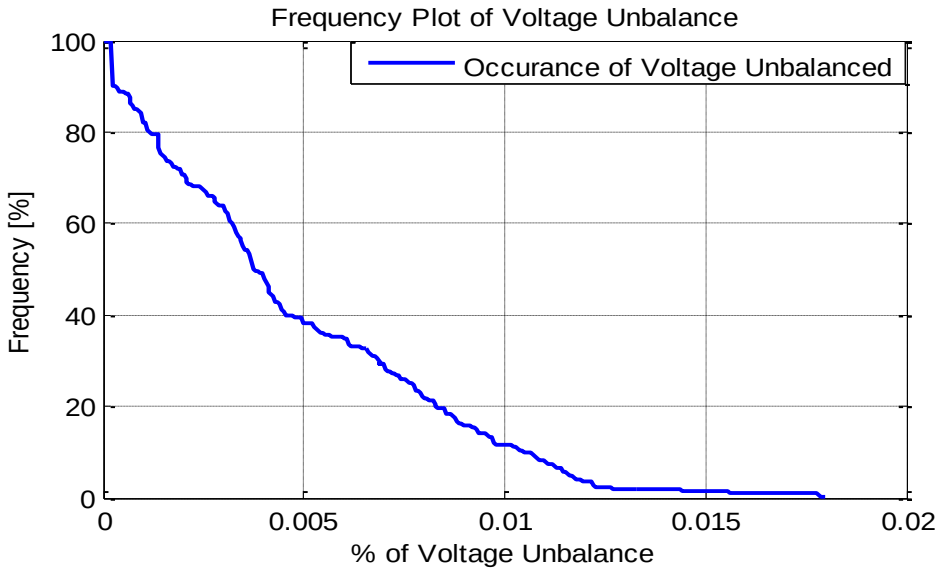

Figure 5.5 : Frequency vs % of Voltage unbalances at pillar J

Figure 5.6 shows the boxplot of three voltage profiles namely 1st, 73rd and 74th nodes (designated by (a), (b) and (c)) under different techniques namely UPF, Q (U), PF (P), PF (U), Q(U) & P(U) and PF(U) & PF(P). As shown, when all GTIs are embedded with UPF, 73rd and 74th nodes exceed the overvoltage limitation which is +10 % of nominal value. In such a situation, the number of PVDG installations upstream, the far end node, i.e. node 74th, is affected severely without any PVDG installation at its premises. Managing voltage under increased penetration of PVDGs thus becomes an important aspect for all the PV GTIs to alleviate any the voltage fluctuation in the LVDN. From Figure 5.6, when different RPCs are embedded in each of the PV GTIs, it can be seen that voltage management controllability is insufficient and inefficient. For example, with Q (U) and PF (U) alone, voltage management is insufficient as both nodes 73 and 74 nearly exceed 1.1 p.u. even after utilizing the maximum available kVAr from each GTI as shown in Figure 5.6 (b) for node 73. Referring to PF (P) technique, over voltage is alleviated in both nodes 73 and 74 with a higher voltage fluctuation at node 1 when compared to UPF. The reason for such uneven voltage management is due to its controlling technique of PF (P) where the PF

is regulated as a function of PV active power. The consequences for the PF (P) technique is that irrespective of the instantaneous node voltage, all the PV GTIs will regulate their PF in which reactive power exchange is the same for all the PVDG installed nodes. Such phenomena can be observed in Figure 5.7 (a) and (b) at nodes 1 and 73 respectively, where an equal amount of reactive power is exchanged for the PF (P) techniques.

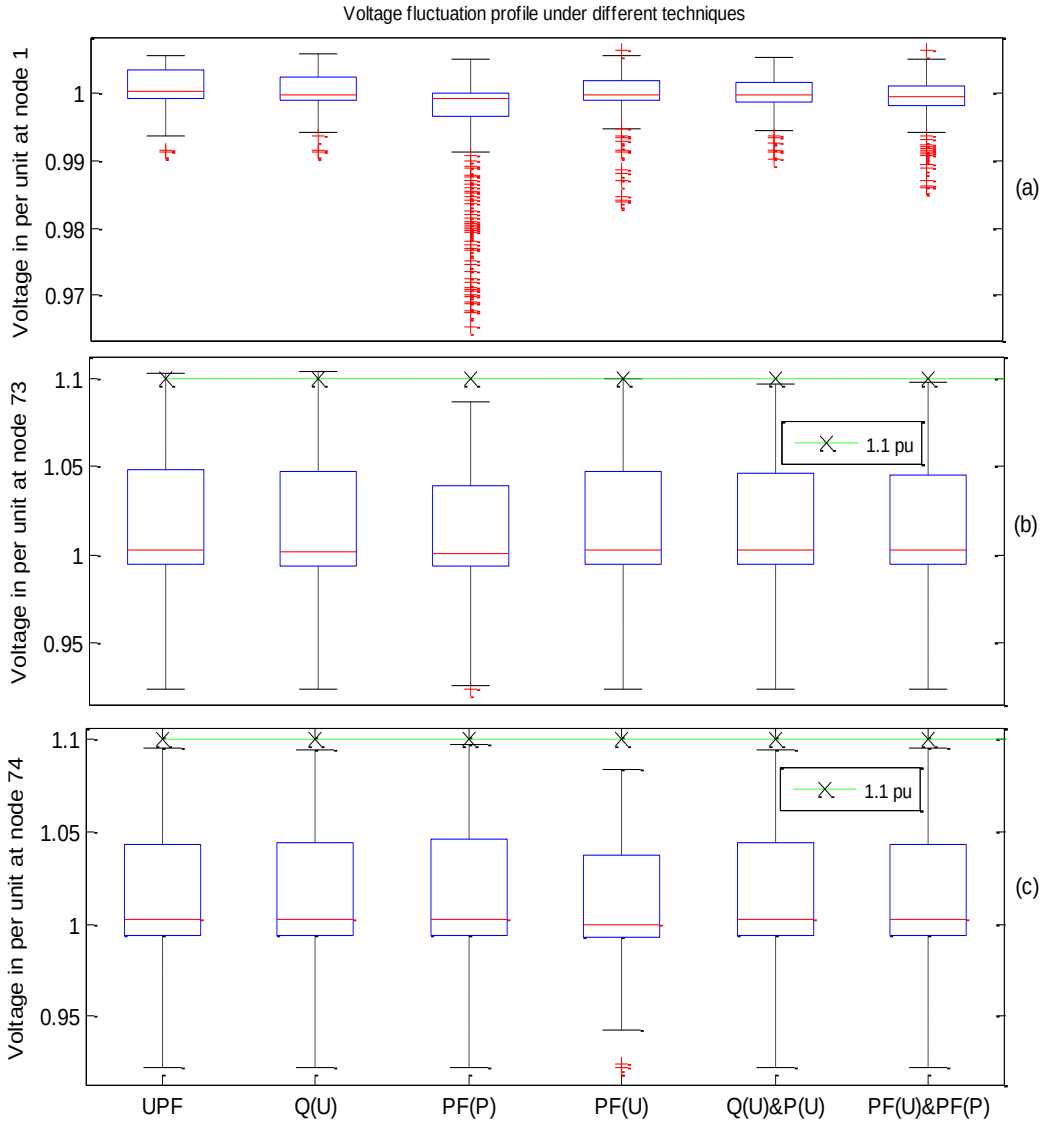

Figure 5.6 : Boxplot of voltage fluctuation profile at nodes (a) 1 (b) 73 and (c) 74 under different techniques when 58 PVDG are installed in LVDN

To overcome each individual controllability limitations of RPCs, the two coordination algorithms namely Q(U) & P(U)and PF(U) & PF(P) shows significant

improvement in managing the voltage in all the nodes evenly as shown in Figure 5.6. Furthermore, PF (U) & PF (P) and Q (U) & P (U) introduce less voltage fluctuation at node 1 as compared with PF (P) and PF (U). As shown in Figure 5.7 (a) apart from the PF (P) technique, all other techniques do not exchange any reactive power as the voltage at node 1 is under the limit. On the other hand, in Figure 5.7 (b), except for the UPF technique, all other techniques exchange reactive power to manage the voltage fluctuation at node 73. It can be observed from Figure 5.7 (b), with coordinating algorithm techniques; the amount of reactive power is optimally utilized to combat any overvoltage violation at node 73. In terms of reactive power exchange, Q (U) & P (U) absorb the least amount of reactive power (with no reactive power exchange in most cases) as compared with other techniques in combating the voltage fluctuation which is shown in Figure 5.7 (b).

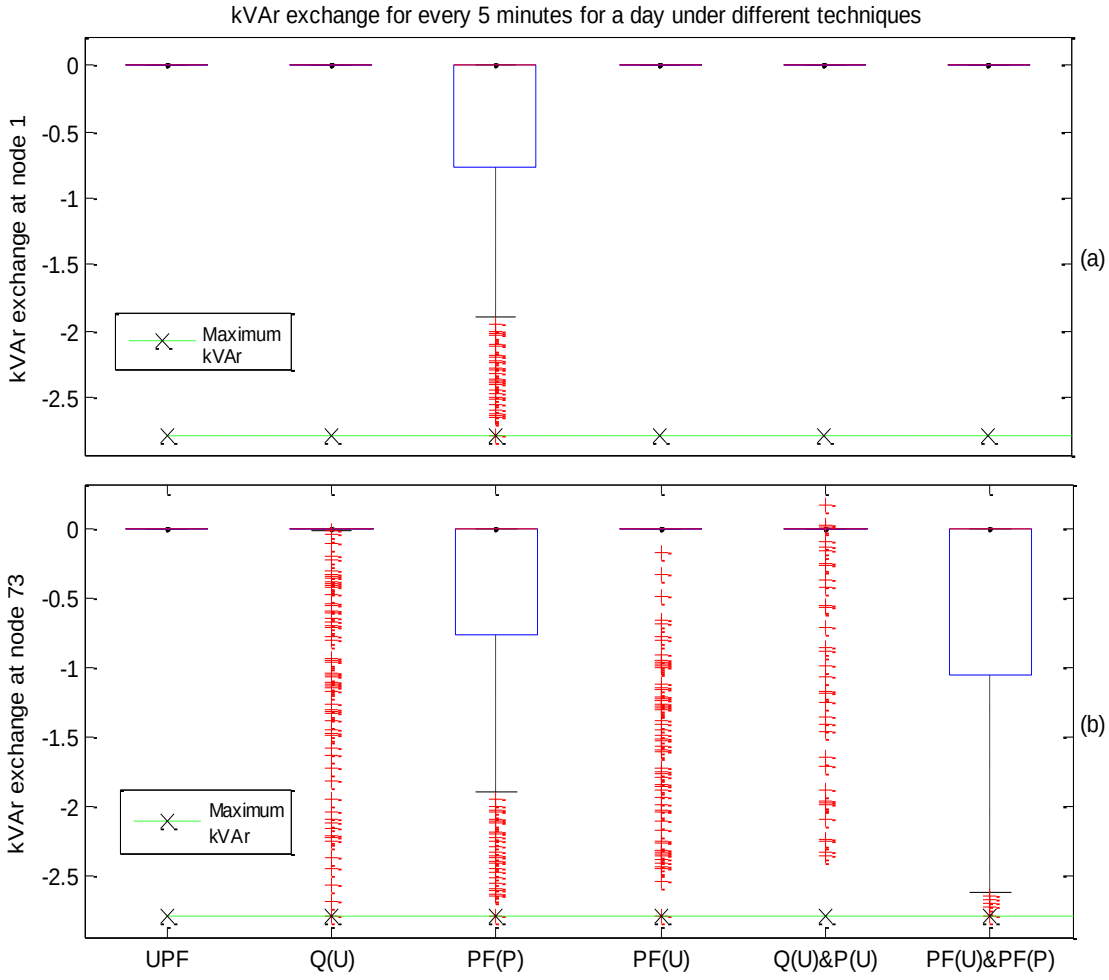

Figure 5.7 : Boxplot of the amount of reactive power exchange for every 5 minutes for an entire day at nodes (a) 1 and (b) 73 under different techniques when 58 PVDG are installed in LVDN

Table 5.3 shows average reactive and active power exchange for one day at node 73 under different techniques. Among RPCs, PF (P) absorbs the highest average reactive power which is about 0.47 kVAr for the whole day. The two coordinating algorithms, namely, PF (U) & PF (P) and Q (U) & P (U) absorb fairly same average reactive power as compared with Q (U) and PF (U). However, in the Q (U) & P (U) technique, a small average amount of active power is curtailed which is almost negligible. With respect to voltage alleviation, PF (U) & PF(P) and Q(U) & P(U) is similar as it can be seen in Figures 5.6 (b) and (c).

Table 5.3 : Average reactive and active power exchange for a day at node 73 under different techniques

Techniques	UPF	Q(U)	PF(P)	PF(U)	Q(U) & P(U)	PF(U) & PF(P)
kVAr absorbed/day	0	0.30	0.47	0.35	0.230	0.23
kVAr exported/day	0	0	0	0	0.002	0
kW curtailed/day	0	0	0	0	0.018	0

Figure 5.8 shows the demonstration of voltage fluctuation management at node 73 through the proposed two coordinating algorithms. Here, instantaneous PV installed node voltage is continuously measured and appropriately the control actions are taken as described in the above paragraph. It can be observed from Figure 5.8 that the proposed two coordinating algorithms not only alleviate the overvoltage but also try to smoothen and stabilize the voltage.

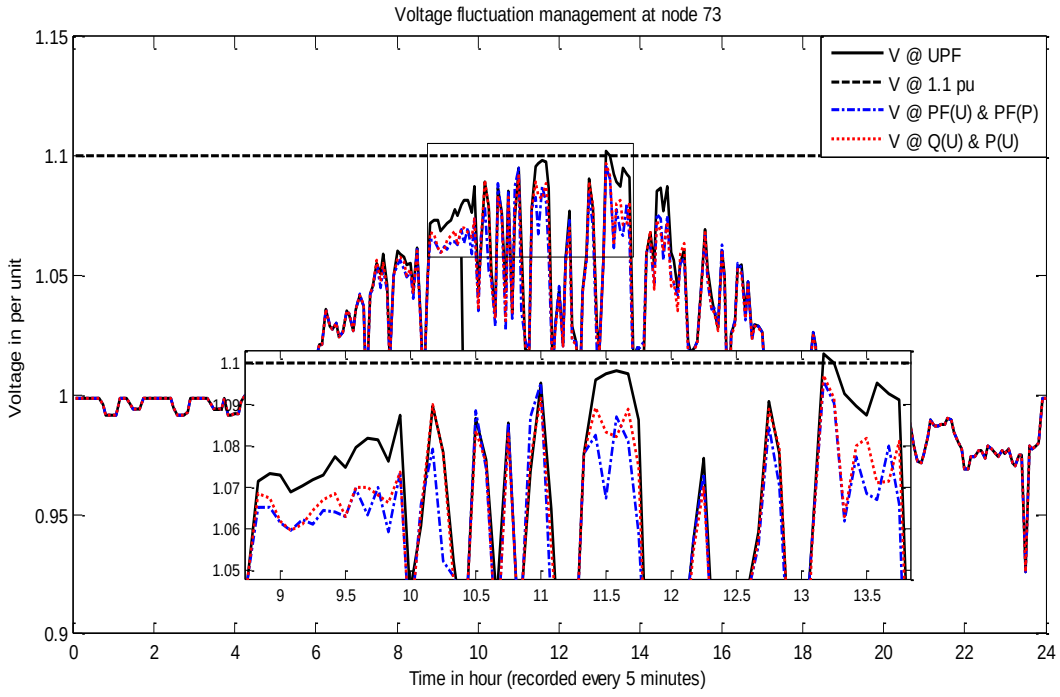

Figure 5.8 : Demonstration of voltage fluctuation management through two coordination algorithms

Table 5.4 presents a performance summary on different techniques when 58 PVDGs are integrated into the LVDN. As presented in Table 5.1, PF (P) maintains the over voltage fluctuation at a cost of high average circuit losses and transformer loading for a

day, whereas Q (U) and PF (U) show an inability to alleviate the over voltage. On the other hand, coordinating algorithm Q (U) & P (U) maintains the over voltage and the least transformer loading at a cost of curtailing an average active power of 0.018 kW per day. In terms of voltage management, the two proposed algorithms Q (U) & P (U) and PF (U) & PF (P) manage to stabilise each and every PV installed node voltage under the limit. In contrast to the controllability of effective voltage management, circuit losses, and transformer loading; Q (U) & P (U)and PF (U) & PF (P) techniques show significant improvement where PF (U) & PF (P) imposes higher circuit and transformer losses as compared to Q (U) & P(U).

Table 5.4: Performance table of all the techniques

Techniques applied under 58 rooftop PVDGs penetration	**Average losses (CL) for a day CL=(Line +Transformer) losses**		**Average transformer loading for a day**		**Average reactive and active power exchange for a day at node 73**			**Voltage at Node 73 in pu**	**Voltage at Node 74 in pu**
	kW	**kVAr**	**In kVA**	**In % of DT**	**kVAr absorb/day**	**kVAr export/day**	**kW curtail/day**		
UPF	3.90	3.74	85.02	59.78	0	0	0	1.102	1.099
Q(U)	4.03	3.81	85.47	59.61	0.30	0	0	1.103	1.100
PF(P)	4.55	4.43	89.60	65.00	0.47	0	0	1.086	1.083
PF(U)	4.09	3.85	85.57	59.63	0.35	0	0	1.100	1.097
Q(U) & P(U)	3.89	3.72	84.58	59.64	0.23	0.002	0.018	1.097	1.094
PF(U)& PF(P)	4.19	3.93	86.00	60.10	0.23	0	0	1.097	1.095

Voltage fluctuation distribution at node 74, where PVDG is not installed in its premises, is shown in Figure 5.9. Referring to Figure 5.9, almost 90% of all the techniques export electricity at 1 p.u but with UPF operation the voltage fluctuation reaches up to 1.1p.u. for almost 20 % of the time. In terms of the voltage distribution profile PF (P) shows significant improvement in maintaining the voltage within the limit at node 74 followed by Q (U) & P (U) and PF (U) & PF (P). Both PF (U) and Q (U) techniques show inadequacy in maintaining the voltage within the limit where

almost above 10% of the voltage fluctuates within the critical limit. However, with respect to circuit losses and transformer loading, Q (U) & P (U) is one of the best voltage management techniques where it maintains and stabilises the voltage below the critical limit with the negligible amount of active power curtailment.

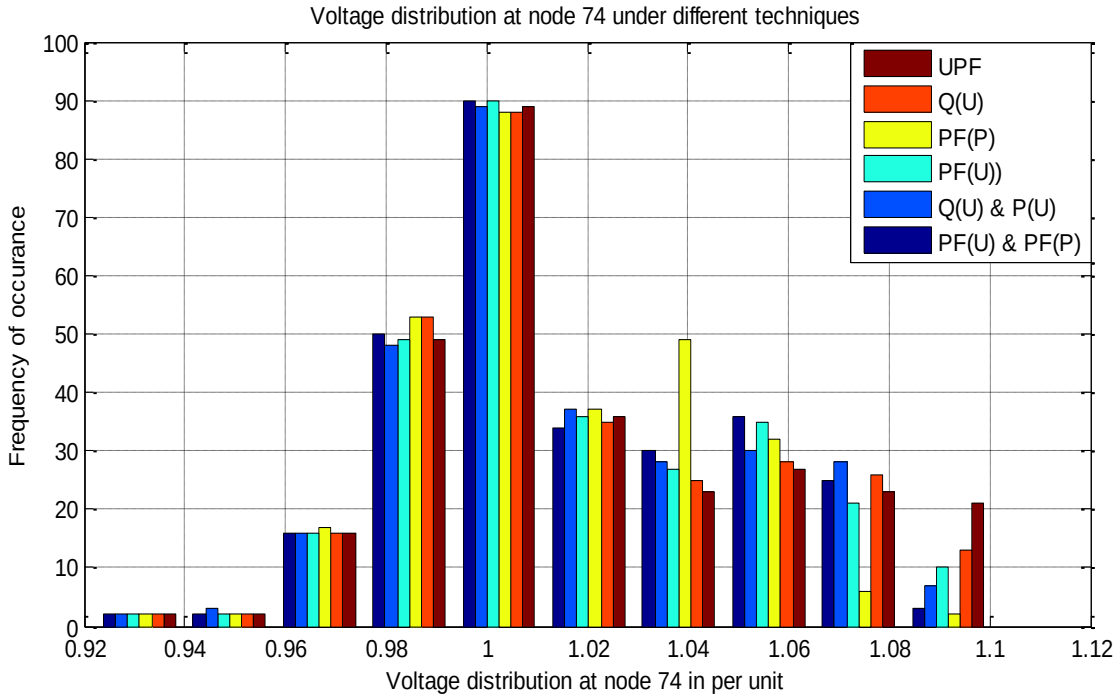

Figure 5.9 : Voltage distribution for node 74 under different techniques

5.5 Conclusion

The results and comparative studies presented here show that a co-ordination of Q (U) & P (U) provides higher compliance with the allowable voltage regulation level. It also significantly facilitates to increase the PVDG penetration level from 35.65 % to 66.7% of DT kVA rating. Further, it can be seen from the histogram of the most remote node in the network (node 74, Figure 5.9) that Q (U) & P (U) is one of the best voltage management technique where it maintains and stabilises the voltage below the critical limit with a negligible amount of active power curtailment. On the other hand, PF (U) & PF (P) impose higher circuit losses and transformer loading as compared to that of Q

(U) & P (U) (see Table 5.4). The ‘Q’ or ‘PF’ limiter algorithm further enhanced the proposed voltage control techniques by alleviating any associated voltage overshoots.

Chapter 6

Conclusion and future work

6.1 Conclusion

The choice of steady state power system study for this research work was highlighted in Chapter 1. As the PVDG penetration increases in an LVDN, the core activities of the DSOs, which are to maintain a stable, reliable and cost-effective electricity supply to all customers are likely to be challenged. The national regulatory authority (NRA) may require careful consideration of these challenges if the policy is to allow for the integration of higher renewable energy. This research has addressed these challenges by proposing three research objectives which is presented in 2.5 Research Objectives.

Chapter 3 investigates and quantifies the steady state impacts due to temporal and spatial characteristics of both load demand and PV generation profiles when integrated into an LVDN. A Monte-Carlo simulation is chosen to quantify the power quality (PQ) impacts and from the results it was observed that site overvoltage is inevitable if the penetration of PVDG increases.

Chapter 4 further evidenced that, as the PVDG integration increases, the DSO's core activities will increase, and they need to be incentivised if they maintain their core activities. The incentives to maintain their core activities under such a situation will be impacted if the net-metering system in conjunction with a volumetric tariff structure is adopted. However, the consideration of a capacity-based tariff structure with a net-

metering system in conjunction with a volumetric tariff structure shows an improvement in the total revenue generated for the DSO which further incentivises it to maintain its core activities.

Chapter 5 proposes an enhanced co-ordinating method to alleviate the overvoltage that may arise during the increased integration of PVDG in an LVDN. This method focuses in mitigating the most likely PQ impact, i.e. site overvoltage without any requirement of grid reinforcement. The smart inverter functionality is leveraged by optimally controlling the active and reactive power to alleviate the site overvoltage.

6.2 Future work

The subsequent future work of this research is discussed in the following paragraphs by recalling the completed work and addressing further potential contribution.

6.2.1 Reactive power planning

In Chapter 3, three PQ impact metrics of overvoltage, voltage unbalance and voltage sags were considered to quantify the impacts within the LVDN due to the increased integration of PVDG. Apart from these PQ impact metrics, there is a high likelihood of declining reactive power requirement in the distribution network. Traditionally the direction of reactive power flow has been from the sub-transmission network into the distribution network and the DSO plans according to this assumption. However, this situation may be impacted in the future when the load demand is at a minimum, and the PV generation is at a maximum leading to reactive power injection

back to the sub-transmission and transmission networks. This could impact seriously in the voltage regulation at these networks resulting to further challenges for the transmission system operators (TSO). Adopting the same method for quantifying the PQ impact metrics, the reactive power exchange at the distribution transformer of the LVDN can be monitored. This monitored reactive power flow can be quantified and better plan the alleviation of voltage regulation issues as describe in [119] and manage the TSO-DSO interaction in relation to voltage regulation. Apart from reactive power planning, consideration of the time durations and the expected number (frequency) of voltage sags are to be considered in an LVDN with increased integration of PVDG [120].

6.2.2 Capacity-based tariff structure

From Chapter 4, the method of including a capacity-based tariff structure with net metering in conjunction with volumetric tariff as a means to recover the sunk cost of the DSO will require further exploration. Firstly, whether the method of computing capacity-based tariffs on a twelve-month hourly peak demand is a cost-reflective way for recovering DSOs' sunk costs may be of significant question. Multiple alternatives are being discussed in [121], such as more frequent peak demand measures, highest measured hourly power over a month and considering demand which coincides with system-wide critical peaks. The selection of these alternatives may have a significant effect on designing the network tariffing structure and thus, this would require a justification on the selection of any alternative. Another aspect is to investigate how customers behave under the revised tariff i.e. a capacity-based tariff structure with net metering in conjunction with volumetric tariff. The follow up question is how does the price elasticity of the demand in the short and long run relate with the marginal revenue

of the DSO [122]. There is no one solution in designing a network tariff structure where there are multiple objectives from the policy makers in promoting a retail tariff structure that underpin the decarbonising of the electricity system through improved energy efficiency and higher adoption of renewable electricity within future electricity markets [122].

6.2.3 Cost benefit analyses

From the Chapter 5, the subsequent future work of these two novel autonomous local voltage control techniques is to carry out a cost-benefit-analysis (CBA) as seen in [123] against the standard voltage control techniques such as the implementation of OLTC in distribution transformers, grid reinforcement to accommodate higher DG and application of advanced agent based optimal voltage control through communication with neighboring agents [124]. This assessment may further explore the consideration of uncertain load demands and intermittent solar energy injection. Another interesting factor apart from CBA is to review the accessibility and readiness of each of these control techniques during the implementation phase. The choice of any control techniques requires an understanding of the core business of the DSO. An optimal solution need not be the best solution if the associated cost of implementation is higher than the allowed revenue that can be recovered from the NRA (National Regulatory Authority).

Appendix A: Voltage fluctuation

Appendix A1: Illustration of voltage rise

Figure A1 illustrates a typical phenomenon when a significant amount of PVDGs are installed at unity power factor (i.e. Φ =0°, where Φ is the phase angle between current and voltage at the point of connection of PVDG) for a typical radial feeder with an impedance phase angle of φ (where φ is the phase angle between resistive and reactive component of the line). Therein, voltage rise is realized due to $I_{PVDG} > I_{LINE}$ where, I_{PVDG} is the current flowing from the installed PVDG and I_{LINE} is current flowing through the line. With respect to Figure A1, *E* represents the voltage at the upstream node, V_{POC} is a representation of the voltage at the *POC* (Point Of Connection) where PDVG is installed, *R* is line resistance, *X* is line reactance, I_F is forward current (I_{LINE}-I_{PVDG} >0) , I_R is reverse current (I_{LINE}-I_{PVDG}< 0) and V_{DROP} represents the voltage drop on the line.

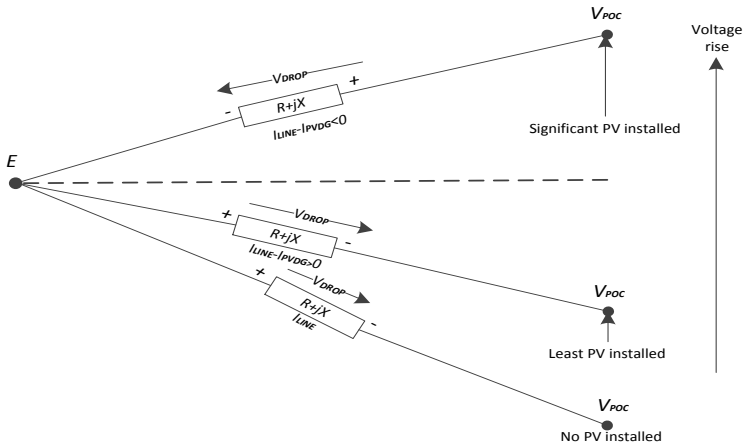

Figure A. 1 : Illustration of the flow of power during significant PVDG installed at V_{POC}

This typical phenomenon can be studied using a phasor representation of Figure A1 which is illustrated in Figure A2. As shown in Figure A2, E is considered as the reference in the phasor diagram. From earlier discussion, PVDG is injecting power at unity power factor, which means I_{PVDG} is in phase with V_{POC} i.e. Φ =0°. Let us assume that PVDG is injecting power into the line at a phase lead of an angle δ i.e. V_{POC} is in phase lead of an angle (from the reference point E). Moreover, Correspondingly, V_{R_LINE} (the voltage drop in the resistive component of the line) is plotted in phase with I_{PVDG}. Subsequently, V_{X_LINE} (the voltage drop across the reactive component of the line) is also plotted orthogonal to V_{R_LINE}. The resultant phasor V_{DROP} is the vector sum of V_{R_LINE} and V_{X_LINE}.

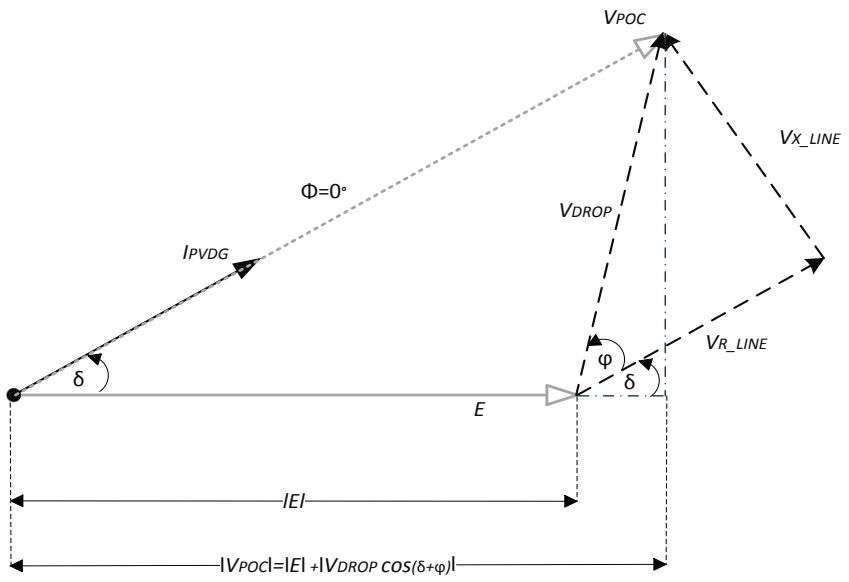

Figure A. 2 : Phasor illustration of voltage rise during PVDG installed at V_{POC}

The angle between V_{R_LINE} and V_{X_LINE} is also the impedance phase angle φ. Finally, the voltage at the point of connection V_{POC} is obtained as a vector sum of E and V_{DROP} i.e. in magnitude,

$$|V_{POC}|=\{|E|+|V_{DROP}\cos(\delta+\varphi)|\} \quad \text{(A1)}$$

The angle δ is also the phase voltage difference between phasors V_{POC} and E. It is clear in Figure A2 that $|V_{POC}|>|E|$ due to PVDG integration. If significant PVDG are installed, this voltage rise phenomena will aggregate and will be highest at the end of the feeder. A further consequence of resultant reverse power flow is that it could also increase the loading at the upstream transformer and thereby restrict the PVDG penetration level in the LVDN. Authors in [125], applied an impedance monitoring method for detecting the current distribution system state in which PVDG penetration level can be observed to monitor its reverse power flow. The voltage rise phenomenon can be further studied by varying the PVDG power factor i.e. Φ and the impedance angle i.e. φ of the network [126].

Appendix A2: Two Bus Systems

Referring to Figure A3, let us consider a two-bus system with PVDG connected at V_{POC}. Here *P* and *Q* are the resultant active and reactive power respectively exchanged at the V_{POC} depending on the availability of the solar irradiation and loading demand. All the following calculations are assumed as per phase quantity considering a balance network.

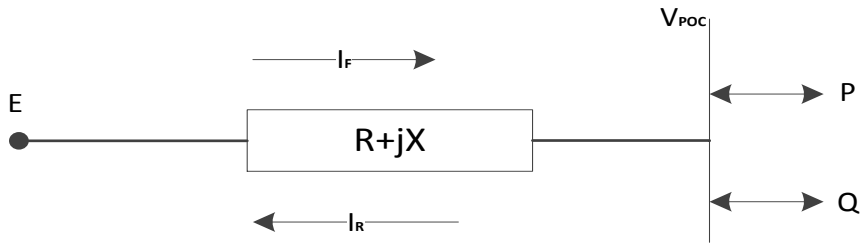

Figure A. 3 : Two bus systems with PVDG connected at V_{POC}

Now, the upstream voltage '*E*' is given by,

$$\vec{E}=V_{POC}+\vec{I}\ (R+jX) \tag{A2}$$

where, *I* could be either I_F or I_R depending on the values of I_{LINE} and I_{PVDG}. However, the complex power is defined by,

$$P+jQ=V_{POC}.I^{*} \tag{A3}$$

Then, $\vec{I}$ equals,

$$I^{*}=\frac{P+jQ}{V_{POC}}\text{, therefore }\vec{I}=\frac{P-jQ}{V_{POC}} \tag{A4}$$

Equation (A2) becomes,

$$\vec{E}=V_{POC}+\frac{P-jQ}{V_{POC}}(R+jX) \tag{A5}$$

Solving for V_{POC}, we get

$$V_{POC}=+\sqrt{a+\sqrt{(a^2-b)}} \tag{A6}$$

Where,

$$a=\frac{|\vec{E}|^2}{2}-(PR+XQ) \tag{A7}$$

$$b=(PR+XQ)^2+(XP-RQ)^2 \tag{A8}$$

Considering only the positive roots, the voltage fluctuation at POC is a function of *E*, *P*, *Q*, *R* and *X* according to Equation (A6).

Let us assume that there is no load connected at POC. In this simple illustration, the power factor i.e. Φ of the PVDG is allowed to vary from phase angle 90° to 270° i.e. from being a capacitive element to an inductive element. Also, the phase angle i.e. φ of the impedance of the line is allowed to vary from 0° to 90° i.e. from being a resistive element to a reactive element. It is further assumed that the upstream voltage *E* is 230 V, rating of PVDG is 5 kVA and the impedance of the line i.e. *Z* is 0.5 ohms/km. Then the voltage fluctuation under such a scenario with unit length of the line can be plotted in a contour plot as shown in Figure A4.

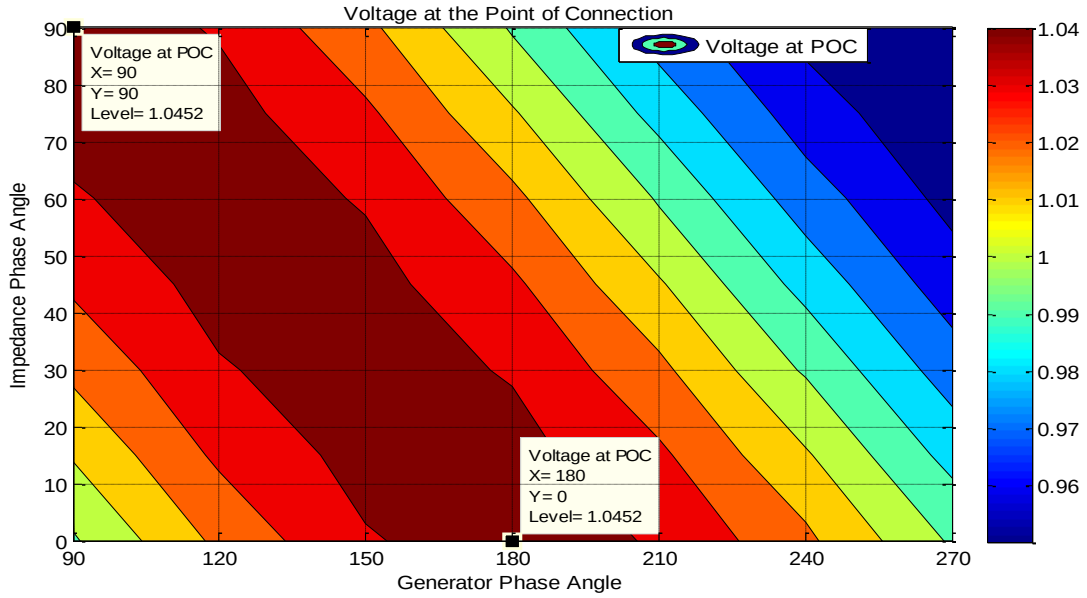

Figure A. 4 : The voltage fluctuation (pu) at the POC as a function of PVDG and impedance phase angle

From Figure A4, maximum voltage fluctuation occurs in two extreme points. They are:

1. When the line impedance is purely resistive (i.e. when the impedance phase angle is 0°) and the PV generator is injecting purely active power (i.e. when the generator phase angle is 180°) to the grid.
2. When the line impedance is purely reactive (i.e. when the impedance phase angle is 90°) and the PV generator is injecting purely reactive power (i.e. when the generator phase angle is 90°) to the grid.

Since LVDN is mostly characterized by high *R*/*X i.e.* $\varphi \approx 0°$, exporting pure active power i.e. $\Phi = 180°$ will lead to voltage fluctuation as shown in Figure A4.

Appendix A3: Analysis of voltage rise in a radial feeder

The above analysis can further extend into a radial feeder. From Equation (A5), we can write,

$$\vec{E} - V_{POC} = \left[\frac{P\text{-}jQ}{V_{POC}}(R+jX) + V_{POC}\right] - V_{POC} \tag{A9}$$

$$\frac{\vec{E} - V_{POC}}{V_{POC}} = \left[1 + \frac{RP+XQ}{{V_{POC}}^2} + j\,\frac{XP\text{-}RQ}{{V_{POC}}^2}\right] - 1 \tag{A10}$$

$$\left|\frac{E - V_{POC}}{V_{POC}}\right| = \sqrt{\left(\left(1 + \frac{RP+XQ}{{V_{POC}}^2}\right)^2 + \left(\frac{XP\text{-}RQ}{{V_{POC}}^2}\right)^2\right)} - 1 \tag{A11}$$

Considering only the real component of Equation (A10), then the right-hand side of Equation (A10) becomes, if $(1+x)^2 \approx 1+2x$ as seen in [127], then

$$\sqrt{\left(\left(1+\frac{RP+XQ}{{V_{POC}}^2}\right)^2\right)} - 1 = \sqrt{1+2\frac{RP+XQ}{{V_{POC}}^2}} - 1 \tag{A12}$$

And if $\sqrt{(1+x)} \approx 1+\frac{1}{2}$ as seen in [127] then

$$1+\frac{2}{2}\left(\frac{RP+XQ}{{V_{POC}}^2}\right) - 1 = \frac{RP+XQ}{{V_{POC}}^2} \tag{A13}$$

Then Equation (A11) can be written as,

$$\left|\frac{E - V_{POC}}{V_{POC}}\right| = \frac{RP+XQ}{{V_{POC}}^2} \tag{A14}$$

$$E - V_{POC} = \Delta E = \frac{RP+XQ}{V_{POC}} \tag{A15}$$

Equation (A15) shows the approximate voltage fluctuation due to the PVDG integration. The slope of the contour plot in Figure A4 is obtained by differentiation Equation (A15) w.r.t to either change in P and Q. Therefore, from Equation (A15), we get

$$\frac{d\,\Delta E}{d\,P} = \frac{R}{V_{POC}}$$

$$\frac{d\,\Delta E}{d\,Q} = \frac{X}{V_{POC}}$$

According to M. Bollen *et al.* [40], any PVDG connected along the feeder is linear with the distance up to the PVDG location and remains constant beyond the PVDG location.

Now, from (A14) and (A15) we have

$$\left|\frac{\Delta E}{V_{POC}}\right| = \begin{cases} \lambda \dfrac{R(P_{gen}-P_{load})+X(Q_{gen}-Q_{load})}{{V_{POC}}^2}, \lambda \leq \lambda_{gen} \\ \lambda_{gen} \dfrac{R(P_{gen}-P_{load})+X(Q_{gen}-Q_{load})}{{V_{POC}}^2}, \lambda > \lambda_{gen} \end{cases} \tag{A16}$$

Here, P_{gen} and Q_{gen} are the active and reactive power produced by the PVDG located at λ_{gen} per unit distance. P_{load} and Q_{load} are the active and reactive power

consumed by the load located at λ_{gen} per unit distance. λ=0 corresponds to the beginning of the feeder and λ=1 corresponds to the end of the feeder.

To alleviate the voltage fluctuation, the right-hand side of Equation (A16) is equated to zero and the required Q_{gen} to compensate the is given by

$$Q_{gen}=Q_{load}-\frac{R}{X}\left[\frac{\left(\frac{\Delta E}{V_{POC}}\right)V_{POC}^{\ 2}}{\lambda_{gen}R}-(P_{gen}-P_{load})\right] \qquad \text{(A17)}$$

From equation (A17), the contributing factors in compensating Q_{gen} are:

1. Source impedance at the point of PVDG connection i.e. $\frac{R}{X}$. In low voltage distribution network, the resistance of the line is a higher than the reactance of the line.
2. Over voltage margin i.e. $\frac{\Delta E}{V_{POC}}$. The over voltage margin is complied with the EN 50160 which is ±10%.
3. The amount of active power generated P_{gen} and consumed P_{load}.
4. The location of PVDG i.e. λ_{gen}.
5. Finally, the reactive power consumed by the load i.e. Q_{load}.

Appendix B: Short Circuit Analyses

Appendix B1: Short Circuit Level

Determining the maximum short circuit current or the fault current at the connection point is important for the protection planning process. The concept of short circuit level or fault level or short circuit capacity can be studied through a Thevenin equivalent of a network as illustrated in Figure B1 [128]. Here the Thevenin voltage source V_{th} is the voltage at the connection point before the fault occurs and Thevenin impedance $Z_{th.}$ is the series impedance seen from the connection point back into the network.

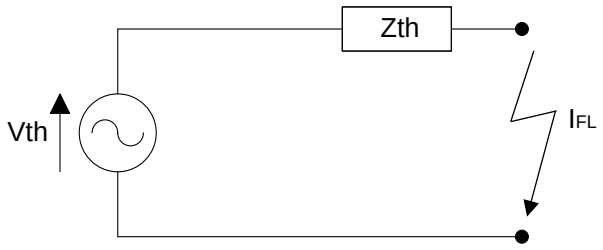

Figure B. 1: Thevenin equivalent of a network

The fault current magnitude at the connection point I_{FL} is given by

$$|I_{FL}| = \frac{|V_{th}|}{Z_{th.}} \qquad \text{(B1)}$$

Determining the fault current at each connection point could be a cumbersome and instead a fault level is computed to identify the proximity of a particular point from the sources of the system. The fault level or short circuit capacity at a bus or at a substation is expressed in MVA (in general) and is given by Equation (B2) where $V_{nominal}$ is the nominal line-line voltage and I_{FL} is the fault current. Herein, the fault level describes how to compensate the effect of the voltage level under potential fault in the system.

$$FL = \sqrt{3}\ V_{nominal}\ I_{FL}\ MVA \quad (B2)$$

Dividing Equation (C2) by the base quantities i.e. $MVA_{Base} = \sqrt{3}\ V_{Base}\ I_{Base}$, the per unit value of the fault level is equal to the per unit value of the fault current and the final expression is given by

$$FL^{pu} = I_{FL}{}^{pu} = \frac{1}{|Z_{th}{}^{pu}|} \quad (B3)$$

From Equation (B3), it is evidenced that if a new generating unit or lines are to be connected in parallel to the network, the Thevenin impedance of the network reduces thereby increasing the fault level of the bus or the substation. This means that before connecting any generating unit, the knowledge of fault level and the source impedance at that point is important during planning process [128].

Appendix B2: Short Circuit Ratio

The short circuit ratio (SCR) indicates the strength of the network at a specified point or a bus. In other words, the SCR defines the ability of a specific bus to retain its nominal voltage in response to the reactive power variation i.e. a network with high SCR will experience less variation in its bus nominal voltage than a network with low SCR [129]. An entire network consisting of several generating units and lines will have different SCR value at each specific bus. In case of connecting distributed generation (DG), the point of common coupling (PCC) is treated as the specific bus. The SCR at PCC is defined as the ratio of the fault level and the nominal or the rated power of the DG P_n at PCC and is given by Equation B4

$$SCR = \frac{FL}{P_n} \quad (B4)$$

If the fault level is considered as a maximum power seen during 3 phase to ground fault at PCC, then using the analogy of the Thevenin circuit, the fault level can be further expressed as Equation (B5).

$$FL = \frac{V_{PCC}{}^2}{Z_{th}} \tag{B5}$$

Considering per unit, the voltage at PCC and rated DG power will be equal to 1 p.u and Equation (B4) becomes

$$SCR_{PCC} = FL_{PCC} = \frac{1}{|Z_{th}{}^{pu}|} \tag{B6}$$

From Equation (B6), the strength of the network at PCC is highly influence by the impedance of the network as seen from the PCC back into the network. Equation (B6) further relates the fault level with the SCR as discussed in Equation (B3). The strength of the network can be identified in three ways using SCR as a metric. They are:

1. Network with low SCR as a result of low voltage level at PCC.
2. High impedance of the network resulting into low SCR.
3. Low impedance network with long cables resulting into high impedance.

Appendix B3: Short Circuit Level calculation in Low Voltage Distribution Network (LVDN)

The short circuit level or short circuit power or fault level signifies the strength of the given network and therefore for any grid reinforcement procedure, identifying the fault level due to the connection of new generating units and lines is a traditional approach. Recalling Equation (B5), we can rewrite as

$$FL = \frac{V_{PCC}{}^2}{Z_{SC}} \tag{B7}$$

From Equation (B7), considering a nominal voltage at the PCC as V_{PCC}, the only way to reinforce (i.e. to increase the fault level) the grid is to lower the source impedance Z_{SC} value. From Equation (A15), reducing the real part of the impedance could lower the voltage variation under the real power injection from the generating unit. Further from Equation (A17), it is evidenced that the source impedance plays a crucial role in alleviating any voltage fluctuation. To calculate the fault level in an LVDN a simplified feeder is presented in Figure B2 is considered [130].

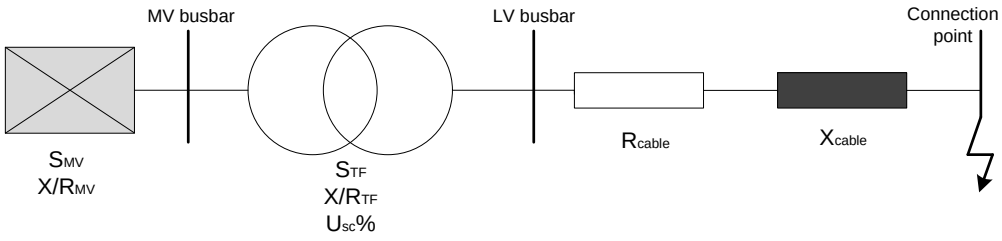

Figure B. 2 : A simplified LVDN feeder

From Figure B2, the fault level at the connection point depends on the short circuit power at the upstream MV level i.e. S_{MV}[VA], rated distribution transformer power S_{TF} [VA] (including the short circuit voltage U_{SC}%), the distribution transformer X/R ratio and the impedance of the line/cable (R_{Cable} and X_{Cable}). Here V_{MV} and V_{LV} are the voltage at the medium and low voltage side of the distribution transformer.

Rewriting the Equation (B7) based on the Figure 43, we have,

$$FL = \frac{V_{LV}{}^2}{Z_{SC}} \qquad \text{(B8)}$$

Recalling Equation (B8), the source impedance of the simplified LVDN feeder as presented in Figure B2 is given by

$$Z_{SC}=\sqrt{((R_{Cable}+R_{TF}+R_{MV})^2+(X_{Cable}+X_{TF}+X_{MV})^2)} \quad \text{(B9)}$$

The source impedance Z_{SC} depends on the following values.

R_{Cable}= Cable resistance [Ω/km] x length of the cable [km]

X_{Cable}= Cable reactance [Ω/km] x length of the cable [km]

Z_{TF}= Transformer impedance = $\frac{U_{SC} \cdot V_{LV}^2}{100\% \cdot S_{TF}}$ [Ω]

R_{TF}= Transformer resistive part = Z_{TF}. $\frac{U_R}{U_{SC}}$ [Ω], where U_R=voltage drop in resistive part of the transformer.

X_{TF}= Transformer reactive part = $\sqrt{Z_{TF}^2 - R_{TF}^2}$ [Ω]

Z_{MV}= Medium Voltage Impedance = $\frac{c \cdot V_{MV}^2}{S_{MV}}$ [Ω] , where c= Voltage factor

X_{MV}= Medium voltage level reactive part = $\sqrt{\frac{Z_{TF}^2}{1+\frac{R}{X}}}$ [Ω] , where $\frac{R}{X}$ is the X/R ratio at MV level.

R_{MV}= Medium voltage level reactive part = $\sqrt{Z_{MV}^2 - X_{MV}^2}$ [Ω]

Considering the above values is imperative in computing the fault level at a particular point in an LVDN.

Appendix B4: Voltage Sag magnitude in a radial system

As discussed in [131], the voltage sag in a radial network can be simplified through a voltage divider model as shown in the Figure B3. Here, Z_{SC} is the source impedance at the point of common coupling (PCC) and Z_F is the impedance between the PCC and

the fault. At PCC, both load current and fault are fed. However, the load current before as well as during the fault is neglected in this simple voltage divider analyses. E is the source voltage with a pre-fault voltage of 1 per unit (p.u).

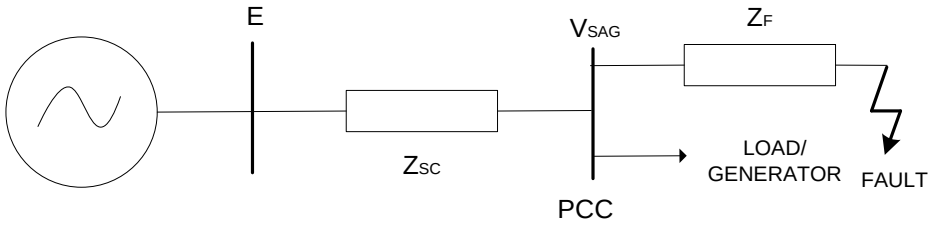

Figure B. 3 : A simplified radial network under fault condition

The voltage sag observed at PCC is calculated as

$$V_{SAG}=E.\frac{Z_F}{Z_{SC}+Z_F} \qquad \text{(B10)}$$

From Equation B10, the V_{SAG} becomes deeper (i.e. the residual voltage after fault is low):

1. for fault nearer to the load or at the site where PVDG is installed since Z_F becomes smaller,
2. for network with smaller fault level since Z_{SC} becomes larger (see equation B7).

Appendix C: Statistical Analyses

Appendix C1: Calculation of CDF and Complementary CDF

Cumulative Distribution Function (CDF) is used to find the probability of a variable taking a value less than or equal to '*x*' for a given function i.e.

$$F_x(x) = P(X \leq x) \quad \text{(C1)}$$

Whereas, Complimentary Cumulative Distribution Function (CCDF) is used find the probability of a variable taking a value greater than '*x*' for a given function i.e.

$$F_x(x) = P(X > x) \quad \text{(C2)}$$

The cumulative distribution function (CDF) and complementary cumulative distribution function (CCDF) are the post analysis methods used in Chapter 3. The CDF of a given impact metric is computed in following method as described in the flowchart given by Figure C1.

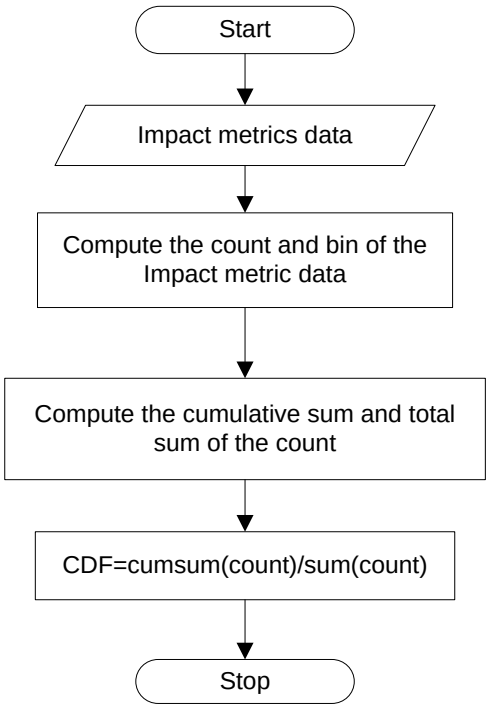

Figure C. 1 : Flowchart to compute CDF

The statistical analysis starts after the Monte-Carlo simulation of 100 different stochastic events. For a given impact metric (such as site overvoltage), the number of site overvoltage observations recorded at each 55 nodes for every 5 minutes for a day (i.e. 288) is the prime data to compute the CDF. In case of site overvoltage metric, there will be 288*55*100= 1584000 observations. Once the number of observations is known, the count[13] and the bin[14] of this particular impact metric is computed. After that, the cumulative sum (cumsum) and the total sum (sum) of the count is computed. The CDF is the ratio of cumulative sum and the total sum. Finally, the post analysis of the impact metric can be plotted by considering the bin as the x-axis and the CDF as the y-axis. The CCDF is the computed in a similar approach arranging the CDF in descending order.

[13] A positive integer statistical data type obtained after counting the number of observations.
[14] Data sorting into class interval.

Appendix C2: Confidence intervals and level

The proposed Monte Carlo simulation considered 100 samples or simulations to estimate the parameter of interest. The choice of this samples was determined to compromise between computational time and the accuracy of the estimation. One specific site PQ variation impact metric i.e., overvoltage was chosen to determine the accuracy of the estimation. 1000 samples size have chosen to perform Monte Carlo simulation to determine the site overvoltage for 5 cases i.e., 0%, 20%, 40%, 60, 80% and 100%. A confidence level of 95% is chosen which contains a true parameter i.e., mean [113]. This true parameter signifies that the mean of the true population of samples size *'n'* is 1. Table C shows the confidence intervals of two samples size namely 100 and 1000 for 5 cases with 95% confidence level. The absolute error from Table I shows that sampling size of 100 is a good estimation for 95% confidence level for the corresponding confidence intervals at a tenth of the computation time as compared with sampling size of 1000.

Table C. 1 : Confidence intervals of two samples size namely 100 and 1000 for 5 cases with 95% confidence level

Penetration in %	**Sample size =100**		**Sample size =1000**		**Absolute Error**	
	Average Time = 180 seconds		**Average Time = 1800 seconds**			
	Confidence interval		**Confidence interval**			
	low	**high**	**low**	**high**	**low**	**high**
0	1.0316	1.0358	1.0329	1.0343	0.0013	0.0016
20	1.0332	1.0373	1.0345	1.0359	0.0014	0.0014
40	1.0353	1.0397	1.0366	1.0381	0.0013	0.0017
60	1.0377	1.0427	1.0392	1.0409	0.0015	0.0019
80	1.0396	1.0453	1.0417	1.0435	0.0021	0.0018
100	1.0426	1.0491	1.0447	1.0468	0.0021	0.0024

Appendix D: COM Interface between MATLAB and OpenDSS

OpenDSS is a comprehensive electrical system simulation engine in the frequency domain designed specifically for electric utility distribution system by EPRI [14], [16]. One of the primary features of Open DSS includes the ability to readily perform grid impact studies that consider the grid interconnection of distributed generators (DG) such as PV and Wind generator. The OpenDSS platform facilitates steady state analyses of the feeder voltage, equipment loading, power flow, losses in the network, harmonics etc. for various times of the day, month, or, year. Application of OpenDSS power flow analysis is briefly described in the following paragraph.

Initially the primitive Z and Y matrices for each element are built along with the bus data. The overall system admittance (Y) matrix is subsequently created using a sparse matrix solver after collecting all the element matrices. In the circuit model, all the series connected power delivery elements are kept connected while all shunt elements are disconnected to maintain a proper relationship of all phase angles and voltage magnitude. The iteration loop starts by obtaining the injection currents from all the power conversion (PC) elements in the system and subsequently, they are systematically added into the appropriate slot in the I_{inj}vector. The sparse set is then solved for the next guess at the voltages. The loop iterates until the voltages converge to typically 0.0001 per unit. The system Y matrix is not rebuilt during this process and hence the iterations are fast. Figure D1 summarises the procedure to perform power flow analyses in OpenDSS.

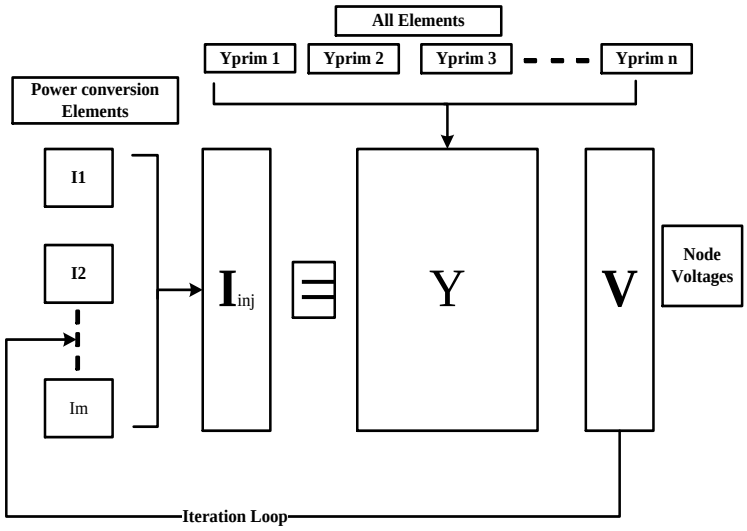

Figure D. 1 :Power flow analysis in OpenDSS [16]

Often, OpenDSS is interfaced with other programs/languages such as MATLAB and VBA in MS office. In this work, MATLAB is used to interface OpenDSS through the COM server of OpenDSS. In this way, any developed algorithm in MATLAB can be integrated with the network model developed in OpenDSS. Particularly in this work, MATLAB is used to interface with OpenDSS via COM server of OpenDSS. COM server of OpenDSS allows script developed in MATLAB to control the OpenDSS model and other various objects within the model.

References

[1] K. Bhattacharya, M. H. J. Bollen, and J. E. Daalder, "Deregulation of the Electricity Supply Industry," in *Operation of Restructured Power Systems*, Boston, MA: Springer US, pp. 1–27, 2001.

[2] Y. Huang, K. Alvehag, and L. Soder, "Regulation impact on distribution systems with distributed generation," in *2012 9th International Conference on the European Energy Market*, pp. 1–8, 2012.

[3] M. Bollen and F. Hassan, *Integration of Distributed Generation in the Power System*, IEEE Press, John Wiley & Sons, Inc., 2011.

[4] R. Cossent, "Economic Regulation of Distribution System Operators and its Adaptation to the Penetration of Distributed Energy Resources and Smart Grid Technologies," *Ph.D dissertation, Comillas Pontifical University*, 2013.

[5] E. Christine Aprilia, "Modelling of Photovoltaic (PV) Inverter for Power Quality Studies," *M. Sc. Dissertation, Dept. Elec. Eng., Univ. Technology, Eidhen, Netherland*, 2012.

[6] S. Hay and A. Ferguson, "A Review of Power System Modelling Platforms and Capabilities," *The Institution of Engineering and Technology (IET), Paper 3*, 2015.

[7] B. Kroposki, "Distribution System Models. Power System Studies and Modeling PV Inverters," *Utility/Lab Workshop on PV Technology and Systems*, pp. 8-9, 2010.

[8] "PSCAD™ | HOME." [Online]. Available: https://hvdc.ca/pscad. [Accessed: 16-Apr-2018].

[9] "Electrical Engineering Software | Plexim." [Online]. Available: http://www.plexim.com/. [Accessed: 16-Apr-2018].

[10] "PSS®E – high-performance transmission planning and analysis software - PSS® power system simulation and modeling software - Siemens Global Website." [Online]. Available: https://www.siemens.com/global/en/home/products/energy/services/transmission-distribution-smart-grid/consulting-and-planning/pss-software/pss-e.html. [Accessed: 16-Apr-2018].

[11] "PowerWorld » The visual approach to electric power systems." [Online]. Available: https://www.powerworld.com/. [Accessed: 16-Apr-2018].

[12] "Energy Management System | PSLF | GE Energy Consulting." [Online]. Available: https://www.geenergyconsulting.com/practice-area/software-products/pslf. [Accessed: 16-Apr-2018].

[13] "CYME - Distribution System Analysis." [Online]. Available: http://www.cyme.com/software/cymdist/. [Accessed: 16-Apr-2018].

[14] “EPRI | Smart Grid Resource Center; Simulation Tool – OpenDSS.” [Online]. Available: http://smartgrid.epri.com/SimulationTool.aspx. [Accessed: 16-Apr-2018].

[15] R. F. Arritt and R. C. Dugan, “Distribution system analysis and the future Smart Grid,” *IEEE Trans. Indus Appl.*, vol. 47, no. 6, pp. 2343–2350, 2011.

[16] R.C. Dugan, “OpenDSS Manual,” *Electric Power Research Institute*, 2016.

[17] A. Keane *et al.*, “State-of-the-art techniques and challenges ahead for distributed generation planning and optimization,” *IEEE Trans. Power Syst.*, vol. 28, no. 2, pp. 1493–1502, 2013.

[18] J. A. Martinez, M. H. Nehrir, C. Wang, and V. Dinavahi, “Tools for Analysis and Design of Distributed Resources — Part II : Tools for Planning , Analysis and Design of Distribution Networks With Distributed Resources,” *IEEE Trans. Power Deliv.*, no. January, pp. 1–10, 2011.

[19] C. P. Steinmetz, “Complex Quantities and their use in Electrical Engineering,” *AIEE Proceedings of International Electrical Congress*. pp. 33–74, 1893.

[20] A. E. A. Araújo and D. A. V Tonidandel, “Steinmetz and the concept of phasor: A forgotten story,” *J. Control. Autom. Electr. Syst.*, vol. 24, no. 3, pp. 388–395, 2013.

[21] P. P. Barker and R. W. De Mello, “Determining the impact of distributed generation on power systems: Part I-Radial distribution systems,” in *Power Engineering Society Summer Meeting (Cat. No.00CH37134)*, vol. 3, no. c, pp. 1645–1656, 2000.

[22] T. Ackermann, G. Andersson, and L. Söder, “Distributed generation: A definition,” *Electr. Power Syst. Res.*, vol. 57, no. 3, pp. 195–204, 2001.

[23] P. Dondi, D. Bayoumi, C. Haederli, D. Julian, and M. Suter, “Network integration of distributed power generation,” *J. Power Sources*, vol. 106, no. 1–2, pp. 1–9, 2002.

[24] J. A. P. Lopes, N. Hatziargyriou, J. Mutale, P. Djapic, and N. Jenkins, “Integrating distributed generation into electric power systems: A review of drivers, challenges and opportunities,” *Electr. Power Syst. Res.*, vol. 77, no. 9, pp. 1189–1203, 2007.

[25] A. Canova, L. Giaccone, F. Spertino, and M. Tartaglia, “Electrical impact of photovoltaic plant in distributed network,” *IEEE Trans. Ind. Appl.*, vol. 45, no. 1, pp. 341–347, 2009.

[26] K. Balamurugan, D. Srinivasan, and T. Reindl, “Impact of distributed generation on power distribution systems,” *Energy Procedia*, vol. 25, pp. 93–100, 2012.

[27] Smith, J. and Rylander, M., “Stochastic Analysis to Determine Feeder Hosting Capacity for Distributed Solar PV,” *Electric Power Resecarh Institute*, 2011.

[28] European Commission Smart Grid Task Force, “Regulatory Recommendations

for the Deployment of Flexibility," *EU SGTF-EG3 Report*, 2015.

[29] G. P. Harrison, A. Piccolo, P. Siano, and A. R. Wallace, "Exploring the Tradeoffs Between Incentives for Distributed Generation Developers and DNOs," *IEEE Trans. Power Syst.*, vol. 22, no. 2, pp. 821–828, May 2007.

[30] European Distribution System Operators for Smart Grids, "Adapting distribution network tariffs to a decentralised energy future," *EDSO Report*, 2015.

[31] A. Picciariello, K. Alvehag, and L. Soder, "Impact of Network Regulation on the Incentive for DG Integration for the DSO: Opportunities for a Transition Toward a Smart Grid," *IEEE Trans. Smart Grid*, vol. 6, no. 4, pp. 1730–1739, 2015.

[32] J. R. Snape, "Spatial and temporal characteristics of PV adoption in the UK and their implications for the smart grid," *Energies*, vol. 9, no. 3, pp. 1–18, 2016.

[33] M. David, F. H. R. Andriamasomanana, and O. Liandrat, "Spatial and temporal variability of PV output in an insular grid: Case of Reunion Island," *Energy Procedia*, vol. 57, pp. 1275–1282, 2014.

[34] R. C. Dugan, M. F. McGranaghan, S. Santoso, and H. W. Beaty, "Long-Duration Voltage Variations," in *Electrical Power Systems Quality*, pp. 295–325, 2004.

[35] T. A. Short, "Voltage Regulation," in *Electric Power distribution handbook*, pp. 249–283, 2004.

[36] F. Katiraei and J. R. Agüero, "Solar PV integration challenges," *IEEE Power Energy Mag.*, vol. 9, no. 3, pp. 62–71, 2011.

[37] A. Woyte, V. Van Thong, R. Belmans, and J. Nijs, "Voltage fluctuations on distribution level introduced by photovoltaic systems," *IEEE Trans. Energy Convers.*, vol. 21, no. 1, pp. 202–209, 2006.

[38] R. Tonkoski, D. Turcotte, and T. H. M. El-Fouly, "Impact of high PV penetration on voltage profiles in residential neighborhoods," *IEEE Trans. Sustain. Energy*, vol. 3, no. 3, pp. 518–527, 2012.

[39] D. Santos-martin and S. Lemon, "Simplified Modeling of Low Voltage Distribution Networks for PV Voltage Impact Studies," vol. 7, no. 4, pp. 1–8, 2014.

[40] M. Bollen and F. Hassan, "Voltage Magnitude Variations," in *Integration of Distributed Generation in the Power System*, Wiley, pp. 141–222, 2011.

[41] R. J. Broderick *et al.*, "Time Series Power Flow Analysis for Distribution Connected PV Generation," *Sandia Natl. Lab.*, no. January, 2013.

[42] R. A. Walling, R. Saint, R. C. Dugan, J. Burke, and L. A. Kojovic, "Summary of distributed resources impact on power delivery systems," *IEEE Trans. Power Deliv.*, vol. 23, no. 3, pp. 1636–1644, 2008.

[43] J. E. Quiroz, M. J. Reno, and R. J. Broderick, "Time series simulation of voltage

regulation device control modes," in *2013 IEEE 39th Photovoltaic Specialists Conference (PVSC)*, pp. 1700–1705, 2013.

[44] Y. P. Agalgaonkar, B. C. Pal, and R. A. Jabr, "Distribution voltage control considering the impact of PV generation on tap changers and autonomous regulators," *IEEE Trans. Power Syst.*, vol. 29, no. 1, pp. 182–192, 2014.

[45] M. Ebad and W. M. Grady, "An approach for assessing high-penetration PV impact on distribution feeders," *Electr. Power Syst. Res.*, vol. 133, pp. 347–354, 2016.

[46] Papathanassiou, S *et al.*, "Capacity of Distribution Feeders for Hosting DER," *CIGRÉ Working Group C6, 24,* 2014.

[47] M. H. J. Bollen and Fainan Hassan, "Protection," in *Integration of Distributed Generation in the Power System*, vol. 1, Wiley, pp. 299-366, 2011.

[48] R. C. Dugan, M. F. McGranaghan, S. Santoso, and H. W. Beaty, "Distributed Generation and Power Quality," in *Electrical Power Systems Quality*, pp. 373–435, 2004.

[49] M. M. Begovic, I. Kim, D. Novosel, J. R. Aguero, and A. Rohatgi, "Integration of Photovoltaic Distributed Generation in the Power Distribution Grid," in *2012 45th Hawaii International Conference on System Sciences*, pp. 1977–1986, 2012.

[50] R. Shah, N. Mithulananthan, R. C. Bansal, and V. K. Ramachandaramurthy, "A review of key power system stability challenges for large-scale PV integration," *Renew. Sustain. Energy Rev.*, vol. 41, pp. 1423–1436, 2015.

[51] M. J. Reno, R. J. Broderick, and S. Grijalva, "Smart inverter capabilities for mitigating over-voltage on distribution systems with high penetrations of PV," in *2013 IEEE 39th Photovoltaic Specialists Conference (PVSC)*, pp. 3153–3158, 2013.

[52] J. Jung, A. Onen, R. Arghandeh, and R. P. Broadwater, "Coordinated control of automated devices and photovoltaic generators for voltage rise mitigation in power distribution circuits," *Renew. Energy*, vol. 66, pp. 532–540, 2014.

[53] W. Zhang, M. Baran, A. De, and S. Bhattacharya, "Fast Volt-VAR Control on PV Dominated distribution systems," *2014 IEEE PES T&D Conf. Expo.*, pp. 1–5, 2014.

[54] V. Calderaro, G. Conio, V. Galdi, G. Massa, and A. Piccolo, "Optimal decentralized voltage control for distribution systems with inverter-based distributed generators," *IEEE Trans. Power Syst.*, vol. 29, no. 1, pp. 230–241, 2014.

[55] C.H. Chang, Y.-H. Lin, Y.-M. Chen, and Y.-R. Chang, "Simplified Reactive Power Control for Single-Phase Grid-Connected Photovoltaic Inverters," *IEEE Trans. Ind. Electron.*, vol. 61, no. 5, pp. 2286–2296, 2014.

[56] G. BDEW, "Technical Guideline, Generating Plants Connected to the Medium-

Voltage Network," 2008.

[57] B. VDE VERLAG GmbH and Germany, "Generators connected to the low-voltage distribution network – Technical requirements for the connection to and parallel operation with low-voltage distribution networks," 2011.

[58] E. Demirok, P. C. González, K. H. B. Frederiksen, D. Sera, P. Rodriguez, and R. Teodorescu, "Local reactive power control methods for overvoltage prevention of distributed solar inverters in low-voltage grids," *IEEE J. Photovoltaics*, vol. 1, no. 2, pp. 174–182, 2011.

[59] L. Collins and J. K. Ward, "Real and reactive power control of distributed PV inverters for overvoltage prevention and increased renewable generation hosting capacity," *Renew. Energy*, vol. 81, no. October, pp. 464–471, 2015.

[60] X. Liu, A. M. Cramer, and Y. Liao, "Reactive-power control of photovoltaic inverters for mitigation of short-term distribution-system voltage variability," *2014 IEEE PES T&D Conf. Expo.*, pp. 1–5, 2014.

[61] S. Weckx, C. Gonzalez, and J. Driesen, "Combined central and local active and reactive power control of PV inverters," *IEEE Trans. Sustain. Energy*, vol. 5, no. 3, pp. 776–784, 2014.

[62] R. Caldon, M. Coppo, and R. Turri, "Distributed voltage control strategy for LV networks with inverter-interfaced generators," *Electr. Power Syst. Res.*, vol. 107, pp. 85–92, Feb. 2014.

[63] S. B. Kjær, "Grid voltage control by PF(U) regulation," in *Proc. 29th Eur. Photovolt. Solar Energy Conf. Exhibit., Amsterdam,The Netherlands*, pp. 2960–2964, 2014.

[64] A. Samadi, R. Eriksson, L. Soder, B. G. Rawn, and J. C. Boemer, "Coordinated Active Power-Dependent Voltage Regulation in Distribution Grids With PV Systems," *IEEE Trans. Power Deliv.*, vol. 29, no. 3, pp. 1454–1464, Jun. 2014.

[65] E. Serban, M. Ordonez, and C. Pondiche, "Voltage and Frequency Grid Support Strategies Beyond Standards," *IEEE Trans. Power Electron.*, vol. 32, no. 1, pp. 298–309, Jan. 2017.

[66] ESB, "Distribution Code Summary,"April, 2017.

[67] T. N. Boutsika and S. A. Papathanassiou, "Short-circuit calculations in networks with distributed generation," *Electr. Power Syst. Res.*, vol. 78, no. 7, pp. 1181–1191, 2008.

[68] A. Ballanti and L. F. Ochoa, "On the integrated PV hosting capacity of MV and LV distribution networks," *2015 IEEE PES Innov. Smart Grid Technol. Lat. Am. ISGT LATAM 2015*, no. March, pp. 366–370, 2016.

[69] H. V. Padullaparti, P. Chirapongsananurak, M. E. Hernandez, and S. Santoso, "Analytical Approach to Estimate Feeder Accommodation Limits Based on Protection Criteria," *IEEE Access*, vol. 4, pp. 4066–4081, 2016.

[70] M. E. Baran and I. El-Markaby, “Fault Analysis on Distribution Feeders With Distributed Generators,” *IEEE Trans. Power Syst.*, vol. 20, no. 4, pp. 1757–1764, 2005.

[71] M. Bollen and F. Hassan, “Overloading and losses,” in *Integration of Distributed Generation in the Power System*, Wiley, pp. 102–140, 2011.

[72] M. Braun, “Economic Potential of Providing Ancillary Services by Distributed Generators,” in *Provision of Ancillary Services by Distributed Generators*, pp. 49–122, 2008.

[73] V. H. Méndez Quezada, J. Rivier Abbad, and T. Gómez San Román, “Assessment of energy distribution losses for increasing penetration of distributed generation,” *IEEE Trans. Power Syst.*, vol. 21, no. 2, pp. 533–540, 2006.

[74] A. G. Marinopoulos, M. C. Alexiadis, and P. S. Dokopoulos, “A correlation index to evaluate impact of PV installation on Joule losses,” *IEEE Trans. Power Syst.*, vol. 26, no. 3, pp. 1564–1572, 2011.

[75] European Parliament, “Directive 2009/28/EC of the European Parliament and of the Council on the promotion of the use of energy from renewable sources and amending and subsequently repealing Directives 2001/77/EC and 2003/30/EC,” 2009.

[76] CEER, “The Future Role of DSOs - A CEER Conclusions Paper,” 2015.

[77] T. Gómez, “Electricity Distribution,” in *Regulation of the Power Sector*, I. J. Pérez-arriaga, Ed. Springer New York, pp. 199–250, 2013.

[78] A. Picciariello, J. Reneses, P. Frias, and L. Söder, “Distributed generation and distribution pricing: Why do we need new tariff design methodologies?,” *Electr. Power Syst. Res.*, vol. 119, pp. 370–376, 2015.

[79] Eurelectric, “Network Tariffs,” *Eurelectric Report*, 2016.

[80] C. Eid, J. Reneses Guillén, P. Frías Marín, and R. Hakvoort, “The economic effect of electricity net-metering with solar PV: Consequences for network cost recovery, cross subsidies and policy objectives,” *Energy Policy*, vol. 75, pp. 244–254, 2014.

[81] Jenkins and et al., “Economics of Embedded Generation,” in *Embedded Generation*, Institution of Engineering and Technology, pp. 231–256, 2000.

[82] CEER, “Electricity Distribution Network Tariffs - CEER Guidelines of Good Practice,” no. January, pp. 1–40, 2017.

[83] S. Pukhrem, M. Basu, M. F. Conlon, and K. Sunderland, “Enhanced Network Voltage Management Techniques Under the Proliferation of Rooftop Solar PV Installation in Low-Voltage Distribution Network,” *IEEE J. Emerg. Sel. Top. Power Electron.*, vol. 5, no. 2, pp. 681–694, 2017.

[84] M. A. Akbari *et al.*, “New Metrics for Evaluating Technical Benefits and Risks

of DGs Increasing Penetration," *IEEE Trans. Smart Grid*, vol. 3053, no. c, pp. 1–1, 2017.

[85] A. Navarro-Espinosa and L. F. Ochoa, "Probabilistic Impact Assessment of Low Carbon Technologies in LV Distribution Systems," *IEEE Trans. Power Syst.*, vol. 31, no. 3, pp. 2192–2203, May 2016.

[86] J. Reneses., M. P. Rodríguez., and I. J. Pérez-Arriaga, "Electricity Tariff," in *Regulation of the Power Sector*, I. J. Pérez-arriaga, Ed., pp. 397–441, 2013.

[87] EDSO, "Adapting distribution network tariffs to a decentralised energy future Key messages," *EDSO Report*, 2015.

[88] Eurelectric, "Network tariff structure for a smart energy system," *Eurelectric Report*, 2013.

[89] Energy Network Association, "The Distribution Code and The Guide To the Distribution Code of Licensed Distribution Network Operators of Great Britain," *October*, no. 17, 2011.

[90] ESB, "Conditions Governing the Connection and Operation of Micro-generation," 2009.

[91] EN 50438, "Requirements for micro-generating plants to be connected in parallel with public low-voltage distribution networks," 2012.

[92] N. Hatziargyriou *et al.*, "Connection criteria at the distribution network for distributed generation," *CIGRE Task Force C6.04.01*, 2007.

[93] G. P. Harrison and A. R. Wallace, "Optimal power flow evaluation of distribution network capacity for the connection of distributed generation," *IEE Proc. - Gener. Transm. Distrib.*, vol. 152, no. 1, p. 115, 2005.

[94] N. S. Rau and Yih-Heui Wan, "Optimum location of resources in distributed planning," *IEEE Trans. Power Syst.*, vol. 9, no. 4, pp. 2014–2020, 1994.

[95] L. F. Ochoa, C. J. Dent, and G. P. Harrison, "Distribution Network Capacity Assessment: Variable DG and Active Networks," *IEEE Trans. Power Syst.*, vol. 25, no. 1, pp. 87–95, 2010.

[96] L. F. Ochoa and G. P. Harrison, "Minimizing Energy Losses : Optimal Accommodation and Smart Operation of Renewable Distributed Generation," vol. 26, no. 1, pp. 198–205, 2011.

[97] Eurelectric, "Active distribution system management: A key tool for the smooth integration of distributed generation," *Eurelectric Report*, 2013.

[98] P. Caramia, G. Carpinelli, P. Verde, and Wiley InterScience (Online service), *Power quality indices in liberalized markets*. J. Wiley, 2009.

[99] A. Russo and P. Verde, "Site and System Indices for Power-Quality Characterization of Distribution Networks With Distributed Generation," vol. 26, no. 3, pp. 1304–1316, 2011.

[100] M. H. J. Bollen, "Understanding power quality problems", *Voltage sags and Interruptions, IEEE Press*, 2000.

[101] R. Brown, *Electric Power Distribution Reliability, Second Edition*, 2nd Editio. CRC Press, Taylor & Francis Group, 2009.

[102] J. C. Das, *Power System Analysis*. CRC Press, Taylor & Francis Group, 2012.

[103] M. H. . Bollen, "Voltage Sags in Three-Phase System," *IEEE Power Eng. Rev.*, vol. 21, no. September, pp. 8–15, 2001.

[104] E. 50160, "Voltage characteristics of electricity supplied by public electricity networks," vol. 44, no. 0, pp. 0–1, 2013.

[105] V. Klonari, J.-F. Toubeau, J. Lobry, and Vall, "PV integration in smart city power distribution A probabilistic PV hosting capacity assessment based on smart metering data," *Smartgreens*, no. May, 2016.

[106] Z. Ren, W. Li, R. Billinton, and W. Yan, "Probabilistic Power Flow Analysis Based on the Stochastic Response Surface Method," vol. 31, no. 3, pp. 2307–2315, 2016.

[107] G. H. Givens and J. A. Hoeting, *Computational Statistics*, Wiley, 2013.

[108] A. Dubey and S. Santoso, "On Estimation and Sensitivity Analysis of Distribution Circuit's Photovoltaic Hosting Capacity," *IEEE Trans. Power Syst.*, vol. 32, no. 4, pp. 2779–2789, 2017.

[109] IEEE, "IEEE EU Low Voltage Distribution Test Feeders." [Online]. Available: http://www.ewh.ieee.org/soc/pes/dsacom/testfeeders/index.html. [Accessed: 28-May-2017].

[110] K. Sunderland, M. Coppo, M. Conlon, and R. Turri, "A correction current injection method for power flow analysis of unbalanced multiple-grounded 4-wire distribution networks," *Electr. Power Syst. Res.*, vol. 132, pp. 30–38, 2016.

[111] The University of Manchester, "The Whitworth Observatory (Centre for Atmospheric Science - The University of Manchester)." [Online]. Available: http://www.cas.manchester.ac.uk/restools/whitworth/. [Accessed: 28-May-2017].

[112] ENWL, "Low Voltage Network Solutions." [Online]. Available: https://www.enwl.co.uk/zero-carbon/smaller-projects/low-carbon-networks-fund/low-voltage-network-solutions/. [Accessed: 28-May-2017].

[113] W. L. Martinez and A. R. Martinez, *Computational Statistics handbook with MATLAB, Second Edition*. Taylor & Francis Group, 2007.

[114] Econ Pöyry AS, "Optimal network tariffs and allocation of costs," *NVE Olso*, 2008.

[115] K. Lummi, A. Rautiainen, P. Jarventausta, P. Heine, J. Lehtinen, and M. Hyvarinen, "Cost-causation based approach in forming power-based distribution network tariff for small customers," in *International Conference on the*

European Energy Market, EEM, pp. 1–5, 2016.

[116] K. Lummi, A. Rautiainen, P. JäRventausta, P. Heine, J. Lehtinen, and M. Hyvärinen, "Electricity Distribution Network Tariffs - Present Practices, Future Challenges and Development Possibilities," in *CIRED Workshop 2016*, 2016.

[117] I. Pérez-Arriaga, "New regulatory and business model approaches to achieving universal electricity access," *Papeles Energ.*, no. June, pp. 7–48, 2016.

[118] J. Tuunanen, S. Honkapuro, and J. Partanen, "Power-based distribution tariff structure: DSO's perspective," *Int. Conf. Eur. Energy Mark. EEM*, 2016.

[119] C. G. Kaloudas, L. F. Ochoa, B. Marshall, S. Majithia, and I. Fletcher, "Assessing the Future Trends of Reactive Power Demand of Distribution Networks," *IEEE Trans. Power Syst.*, vol. 32, no. 6, pp. 4278-4288, 2017.

[120] J. E. R. Baptista, A. B. Rodrigues, M. G. Silva, and S. Member, "Probabilistic Analysis of PV Generation Impacts on Voltage Sags in LV Distribution Networks Considering Failure Rates Dependent on Feeder Loading," *IEEE Trans. Sustain. Energy*, vol. 10, no. 3, pp. 1342–1350, 2019.

[121] S. Honkapuro and J. Haapaniemi, *Development options and impacts of distribution tariff structures*, no. 65. 2017.

[122] L. Ryan, S. La, L. Mastrandrea, and P. Spodniak, "Harnessing electricity retail tariffs to support climate change policy," *The 6th World Congress of Environmental and Resource Economists*, Gothenburg, Sweden, pp. 1–39, 25-29 June 2018.

[123] T. Stetz, K. Diwold, M. Kraiczy, D. Geibel, S. Schmidt, and M. Braun, "Techno-economic assessment of voltage control strategies in low voltage grids," *IEEE Trans. Smart Grid*, vol. 5, no. 4, pp. 2125–2132, 2014.

[124] M. Zeraati, M. E. H. Golshan, and J. M. Guerrero, "Voltage Quality Improvement in Low Voltage Distribution Networks Using Reactive Power Capability of Single-Phase PV Inverters," *IEEE Trans. Smart Grid*, vol. 10, no. 5, pp. 5057–5065, 2018.

[125] H. Mortazavi, H. Mehrjerdi, M. Saad, S. Lefebvre, D. Asber, and L. Lenoir, "A Monitoring Technique for Reversed Power Flow Detection With High PV Penetration Level," *IEEE Transactions on Smart Grid*, vol. 6, no. 5, pp. 2221–2232, 2015.

[126] M. Braun, "Characterisation of Ancillary Services," in *Provision of Ancillary Services by Distributed Generators*, vol. 10, University of Kassel, pp. 23–31, 2008.

[127] M. Bollen and I. Gu, "Signal processing of power quality disturbances," vol. 30, John Wiley & Sons, 2006.

[128] N. Jenkins, R. Allan, P. Crossley, D. Kirschen, and G. Strbac, "System Studies," in *Embedded Generation*, IET Power and Energy Series, pp. 1-49–93, 2000.

[129] A. Gavrilovic, “AC/DC System strength as indicated by short circuit ratios,” in *International Conference on AC and DC Power Transmission, London, UK*, pp. 27–32,1991.

[130] T. Stetz, “Hosting Capacity of Distribution Grids,” in *Autonomous Voltage Control Strategies in Distribution Grids with Photovoltaic Systems - Technical and Economic Assessment*, pp. 27–61, 2005

[131] M. H. J. Bollen, "IEEE Tutorial on Voltage Sag Analysis," *IEEE Power Engineering Society*, 1999.

List of Publications

1. S. Pukhrem, M. Basu, and M. F. Conlon, "**Probabilistic Risk Assessment of Power Quality Variations and Events under Temporal and Spatial characteristic of increased PV integration in low voltage distribution networks**," IEEE Trans. Power Syst., vol. 33, no. 3, pp. 3246-3254, 2018.
2. S. Pukhrem, M. Conlon, and M. Basu, "**The relationship between PVDG technical impacts and DSO revenue : An approach to foster a higher share of non-firm PVDG integration**," in CIGRE Symposium, 2017.
3. S. Pukhrem, M. Basu, M. F. Conlon, and K. Sunderland, "**Enhanced Network Voltage Management Techniques Under the Proliferation of Rooftop Solar PV Installation in Low-Voltage Distribution Network**," IEEE J. Emerg. Sel. Top. Power Electron., vol. 5, no. 2, pp. 681–694, 2017.